

**UNCLASSIFIED**

**AD 414412**

**DEFENSE DOCUMENTATION CENTER**

**FOR**

**SCIENTIFIC AND TECHNICAL INFORMATION**

**CAMERON STATION, ALEXANDRIA, VIRGINIA**



**UNCLASSIFIED**

**NOTICE:** When government or other drawings, specifications or other data are used for any purpose other than in connection with a definitely related government procurement operation, the U. S. Government thereby incurs no responsibility, nor any obligation whatsoever; and the fact that the Government may have formulated, furnished, or in any way supplied the said drawings, specifications, or other data is not to be regarded by implication or otherwise as in any manner licensing the holder or any other person or corporation, or conveying any rights or permission to manufacture, use or sell any patented invention that may in any way be related thereto.

**AEDC-TDR-63-173**



**RESULTS OF  
RAMJET FACILITY MODEL  
TESTS AT MACH 7**

**By**

**James L. Grunnet**

**Fluidyne Engineering Corporation  
Minneapolis, Minnesota**

**TECHNICAL DOCUMENTARY REPORT NO. AEDC-TDR-63-173**

**August 1963**

**Program Element 62405214/6951, Task 695101**

**(Prepared under Contract No. AF 40(600)-946 by the Fluidyne Engineering Corporation, Minneapolis, Minnesota)**

**ARNOLD ENGINEERING DEVELOPMENT CENTER  
AIR FORCE SYSTEMS COMMAND  
UNITED STATES AIR FORCE**

414412  
AS AD NO. 1  
414412

# *NOTICES*

Qualified requesters may obtain copies of this report from DDC, Cameron Station, Alexandria, Va. Orders will be expedited if placed through the librarian or other staff member designated to request and receive documents from DDC.

When Government drawings, specifications or other data are used for any purpose other than in connection with a definitely related Government procurement operation, the United States Government thereby incurs no responsibility nor any obligation whatsoever; and the fact that the Government may have formulated, furnished, or in any way supplied the said drawings, specifications, or other data, is not to be regarded by implication or otherwise as in any manner licensing the holder or any other person or corporation, or conveying any rights or permission to manufacture, use, or sell any patented invention that may in any way be related thereto.

RESULTS OF  
RAMJET FACILITY MODEL  
TESTS AT MACH 7

By

James L. Grunnet  
FluidDyne Engineering Corporation  
Minneapolis, Minnesota

(The reproducibles used in the reproduction  
of this report were supplied by the author.)

August 1963

## ABSTRACT

A test program was conducted under this contract to provide ramjet test facility bypass flow second throat diffuser pressure recovery data at a nominal nozzle exit Mach number of 7.0. During the tests a study was made of the effects of stagnation temperature, Reynolds number, ramjet inlet to facility nozzle exit area ratio, and other geometric variables. Two facility models were tested, the earlier Phase I model having a cowl lip angle of  $35^{\circ}$  with a flare angle of  $30^{\circ}$ , and the Phase II model having a lip and flare angle of  $15^{\circ}$ .

Prior to the tests it was hoped that it would be possible to attain bypass diffuser pressure recoveries approaching the pressure recovery across a normal shock at the nozzle exit Mach number. The best performance, which was obtained with the Phase II model, gave a pressure recovery corresponding to 65% of normal shock recovery. A significant influence of cowl flare angle was noted since the maximum recovery obtained with the Phase I model was 37% of normal shock recovery.

PUBLICATION REVIEW

This report has been reviewed and publication is approved.

  
Marion L. Laster  
Aerospace Engineer  
Propulsion Division  
DCS/Research

  
Donald R. Eastman, Jr.  
DCS/Research

## CONTENTS

	<u>Page</u>
ABSTRACT	iii
CONTENTS	v
LIST OF SYMBOLS	vii
1.0 INTRODUCTION	1
2.0 APPARATUS	2
3.0 TEST PROCEDURE	10
4.0 DATA CORRELATION STANDARDS	12
5.0 RESULTS AND DISCUSSION	24
6.0 EMPIRICAL EQUATIONS FOR ESTIMATION OF RAMJET FACILITY SECOND THROAT DIFFUSER PERFORMANCE	36
7.0 REMARKS CONCERNING THE USE OF BOUNDARY LAYER REMOVAL AND STARTING BLEED OFF	40
8.0 CONCLUSIONS	42
9.0 RECOMMENDATIONS	44
REFERENCES	45

## LIST OF SYMBOLS

A	Area
A*	Throat area (general)
A <sub>core</sub>	Facility nozzle exit potential flow core area
A <sub>effective</sub>	Effective area
A <sub>i</sub>	Ramjet inlet geometric capture area
A <sub>i</sub> *	Ramjet inlet throat area
A <sub>N</sub>	Facility nozzle geometric exit area
A <sub>NE</sub>	Facility nozzle effective exit area
A <sub>NT</sub>	Facility nozzle throat area
A <sub>ST</sub>	Bypass flow diffuser second throat area
K <sub>1</sub>	Constant in empirical equation for minimum starting second throat area
K <sub>2</sub>	Constant in empirical equation for minimum running second throat area
K <sub>3</sub>	Constant in empirical equation for boundary layer thickness
M	Mach number
M <sub>free stream</sub>	Free stream Mach number
M <sub>nozzle</sub>	Nozzle exit Mach number
P	Pressure
P <sub>t</sub>	Stagnation pressure
P <sub>t0</sub>	Upstream nozzle stagnation pressure
P <sub>t1</sub>	Stagnation pressure immediately upstream of shock wave
P <sub>t2</sub>	Stagnation pressure downstream of shock wave
T	Temperature
T <sub>exh</sub>	Bypass diffuser outlet stagnation temperature
T <sub>o</sub>	Nozzle stagnation temperature
T <sub>wall</sub>	Nozzle and diffuser wall temperature
Re	Reynolds number
X	Distance along nozzle from throat
δ	Boundary layer thickness

$\delta^*$	Boundary layer displacement thickness
$\eta$	Efficiency
$\eta_{NS}$	Normal shock efficiency
$\eta_p$	Corrected efficiency
$\lambda$	Pressure ratio - $P_{t0}/P_{t2}$
$\lambda_{MIN}$	Minimum running pressure ratio across bypass diffuser
$\lambda_{START}$	Starting pressure ratio across bypass diffuser
$\theta_c$	Cowl flare angle

## 1.0 INTRODUCTION

In a free-jet ramjet test facility the pressure recovery in the flow which bypasses the engine influences the size and cost of the exhausters required. Furthermore it is important from a cost stand point that the smallest possible facility be built for the engine to be tested. Consequently, the facility designer must have an accurate knowledge of the attainable bypass flow second throat diffuser pressure recovery and be able to select the maximum permissible or optimum inlet to nozzle exit area ratio.

References 1 through 10 contain second throat diffuser pressure recovery data for Mach numbers up to 4.5. These reports usually cover only one specific inlet configuration each, and no attempt is made at a systematic investigation of the parameters affecting pressure recovery. In the current program the data were obtained using a Mach 7.2 nozzle, and the influence of several variables on pressure recovery was defined.

## 2.0 APPARATUS

In order to provide the experimental data required under the subject contract, ramjet test facility models were designed, built and tested at Fluidyne Engineering Corporation. These models and the support facilities used during the tests are described below.

### 2.1 GENERAL FACILITY DESCRIPTION

The AEDC second throat diffuser tests were conducted at Fluidyne Engineering Corporation's Medicine Lake Laboratory. This laboratory contains what is known as the Fluidyne Hypersonic Flight Simulation Facility. Among the facility components used for these diffuser tests were the 500 psi and 5000 psi air supplies, the zirconia storage heater, and the vacuum system.

The 5000 psi air supply was used to provide the primary AEDC facility model air flow. This air is stored in a 60 cu. ft. tank which is recharged between runs. A run time of approximately 50 seconds was attainable at  $P_0 = 1500$  psi. Air from the 500 psi storage tank was the driving fluid in the exhaust ejector which was used to pump the combined inlet and bypass diffuser flows for the initial tests.

The facility model air flow was heated to the desired temperature by passing it through the zirconia pebble bed storage heater. Initial pebble bed temperatures as high as 4200 R were attainable. The heater outlet air temperature depended upon the initial bed temperature, the air flow and the run time.

Starting bleed off air was run through the air cooler and absorbed by Fluidyne's 33500 cu. ft. vacuum tank for the initial tests. For most of the tests the bleed off system was not used, instead the bypass flow and inlet flow were run into the vacuum tank to provide adequate overall pressure ratio.

The facility model consisting of Mach 7.2 nozzle, inlet diffuser, bypass flow diffuser, etc., was attached directly to the pebble bed heater air outlet. Figure 1 shows the layout of the test setup. The individual facility model components are discussed in detail in

the following subsections.

## 2.2 NOZZLE AND CALIBRATION

The nozzle used to produce flow for the facility model was designed to generate  $M = 7.0$  at  $P_{t_0} = 2000$  psi and  $T_0 = 4000R$ . Coordinates computed by WADC using the Cresci method and having a source flow half angle of  $12^\circ$  were used for the nozzle potential flow contour. The additive correction to the contour for boundary layer displacement thickness was calculated using the method of reference 11. A geometric nozzle exit diameter of 8.0 inches was selected for the design. A nozzle calibration obtained at  $P_{t_0} = 1000$  psi and  $T_0 = 1300F$  appears as figure 2. The Mach number attained at  $T = 4000R$  would then be 7.16 and the Mach number cold would be 7.70. This corresponds to a ratio of effective to geometric nozzle exit area of  $A_{NE}/A_N = 0.86$ . This is a somewhat larger effective area ratio than was originally estimated during the design. Consequently the actual inlet to nozzle effective area ratios for the Phase I tests were  $A_i/A_{NE} = 0.39, 0.51, \text{ and } 0.62$  rather than 0.45, 0.55, and 0.67. Similarly the Phase II model had an  $A_i/A_{NE}$  equal to 0.56 rather than the nominal value of 0.60 referred to in 2.3.2.

Since the nozzle was to be used with high stagnation pressures and temperatures, it was necessary to estimate the heat transfer rate to the nozzle walls in order to determine the cooling required. The nozzle heat transfer rate was calculated using the method of Bartz outlined in reference 12. It was found that backside convective water cooling was required for the entire length of the nozzle. Consequently double wall construction was used. The nozzle was built in three sections axially. The first two sections have beryllium copper inner liners because of the combined requirements for high strength and high thermal conductivity. The downstream liner was made of mild steel because of the reduced heat transfer rate.

### 2.3 INLET DIFFUSER

Two inlet and bypass diffuser configurations were tested under the current contract test series. During the initial tests it was found that the high cowl flare angle was adversely effecting pressure recovery. Consequently a second model was built with a lower cowl flare angle. A simple inlet design was used in both cases.

#### 2.3.1 Phase I Inlet Design

It was the purpose of the tests to obtain bypass diffuser pressure recovery data with a typical inlet configuration. The primary geometric parameter considered was the cowl lip angle which in the current tests was closely related to the cowl flare angle. Reference 13 was reviewed to determine the range of lip angles which might be encountered and it was decided that the worst condition (greatest angle) would be simulated in the initial inlet design. This was a cowl lip angle of 35°. The Oswatich method as described on pp. 255 to 263 of reference 14 was used to optimize the simple two-shock design selected. The important geometric parameters are shown in figure 3. It was estimated that the maximum recovery would approach  $P_{t_2}/P_{t_0} = 0.035$ .

The mechanical design of the Phase I inlet model was largely dictated by the necessity of cooling the model and by the practical requirement that three nozzle exit area ratios be attainable with one piece of basic hardware and three cowl lips. A heat transfer analysis using reference 15 as a guide showed that 4000°R testing made it necessary to either cool the entire inlet model or use high temperature materials in its construction. To take care of this problem, the cowl lips were made from molybdenum and coated to prevent oxidation, while the rest of the inlet model was built from mild steel with water passages for cooling. The steel parts were given a nickel plating to prevent rust. Figure 5 shows the basic method used in the construction of the inlet model and bypass diffuser. A throttling plug was installed in the inlet model exhaust pipe so that subcritical operation was possible. Capture

ratio could be calculated by means of the metering nozzle built into the inlet model. Photographs of the inlet model appear as figure 7.

The contract specified that three inlet sizes were to be tested. These were to correspond to inlet to effective nozzle exit area ratios of 0.45, 0.55, and 0.67. The resulting inlet to geometric nozzle exit area ratios were 0.34, 0.44, and 0.53 respectively. The inlet contraction in all cases was  $A_i^*/A_i = 0.225$ .

### 2.3.2 Phase II Inlet Design

As pointed out before, the high cowl flare angle on the initial inlet design had an adverse effect on bypass diffuser pressure recovery. Consequently a second review of inlet design practice was made. On the basis of conversations with people familiar with inlet design, it was concluded that the  $35^\circ$  lip angle -  $30^\circ$  flare angle used in the initial inlet design was much higher than would be ordinarily encountered. Cowl angles of less than  $15^\circ$  were more typical because these give lower cowl drag. For the second inlet design a cowl lip and flare angle of  $15^\circ$  was specified. Although this was still higher than typical, it made the design of the adjustable diffuser easier, and it was felt that it would not reduce bypass diffuser pressure recovery significantly. Based on the influence of  $A_i/A_N$  found during the initial tests, an inlet to effective nozzle exit area ratio of 0.60 was selected which gave an inlet to geometric nozzle exit area ratio of 0.48. Figure 4 shows the basic design features of the second inlet. The internal cowl lip angle of  $5^\circ$  was chosen to avoid shock induced separation on the spike. An inlet contraction of  $A_i^*/A_i = 0.34$  resulted from the design.

Tests at high stagnation temperature during Phase I confirmed the conclusions of section 4.1.2 that the influence of real gas effects on the pressure recovery of a particular piece of hardware is negligible. Consequently, the Phase II tests were run at a moderate stagnation temperature and mechanical design of the second

inlet model was much simpler than the initial model since cooling was not necessary. The basic method of construction appears in figure 6. Mild steel was used throughout. The same inlet support tube and throttling plug was used for both the Phase I and II models. Photographs of the Phase II model appear in figure 7.

#### 2.4 BYPASS FLOW SECOND THROAT DIFFUSER

The bypass flow diffuser is essentially an annular conical passage. The inlet cowl extends to form the inner wall of the diffuser passage and a conical shell forms the outside wall as shown in figures 5 and 6. In the Phase I design the cowl flare angle was  $30^{\circ}$ . The flare angle was reduced to  $15^{\circ}$  in the Phase II model. A separate conical shell was used with each of the two inlet model configurations to account for the different cowl angles. For both inlet configurations the diffuser contraction ratio could be varied by moving the inlet model axially with respect to the bypass diffuser outer shell. Available axial motion was sufficient to permit change of the diffuser throat area from practically zero to a value larger than that needed for starting. Adjustment was accomplished by means of a gear and screw mechanism with a Veeder-Root Counter. The counter reading was related to the diffuser contraction as shown in figures 9 and 10. The slant height (length) of the conical diffuser passage was made long for adequate pressure recovery. Test results reported in reference 9 were used as a guide in determining what length was needed.

A heat transfer analysis similar to that made for the inlet model showed that cooling would be necessary for the bypass diffuser outer shell at high stagnation temperatures. It was decided that the shell would be externally spray cooled so that expensive double wall construction could be avoided. As a result, the diffuser outer shells are of simple welded construction and are split along a horizontal seam for access to the inlet model and other enclosed components. The photographs comprising figure 8 show the facility model in various stages of assembly.

The various diffuser configuration modifications tested with the two inlet designs appear in figures 11 and 12. The Phase II second throat diffuser configuration included a constant area section and a subsonic diffuser portion while the Phase I configuration had an essentially constant annulus height.

## 2.5 THE STARTING BLEED OFF SYSTEM

With the adjustable second throat diffuser it was mechanically possible to decrease the second throat area after starting to improve pressure recovery. In view of the possible difficulty in providing such adjustment in a large facility, though, a bleed off system was built into configuration 1A so that attempts could be made to start the flow with bypass diffuser second throat areas too small to permit passage of the starting shock system. It was hoped that with such a system a fixed diffuser could be made to provide pressure recoveries approaching those of an adjustable diffuser. In the facility model a gap could be opened between the nozzle exit and bypass diffuser entrance through which the excess flow could be drawn to unchoke the diffuser throat. A manually tripped, quick opening valve opened the bleed off vent area at the nozzle exit to the FluidDyne vacuum tank. The existing FluidDyne air operated vacuum valves could then be closed to stop the bleed off so that it could be ascertained if starting had been accomplished. Sufficient bleed off vent area was provided so that a large share of the bypass flow could be handled during starting. The plenum chamber around the bleed off vent area contained flap type relief valves to discharge the facility flow to atmosphere in case of unstart with a small diffuser throat area.

In figure 8 is a photograph showing the quick opening bleed off valve. This valve and the associated ducting were mounted just below the bleed off system plenum which was built as an integral part of the bypass diffuser outer shell. Figure 8 also contains a general view of the assembled facility model which shows the bleed off system ducting.

Because difficulty was encountered in starting the facility, this bleed off system was abandoned after the first few runs.

## 2.6 FACILITY MODEL EXHAUST SYSTEM

Originally the FluidDyne vacuum tank was to be used for the starting bleed off system and an air ejector was built to handle the combined flows from the inlet model and bypass flow diffuser for configuration 1A. The ejector was designed to provide a model back pressure as low as 4 psia, which would correspond to one quarter of Mach 7.0 normal shock recovery at 1500 psia stagnation pressure. The FluidDyne 500 psia air supply system provided the driving gas. With 1000 lb of stored air, a total of 20 seconds of peak ejector operation was possible. With the abandonment of the bleed off system, the entire facility flow was run into the vacuum tank so that higher overall pressure ratios could be obtained.

## 2.7 INSTRUMENTATION

Instrumentation was provided to obtain the following basic test information on all models

- a. facility model nozzle stagnation pressure
- b. facility model nozzle stagnation temperature
- c. facility model nozzle exit static pressure
- d. inlet model pressure recovery
- e. inlet model mass flow (capture ratio)
- f. inlet model spike static pressure distribution
- g. bypass flow second throat diffuser pressure recovery
- h. bypass flow second throat diffuser exit stagnation temperature
- i. bypass flow second throat diffuser axial static pressure distribution

Additional instrumentation was provided on some configurations. Figure 13 and 14 show the location of most of the measuring points on the models. The device used for each measurement is listed along with its stated accuracy in table 1. The accuracy of some

of the transducers used was actually better than that stated in table I because of the care taken in calibration. In other cases, zero drift made the real accuracy somewhat poorer than that stated.

A great deal of difficulty was experienced in measuring the high stagnation temperatures during the Phase I tests. The iridium-iridium-rhodium unshielded thermocouple probe used at the high temperatures never did give useable results, and it was necessary to estimate the high stagnation temperatures by extrapolation from lower temperature data using the bypass flow diffuser outlet stagnation temperature as a reference. No explanation has been found for the type of difficulty experienced with the iridium, iridium-rhodium junction. The platinum, platinum-rhodium junction worked satisfactorily over its useable range of temperatures but it would melt at the high temperatures.

Transducer and thermocouple measurements were read out on an 18 channel Consolidated Electrodynamics recorder. This recorder uses light beam galvanometers with a light sensitive chart paper. A chart speed of four inches per second was used for the tests.

### 3.0 TEST PROCEDURE

Significant modifications to the facility model were made after the first runs with the Phase I inlet configuration. Consequently the discussion of test procedures will be divided into two sections, one covering the preliminary tests and the other the bulk of the tests with the Phase I and Phase II models. A third section is devoted to between run activities.

#### 3.1 PRELIMINARY TESTS

During the preliminary tests the air ejector was used to pump the inlet and bypass flows. The FluidDyne vacuum tank was used to handle the flow bled off from around the nozzle exit during attempts to start the facility model with a diffuser throat area less than that required with no auxiliary pumping. All of the preliminary runs were made at  $P_{t_0} = 1500$  psig and  $T_0 = 1500^{\circ}\text{R}$ .

For a typical run in which the bleed off system was used, the following sequence of events transpired after preliminary steps such as heater securing and turning on cooling water were completed.

1. the air control valve was opened and stagnation pressure was increased (this was a rather slow process since the volume of the pebble bed heater is large and bed flotation must be avoided)
2. at a stagnation pressure of 1000 psi the recorder chart motion was started
3. at a stagnation pressure of 1200 psi the main vacuum tank valve was opened
4. at the desired stagnation pressure of 1500 psi the air ejector was started
5. when peak air ejector performance was achieved the quick opening bleed off valve was actuated
6. manometer photo shadowgraphs were taken
7. the air ejector was shut down
8. the vacuum valve was closed
10. the recorder chart motion was stopped

### 3.2 BASIC TEST PROGRAM

After the preliminary tests the air ejector and bleed off system was abandoned and the entire facility model flow was run into the FluidDyne vacuum tank in order to increase the available overall pressure ratio. The following run procedure is typical.

1. open air control valve and increase stagnation pressure
2. at about 500 psi below desired stagnation pressure actuate main vacuum tank valve (it opens slowly)
3. start recorder chart motion
4. when the desired stagnation pressure is reached adjust bypass diffuser area (inlet model position) as desired
5. take manometer photos or shadowgraphs
6. close main vacuum valve
7. when facility nozzle unstarts shut air control valve
8. shut off recorder chart motion

### 3.3 BETWEEN RUN ACTIVITIES AND DATA REDUCTION

Between runs the vacuum tank was pumped down, the air supply tanks were pumped up and the heater bed temperature brought back up to the required prerun value. Calibration of the pressure transducers was accomplished between runs also. Calibration consisted of applying known pressures to the transducers and measuring the recorder trace deflection. The time between runs was also used to plot up the calibrations (pressure versus trace deflection) and to reduce the data from preceding runs. Data reduction involved reading out the manometer photographs and using the calibrations to read pressures and temperatures off of the recorder chart. From inspection of the recorder chart for a particular run, it was usually possible to tell immediately if and when starting and unstarting of the facility nozzle and inlet took place during the run. The points read out were those corresponding to start or unstart. The pressure data was used to determine overall pressure ratio requirements, inlet recovery, and local pressures.

#### 4.0 DATA CORRELATION STANDARDS

This section is devoted to the development of theoretical and empirical relationships for correlating wind tunnel and ramjet test facility data.

##### 4.1 IDEAL SECOND THROAT DIFFUSER PRESSURE RECOVERY AND A NEW DEFINITION OF DIFFUSER EFFICIENCY

It has been customary for a long time to compare supersonic diffuser pressure recovery data with the theoretical normal shock recovery at the free stream nozzle exit Mach number. This comparison of actual diffuser recovery with normal shock recovery has been called normal shock efficiency, which is defined as follows;

$$\eta_{NS} = \frac{(P_{t2}/P_{t0})_{ACTUAL}}{(P_{t2}/P_{t1})_{NS @ M_{NOZZLE}}} \quad 4.1$$

Under circumstances where the boundary layer is thick or where the final shockdown area is much different from the nozzle area, free stream nozzle exit normal shock recovery is not a good measure of obtainable pressure recovery and normal shock efficiency is a poor measure of the real efficiency of the recovery process. To lay the foundation for a better definition of diffuser efficiency in 4.1.4, the influence of diffuser second throat contraction, stagnation temperature, and boundary layer thickness on pressure recovery will be discussed.

##### 4.1.1 The Influence of Second Throat Diffuser Contraction

For frictionless flow, final deceleration from supersonic to subsonic flow occurs through a normal shock wave. The total pressure ratio or pressure recovery across this normal shock wave is a direct function of the diffuser throat Mach number which, in turn, is a function of the net area ratio through which the flow has been

expanded up to the shock wave. For a wind tunnel with frictionless flow and isentropic contours this implies that the pressure recovery will be a function of the net expansion ratio  $A_{ST}/A_{NT}$ .

The importance of the second throat contraction is apparent on examination of the compressible flow tables and equations in reference 16 where it can be seen that the pressure recovery across a normal shock at high Mach number is very near to being inversely proportional to the area ratio through which the flow has been expanded. For  $\gamma = 1.4$  an approximate relationship can be written as follows;

$$\left(\frac{P_2}{P_1}\right)_{NS} = \frac{1.62}{A/A^*} \quad \text{for } (5.0 < M < \infty) \quad 4.2$$

where:  $A$  is the area at which  
shockdown occurs  
 $A^*$  is the throat area  
corresponding to the flow  
under consideration

From this relationship it is clear for the idealized case that making the diffuser throat area equal to half the nozzle exit area would give a pressure recovery of twice free stream normal shock recovery. It appears, therefore, that any meaningful definition of diffuser efficiency must be based on the actual second throat area which defines the Mach number at which shockdown occurs.

A legitimate question here is; what influence do losses ahead of the diffuser throat (oblique shocks, etc.) have on diffuser pressure recovery? In other words, for frictionless flow given  $A_{ST}/A_{NT}$ , how would an estimate of pressure recovery based on isentropic flow up to the final shock compare with a more elaborate estimate which included oblique shock losses ahead of the shock. One can satisfy himself that such losses have a negligible effect on

overall recovery by setting up a simple flow model and assuming a distributed total pressure loss across the flow upstream of the final normal shock. The effect of this loss is to lower the final normal shock Mach number and reduce the total pressure loss across it. This effectively compensates for the upstream loss giving the same overall recovery for a given  $A_{ST}$  as the case with isentropic flow up to the shock.

#### 4.1.2 The Influence of Stagnation Temperature

High stagnation temperatures may influence pressure recovery in two ways; first through the so called real gas effects, and secondly through its effect on boundary layer displacement thickness (nozzle effective flow area)

Figures 11 through 24 in NACA Report 1135 (Ref. 16) present the real gas corrections to the thermally and calorically perfect flow properties found in the tables. It appears, on examination of these figures and tables, that the normal shock recovery for a particular expansion ratio is independent of stagnation temperature, or, in other words, our approximate relationship for frictionless flow

$$\left( \frac{P_{t2}}{P_{t1}} \right)_{NS} = \frac{1.62}{A/A^*} \quad (5.0 < M < \infty) \quad 4.2$$

is valid regardless of stagnation temperature. As stagnation temperature is raised, the Mach number obtained with a given expansion ratio goes down, thereby offsetting the reduction in recovery which would occur if the Mach number remained constant. The facility designer must account for stagnation temperature by selecting the proper nozzle area ratio for the design Mach number.

The influence of boundary layer displacement thickness on pressure recovery will be discussed in 4.1.3. Changes in stagnation temperature influence the boundary layer displacement thickness

principally through their influence on the temperature distribution in the boundary layer. As stagnation temperature is increased the difference between wall temperature and recovery temperature increases and the ratio  $\frac{T_r - T_w}{T_r}$  increases. This results in a decrease in boundary layer displacement thickness.

#### 4.1.3 The Effect of Frictional Losses

The discussion in 4.1.1 was limited to frictionless flow. The effect of friction (boundary layer growth) must now be considered.

In a duct containing a flowing fluid, frictional losses appear in the boundary layer. These losses can influence the maximum attainable pressure recovery in several ways. First, it is conceivable that frictional losses might influence the pressure recovery for a particular flow geometry defined by the ratio of diffuser throat area to nozzle throat area. Secondly, the frictional losses are liable to influence the amount of diffuser contraction which can be applied without causing unstart (minimum running throat area). Finally, in ramjet test facilities, where the inlet captures part of the flow, the frictional losses influence the portion of flow entering the bypass diffuser. Only the influence of friction on the pressure recovery with a given flow geometry will be discussed here. The other effects will be discussed in sections 4.1.4 and 4.3. These latter effects, though, will be shown to have the most influence on the pressure recovery which can be obtained in ramjet test facility bypass diffusers.

Frictional losses reduce the percent of freestream normal shock recovery which can be obtained in the shockdown of a potential flow plus boundary layer. This can be demonstrated by integrating momentum, energy, and mass flux through a confined boundary layer to determine what pressure recovery might be realized. For high free stream Mach numbers it will be found that, to a close approximation, the potential pressure recovery of a confined boundary layer is equal to

$$\left(\frac{P_{t_2}}{P_{t_0}}\right) = \left(\frac{P_{t_2}}{P_{t_1, NS}}\right) \left(\frac{\delta - \delta^*}{\delta}\right) \quad 4.3$$

for two-dimensional flow

where:  $P_{t_0}$  is free stream stagnation pressure  
 $P_{t_2}$  is recovered stagnation pressure  
 $(P_{t_2}/P_{t_1})_{NS}$  is free stream normal shock stagnation pressure recovery ratio  
 $\delta$  is the boundary layer thickness  
 $\delta^*$  is the boundary layer displacement thickness

The expression  $\frac{\delta - \delta^*}{\delta}$  is equivalent in the boundary layer to  $A_{\text{effective}}/A_{\text{geometric}}$  which implies that the maximum attainable pressure recovery of any potential flow plus boundary layer is equal to free stream normal shock recovery multiplied by the ratio of effective to geometric flow area at shockdown. This implication, along with the results in 4.1.1, leads to an interesting conclusion of practical importance. In a flow passage containing potential flow plus boundary layer, the free stream normal shock recovery can be approximated as

$$\left(\frac{P_{t_2}}{P_{t_1}}\right)_{NS} = \frac{1.62}{A_{\text{effective}}/A^*} \quad 4.2$$

since  $A_{\text{effective}}/A^*$  is the area ratio through which the potential flow has been expanded. The maximum obtainable pressure recovery of the total stream would then be

$$\left(\frac{P_{T2}}{P_{T0}}\right)_{\text{potential}} = \frac{1.62}{A_{\text{effective}}/A^*} \times \frac{A_{\text{effective}}}{A_{\text{geometric}}} = \frac{1.62}{A_{\text{geom}}/A^*}$$

4.4

The important conclusion here is that the maximum attainable pressure recovery of any non-isentropic potential flow plus boundary layer can be accurately estimated by assuming that the flow expands isentropically from the nozzle throat to the geometric diffuser throat area and then passes through a normal shock. This means that if friction is to influence pressure recovery, it must influence it through its effect on flow geometry (permissible diffuser contraction and percent of flow entering the bypass diffuser).

#### 4.1.4 Basis for Correlating Pressure Recovery Data

In 4.1.1, 4.1.2, and 4.1.3 it has been demonstrated that the potential pressure recovery of any flow including boundary layer can be estimated by assuming that the flow is isentropically expanded through the geometrical area ratio between the diffuser throat and nozzle throat and then goes through a normal shock at the ideal diffuser throat Mach number. In this section this will be applied to ramjet test facility bypass flow second throat diffusers and a new definition of efficiency will be presented which adequately measures the efficiency of the recovery process.

In a ramjet test facility the major problem in determining the geometric area ratio through which the bypass flow has been expanded is that of determining the nozzle throat area corresponding to the bypass flow. Generally speaking;

$$A_{\text{bypass}}^* = A_{\text{NT}} \frac{\dot{W}_{\text{bypass}}}{\dot{W}_{\text{total}}} \quad 4.5$$

If  $A_i$  is the inlet capture area and  $A_{NE}$  is the effective nozzle exit area (which determines nozzle exit Mach number) equation 4.5 becomes

$$A_{\text{bypass}}^* = A_{NT} \frac{(A_{NE} - A_i)}{A_{NE}} \quad 4.6$$

Since  $A_{ST}$  is the diffuser throat area where shockdown occurs, the geometric area ratio through which the flow is expanded becomes

$$\frac{A}{A^*} = \frac{A_{NE}}{A_{NT}} \frac{A_{ST}}{(A_{NE} - A_i)} \quad 4.7$$

By rearranging 4.7 one can write it so that it is expressed in terms of more familiar parameters

$$\frac{A}{A^*} = \left( \frac{A_N}{A_{NT}} \right) \left( \frac{A_{NE}}{A_N} \right) \left( \frac{1 - A_i/A_N}{\frac{A_{NE}}{A_N} - \frac{A_i}{A_N}} \right) \left( \frac{A_{ST}}{A_N - A_i} \right) \quad 4.8$$

The boundary layer displacement thickness enters this equation directly through  $A_{NE}$  as it influences the amount of flow entering the bypass flow diffuser.

Using the explicit relationship for pressure recovery (eqn 4.2) and substituting in 4.8, an equation for bypass second throat diffuser potential pressure recovery is obtained which is reasonably accurate at high Mach numbers ( $5.0 < M < \infty$ ).

$$\left( \frac{P_{T_2}}{P_{T_0 \text{ potential}}} \right) = \frac{1.62}{\left( \frac{A_N}{A_{NT}} \right) \left( \frac{A_{NE}}{A_N} \right) \left( \frac{1 - A_i/A_N}{\frac{A_{NE}}{A_N} - \frac{A_i}{A_N}} \right) \left( \frac{A_{ST}}{A_N - A_i} \right)} \quad 4.9$$

For accuracy at low Mach numbers one must take the area ratio obtained from equation 4.8 and look up the corresponding normal shock recovery in the flow tables, rather than using the explicit relationship 4.9.

The new definition of efficiency,  $\eta_p$ , will be defined as the ratio of the actual recovery to the real potential pressure recovery defined in the preceding paragraph, or as in equation 4.9 for high Mach numbers. Written in explicit form  $\eta_p$ , which we will call corrected efficiency, becomes

$$\eta_p = 0.618 \left( \frac{P_{t2}}{P_{t0}} \right)_{\text{ACTUAL}} \left( \frac{A_N}{A_{NT}} \right) \left( \frac{A_{NE}}{A_N} \right) \left( \frac{1 - A_i/A_N}{\frac{A_{NB}}{A_N} - \frac{A_i}{A_N}} \right) \left( \frac{A_{ST}}{A_N - A_i} \right)$$

(5.0 < M < ∞) 4.10

For wind tunnel diffusers having adequate second throat lengths, efficiencies on the order of 0.80 are typical. A survey of ramjet facility model data indicates that bypass flow second throat diffusers of good design can produce corrected efficiencies of 0.70 even with unusual inlet configurations.

#### 4.2 THE MINIMUM STARTING SECOND THROAT AREA

For a fixed second throat diffuser, the flow contraction and consequent running pressure ratio are limited by the starting area requirement. At low Mach numbers (normal starting shock), the sum of the inlet throat area,  $A_i^*$ , and the bypass diffuser second throat area,  $A_{ST}$ , must be large enough to permit starting of the facility nozzle (swallowing of the normal shock) without choking (see figure 15). This ordinarily results in a rather large diffuser throat area requirement because, before starting, the inlet throat can only accommodate a small percentage of the flow. After starting, though, the inlet captures a large share of the total flow; and the

flow entering the bypass diffuser experiences little if any deceleration before shockdown occurs. This explains why the pressure recovery of fixed bypass flow diffusers can not equal the pressure recovery of fixed wind tunnel diffusers.

At high Mach numbers the starting shock is characterized by separated supersonic flow in the nozzle and the problem of choking is alleviated to some extent. The minimum starting second throat area in such a case depends in part upon the interaction of shock waves from the inlet with the nozzle boundary layer (see figure 15). The actual starting process observed during the current test series is discussed in section 5.5. It is practically impossible to develop a theoretical model of this flow process which would permit accurate prediction of the minimum starting second throat area. Consequently, estimates of minimum starting second throat area based on the simplified model assuming a normal starting shock wave will be used to correlate the experimental data.

Reference 14 describes the idealized one-dimensional starting process and defines what is referred to as the "swallowing function", which is the ratio of flow area downstream of the nozzle to nozzle exit area required to permit starting of the nozzle. This ratio reaches an asymptotic value as  $M_{\text{nozzle}}$  approaches infinity. For Mach numbers above 5.0 the swallowing function (M) is nearly equal to 0.62 so the ideal value of minimum starting second throat area can be expressed as;

$$\frac{A_{ST,IDEAL} + A_i^*}{A_N} = 0.62 \quad 4.11$$

which can be refined to give the following relationship

$$\left( \frac{A_{ST}}{A_N - A_i} \right)_{\text{MINSTART IDEAL}} = \frac{0.62 - \left( \frac{A_i^*}{A_i} \right) \left( \frac{A_i}{A_N} \right)}{1 - \frac{A_i}{A_N}} \quad 4.12$$

Tests made at Mach number 3.2 (reference 9) indicated that a bypass diffuser second throat area 20% greater than theoretical was needed for starting. For purposes of correlating minimum starting diffuser throat area data, a constant  $K_1$  will be defined as the ratio of actual contraction to ideal contraction for starting i.e.;

$$\left(\frac{A_{ST}}{A_N - A_i}\right)_{\text{MIN START}} = K_1 \left(\frac{A_{ST}}{A_N - A_i}\right)_{\text{MIN START IDEAL}} = \frac{K_1 \left\{ 0.62 - \left(\frac{A_i}{A_i}\right) \left(\frac{A_i}{A_N}\right) \right\}}{1 - A_i/A_N} \quad 4.13$$

#### 4.3 THE MINIMUM RUNNING SECOND THROAT AREA

With an adjustable second throat diffuser the maximum possible contraction of the flow before final shockdown is limited by the boundary layer thickness. If there were no boundary layer the bypass flow could theoretically be decelerated to a Mach number of 1.0 in the second throat and all of the upstream stagnation pressure could be recovered. The presence of a boundary layer limits the rate of pressure rise which can be tolerated and consequently limits the flow contraction. Accurate theoretical estimation of the minimum running second throat area is not possible since it depends on boundary layer thickness, flow passage configuration, the strength of disturbances entering the diffuser, etc. However, it appears possible to correlate minimum running second throat area data by using the following equation

$$\left(\frac{A_{ST}}{A_N - A_i}\right)_{\text{MIN RUN}} = \frac{K_2 \left\{ \frac{(P_2/P_1)_{0c}}{(P_2/P_1)_{0cd}} + 1 \right\} \left(1 - \frac{A_{NE}}{A_N}\right)}{\left\{ \left(\frac{A_N}{A_{NT}}\right) \left(\frac{A_{NE}}{A_N}\right) \right\}^{0.6} \left(1 - \frac{A_i}{A_N}\right)} \quad 4.14$$

where:  $K_2$  is an empirical constant developed from experimental data

$(P_2/P_1)_{\theta_c}$  is the pressure rise ratio associated with wedge turning of the nozzle exit flow through an angle equal to the cowl flare angle

$(P_2/P_1)_{sep}$  is the pressure rise ratio associated with separation of a turbulent boundary layer ahead of a forward facing step (see figure 17)

In ramjet test facilities where the inlet is large with respect to the nozzle exit area and the bypass diffuser captures primarily boundary layer, the permissible diffuser contraction is reduced. This is the primary reason why adjustable bypass flow diffusers give poorer pressure recovery than adjustable wind tunnel diffusers. A correlation of wind tunnel data and existing data from ramjet facility models with adjustable diffusers (references 3 and 17) gave an average  $K_2$  of 16.0. For the wind tunnels it was assumed that  $(P_2/P_1)_{\theta_c} = 0$ .

#### 4.4 MAXIMUM PRACTICAL RAMJET INLET TO NOZZLE EXIT AREA RATIO

The selection of the inlet to nozzle exit area ratio for design purposes will depend primarily on four things;

1. there must be sufficient flow area between the inlet cowl and nozzle exit to permit starting of the facility
2. the nozzle exit disturbance must not enter the inlet or influence the flow into it
3. the inlet must capture only potential flow (none of the boundary layer)
4. the nozzle should not be made so small relative to the inlet that the pressure recovery of the second throat diffuser is significantly impaired (exhaust volume flow increased)

The first two requirements combine to limit the maximum permissible inlet to nozzle exit area ratio at Mach numbers up to about 3.0.

The limit can be estimated by a consideration of the inlet and nozzle exit geometry and application of the normal shock properties to determine how much area is required around the inlet to permit starting of the facility nozzle.

Above Mach number 5.0 an absolute limit of relative inlet size is set by the thickness of the nozzle exit boundary layer, since the inlet must capture only potential flow and the boundary layer may be quite thick. The following empirical relationship can be used to correlate nozzle boundary layer thickness data:

$$\frac{\delta}{X} = \frac{K_3}{Re_{exit}^{0.2}} \quad 4.10$$

where  $Re$  is the Reynolds number per foot at nozzle exit times the nozzle length, and  $K_3$  is a constant evaluated from the data. Data from various (Ref 18 and 19) indicate that  $K_3$  ranges from 0.63 to 0.89 with most of the data for axisymmetric nozzles falling around 0.8. With the substitution of  $K_3 = 0.8$ , it appears that  $A_{CORE}/A_N$  is slightly greater than 0.6 for a good sized nozzle at Mach number 7.0.

The reduction of second throat diffuser pressure recovery with increasing inlet size (item 4 above) may limit the maximum practical inlet to nozzle exit area ratio in certain situations where there is a strong disturbance from the inlet cowl which influences the diffuser wall boundary layer. This effect is characterized by a reduction in  $\tau_p$  as  $A_i/A_N$  is increased. In a practical sense it means that the exhaust volume flow is increased when the nozzle size is decreased below a certain point. As long as  $\tau_p$  remains constant, however, increasing  $A_i/A_N$  will reduce the exhaust volume flow for a given sized inlet. The practical limit to relative inlet size will depend upon a consideration of air supply system cost and exhaust system cost. Some increase in exhaust system size and cost may be tolerated if the air supply system cost is reduced by making the nozzle size relative to the engine and inlet smaller.

## 5.0 RESULTS AND DISCUSSION

### 5.1 GENERAL PRESENTATION AND CORRELATION OF DATA

Figures 18 and 19 present pressure distribution data for the Phase I and Phase II facility models. Data for both started and unstarted flow situations appear. This information will not be discussed further.

The bypass flow second throat diffuser pressure recovery data are plotted in figures 20 through 34. These data appear as overall pressure ratio,  $\lambda$ , required to start and maintain flow, as normal shock efficiency  $\eta_{NS}$ , and as corrected efficiency,  $\eta_p$ , based on the real potential pressure recovery. Included in figures 20 through 34 are the minimum starting and minimum running second throat areas. The best performance, attained with the Phase I model configuration D for  $A_1/A_N = 0.34$ , indicated that an overall pressure ratio of at least 270 would be required to maintain flow. This corresponds to a normal shock efficiency of 0.37. For Phase II configuration B having an  $A_1/A_N = 0.48$ , a pressure ratio of only 152 was needed at the minimum running diffuser throat area, giving a normal shock efficiency of 0.65. Had the Phase II model been built with  $A_1/A_N = 0.34$  it would have given a bypass diffuser pressure recovery nearly equal to normal shock recovery. These data are discussed more completely below.

The pressure ratios and pressure recoveries given in this report are the ratios of nozzle stagnation pressure and bypass diffuser outlet stagnation pressure. These data do not include the pumping effect of the engine flow which can be utilized when the engine and bypass diffuser flows are mixed in an ejector. This effect must be predicted for each specific installation on the basis of engine performance and ejector theory.

Shadowgraphs of started flow are shown in figures 35 and 36 for the Phase I and II models. The gap length and window diameter limited the viewing area. Shadowgraphs of unstarted flow appear as figures 37 and 38.

## 5.2 THE INFLUENCE OF STAGNATION TEMPERATURE

The influence of stagnation temperature on diffuser pressure recovery is discussed in 4.1.2 on the basis of the real gas effect corrections found in NACA Rept 1135 (reference 16). During the Phase I tests the influence of elevated stagnation temperature on diffuser pressure recovery was determined experimentally. The results of these tests are summarized in figure 39 where the corrected second throat diffuser efficiency is plotted as a function of stagnation temperature for  $A_1/A_N = 0.34, 0.43, \text{ and } 0.53$ . It appears from these data that the pressure recovery is not influenced appreciably by high stagnation temperatures.

## 5.3 THE INFLUENCE OF REYNOLDS NUMBER

During the Phase II program, tests were run at reduced Reynolds number with both the closed gap and open gap configurations. These tests simulated a full scale facility Reynolds number altitude of 150,000 ft. based on a full scale effective nozzle diameter of 10 ft. The stagnation pressure for these tests was 300 psi as compared with the value of 1000 psi which was used for the major portion of the tests. In figure 40 the corrected efficiency of both the open and closed gap configurations is plotted vs stagnation pressure. No effect of Reynolds number is apparent. During the reduced Reynolds number tests the minimum starting second throat area was also checked and no significant effect of Reynolds number was noted.

## 5.4 THE INFLUENCE OF GEOMETRIC VARIABLES

In this subsection the influence of the geometric variables on diffuser pressure recovery will be discussed.

### 5.4.1 The Influence of Second Throat Area

A significant feature of the facility models tested under this contract was the mechanically adjustable diffuser second throat area. The influence of second throat diffuser area on bypass diffuser pressure recovery is shown in figures 30 through 34

where  $\eta_p$  is plotted as a function of diffuser second throat area  $\frac{A_{ST}}{A_N - A_i}$ . According to these data  $\eta_p$  is essentially independent of diffuser contraction indicating that pressure recovery is inversely proportional to second throat area as was suggested in subsection 4.1.1.

#### 5.4.2 The Influence of Inlet to Nozzle Exit Area Ratio

During the Phase I tests three different inlet to nozzle exit area ratios were tested (0.34, 0.44, & 0.53) in an attempt to define the maximum practical area ratio for design purposes. Changing the relative inlet size had two effects;

1. an effect on  $\eta_p$
2. an effect on minimum starting and running second throat area

The corrected efficiency,  $\eta_p$ , for the running condition is plotted in figure 41 as a function of  $A_i/A_N$ . The figure contains both Phase I and Phase II data. The Phase I data show  $\eta_p$  remaining relatively constant with  $A_i/A_N$  up to an  $A_i/A_N$  of approximately 0.44 at which point it apparently begins to drop off with increasing  $A_i/A_N$ . According to the discussion in subsection 4.4 this indicates that the maximum practical inlet to nozzle exit area ratio may have been reached. The reduction in  $\eta_p$  with increasing  $A_i/A_N$  is probably related to the strength of the cowl lip shock. Quite possibly there would be no reduction in  $\eta_p$  even at  $A_i/A_N = 0.53$  with the reduced cowl lip angle used during the Phase II tests, however only one value of  $A_i/A_N$  was tested with the reduced cowl lip angle so the effect of  $A_i/A_N$  on  $\eta_p$  was not defined.

Figure 42 contains a plot of experimentally and analytically determined values of minimum starting second throat area versus  $A_i/A_N$ . The analytical variations were obtained by using equation 4.12. The experimental values were obtained during the Phase I testing. The minimum starting throat area was consistently about 30% higher than the theory, indicating that  $K_1$  is not a strong

function of  $A_1/A_N$ . For the Phase I configuration, the diffuser second throat area could not be reduced after starting without causing flow breakdown. Consequently, the minimum starting and minimum running throat areas were equal. Correlation of this data with equation 4.14 for minimum running throat gave  $K_2 = 19.0$  compared to  $K_2 = 16.0$  obtained from existing data.

#### 5.4.3 The Influence of Inlet Cowl Lip Angle

The principal difference between the Phase I and Phase II models was the difference in cowl flare angle. Associated with the reduced cowl flare angle in the Phase II configuration was a reduced inlet spike angle. The change in angles between Phase I and Phase II was made because it appeared that the high angle (nominally  $30^\circ$ ) of the Phase I configuration were adversely influencing pressure recovery (see reference 20) and also because a reduction in angle to something equal to or below  $15^\circ$  seemed to be justifiable on the basis of current inlet design thinking.

Reducing the cowl flare angle influenced  $\eta_p$ , minimum starting second throat area, and minimum running second throat area. The corrected running efficiency,  $\eta_p$ , improved from 0.50 to 0.60 in going from the  $30^\circ$  flare angle to the  $15^\circ$  flare angle configuration (the efficiency attained may be related to diffuser throat length and geometry as much as to cowl lip angle per se - see 5.4.4 and 5.5).

Even more significant than the improvement in  $\eta_p$  was the reduction in minimum starting and minimum running diffuser second throat areas which resulted in lower starting and operating pressure ratios for the Phase II model.

Figure 43 contains a plot of  $K_1$  (the ratio of actual to ideal minimum starting diffuser throat area, equation 4.13) as a function of inlet size.  $K_1$  varied from 1.30 for the  $30^\circ$  cowl closed gap configuration to 0.95 for the  $15^\circ$  cowl.  $K_1$  seldom gets below 0.80 for wind tunnels, so using a value of  $K_1 = 1.00$  to estimate the minimum starting diffuser throat area for ramjet facilities with

moderate cowl angles and closed gap will be reasonably accurate at high Mach numbers.

The  $K_2$  for minimum running diffuser throat (equation 4.14) remained at approximately 19.0 for all of the closed gap Phase I and Phase II tests (see figure 44). Since the correlation equation accounts for cowl flare angle, the constant  $K_2$  implies that the reduction in cowl angle resulted in a considerable reduction in minimum running bypass diffuser second throat area. This is the primary reason why the Phase II model had a diffuser normal shock efficiency almost twice that of the best Phase I configuration. It was possible to contract the second throat area after starting with the Phase II models. This resulted in an improvement of 21% in required running pressure ratio over what would be required with a fixed diffuser (see figures 23 and 24).

#### 5.4.4 The Influence of Minor Geometric Variables

Figures 11 and 12 present the variations in bypass flow diffuser entrance geometry tested during the Phase I and Phase II programs. Configurations 1A and 1C were not tested completely because serious shortcomings in their design became apparent quickly. Configuration 1A was abandoned before starting was accomplished and configuration 1C was abandoned after one run. Configurations 1B and 1A are standard open gap configurations while 1D and 11B have a closed gap. These configurations were given extensive testing. For both the Phase I and Phase II models, the change from an open gap design to the closed gap resulted in lower minimum starting and operating second throat areas and consequently improved diffuser pressure recovery. With the Phase I model and  $A_i/A_N = 0.34$ , going from the open to the closed gap configuration reduced minimum starting and running second throat area by 11%. For the Phase II model the minimum starting second throat area went from  $\frac{A_{ST}}{A_N - A_{i \text{ min start}}} = 0.97$  to 0.84, and the minimum running

area went from  $A_{ST} = 0.82$  to 0.64. Apparently the open gap provides a sort of "short circuit" through which pressure disturbances can influence flow at the nozzle exit. This limits the diffuser contraction since the contraction is varied by moving the inlet model, which in turn moves the point of intersection of the cowl lip shock with the diffuser exterior wall.

With the Phase I model, closing the gap also resulted in an improvement in corrected running efficiency from  $\eta_p = 0.46$  to  $\eta_p = 0.50$ . This improvement in  $\eta_p$  was not noted with the Phase II model; in fact, the limited data obtained with the Phase II open gap configuration indicated a higher running  $\eta_p$  than the closed gap configuration. This does not seem realistic and no explanation has been found for it. The open gap configuration did suffer from a higher starting pressure ratio requirement, however.

In addition to the open versus closed gap variations there was an additional variation in geometry between the Phase I and Phase II models that may partially account for the higher value of  $\eta_p$  found during the Phase II tests. While the Phase I bypass diffuser had essentially a constant annulus height (increasing area in the downstream direction), the Phase II diffuser was designed to have a significant length of constant area throat (approximately 10 annulus heights at typical second throat area settings).

### 5.5 THE FACILITY STARTING PROCESS

Starting pressure ratios at a particular diffuser throat setting varied from 1.50 times running pressure ratio for the open gap configuration to about 1.10 times running pressure ratio for the closed gap configuration. The minimum starting pressure ratios and area ratios obtained during both the Phase I and Phase II tests were closely related to the starting process. In figure 15 the starting process is portrayed as if the starting shock were a

normal shock wave. A more realistic picture of the actual shock system appears in figure 16. The flow separates from the nozzle and forms a supersonic core or jet surrounded by low energy air. Shadowgraphs of unstarted flow appear as figures 37 and 38. As sketched in figure 16A, the jet is centered on the nozzle centerline and consequently on the inlet spike. Two problems may arise when the jet is centered. First of all the jet may be almost completely captured by the inlet and the bypass diffuser starved of high energy air. This results in high starting pressure ratios. Secondly the strong flow turning angles which occur from the spike or cowl increase the minimum starting second throat area. From the Phase II experimental data it appeared that the open gap configuration had a tendency to force the separated core to be centered. With the closed gap configuration, the separated starting shock system or jet flopped over to one side of the nozzle, (see figure 16B) alleviating both the starvation problem and the high flow deflection problem. Starting pressure ratio and minimum starting area ratio were both reduced as shown in figures 23 and 24.

The jet like starting shock system is responsible for the fact that the Phase II closed gap configuration started with a second throat area 5% below the theoretical (normal shock) estimate. The choking problem is alleviated somewhat by the jet of high energy air. This type of phenomenon occurs in wind tunnels also where starting has been accomplished with second throat areas as much as 35% below theoretical.

The ramjet inlet can play a fairly important role in the starting process. This was illustrated during the early Phase II tests. Starting could not be accomplished even though there was adequate second throat area and sufficient overall pressure ratio. The flow picture that developed is sketched in figure 45. The starting shock jet was flopped to one side of the nozzle. The ramjet inlet model captured part of the high energy jet but would spill part of the flow back out on the opposite side from the jet. This low energy flow then passed downstream through the diffuser throat and effectively choked it. After analyzing the problem it

appeared that there was too great a constriction in the inlet model exhaust flow passage, that is, the inlet was in effect throttled. Although the degree of throttling probably would have permitted supercritical operation had the flow been started, it would not handle the required amount of flow during the starting process. The problem was solved by both increasing the minimum passage area inside the inlet exhaust duct and by extending the constant area shockdown length inside the inlet throat to give better inlet pressure recovery (the latter treatment was necessary because the minimum exhaust flow area could not be enlarged indefinitely). Although this type of flow throttling is not likely to be a problem when real ramjet engines are tested, the possibility perhaps ought to be checked in each case, especially at very high Mach numbers where the amount of heat addition is necessarily limited and the nozzle throat size is consequently reduced with respect to the inlet throat area. This problem ought also be considered when tests of turbine engines are contemplated if the engine internal hardware blocks the inlet flow passage during the facility starting process.

#### 5.6 PROSPECTS FOR IMPROVING SECOND THROAT DIFFUSER RECOVERY FURTHER

Improvements in bypass flow second throat diffuser pressure recovery can come from three possible sources; further reduction in the minimum running second throat area, improvements in corrected efficiency (getting back a greater percentage of the potential pressure recovery), or reduction in boundary layer displacement thickness in the nozzle. With no boundary layer removal, reductions in minimum starting or minimum running second throat area will probably be associated with further reductions in cowl flare angle. In subsection 4.3 the minimum running throat area was related to the strength of model induced disturbances entering the diffuser; and on the basis of wind tunnel data it appeared that the empirical constant  $K_2$  equalled 19.0 based upon a correlation which accounted for cowl disturbance strength. If the proposed

relationship between disturbance strength and permissible diffuser contraction is correct, there is a real possibility that reducing the cowl lip angle farther will beneficially affect the minimum running diffuser throat area.

In 4.1.4 it was indicated that wind tunnel diffuser corrected efficiencies approach the value of 0.80. The values obtained in these tests did not exceed  $\eta_p = 0.65$ . Consequently there may be room for improvement. Any improvement which can be realized will probably come from increasing the diffuser throat constant area length. With the type of diffuser configuration used, the flow along the nozzle wall expands around a corner in entering the conical diffuser annulus. The flow on the inside boundary of the annulus (the inlet cowl and extension) has experienced a compression shock. It takes a considerable axial distance for the radial velocity distribution to even out so that reasonable pressure rises can be tolerated on the exterior wall of the diffuser. Consequently the required constant area length for maximum pressure recovery may be 20 or 30 annulus heights instead of only 10 or 12 (which should be adequate for an annular diffuser).

## 5.7 HEAT TRANSFER TO THE DIFFUSER WALLS

A stagnation temperature probe was placed at the exit to the bypass diffuser so that some measure of the heat loss to the nozzle and diffuser walls could be obtained. The most extensive data were gathered during the Phase I tests when stagnation temperature and relative inlet size were varied. From these data the following empirical relationship between nozzle stagnation temperature, wall temperature, relative inlet size, and diffuser outlet temperature was derived.

$$\frac{T_o - T_{\text{exh}}}{T_o - T_{\text{wall}}} = 1.90 \left( \frac{1 - \frac{A_{\text{ns}}}{A_N}}{1 - \frac{A_i}{A_N}} \right) \quad 5.1$$

A fairly substantial difference can exist between nozzle stagnation temperature and bypass diffuser outlet stagnation temperature, (perhaps 1750°R with  $T_0 = 4000^\circ\text{R}$  and  $A_1/A_N = 0.48$ ). This is true because a large share of the flow entering the bypass diffuser is the cooled nozzle boundary layer.

#### 5.8 INLET DIFFUSER PERFORMANCE AND LIMIT OF SUBCRITICAL OPERATION

In this test program the inlet design was of secondary importance. Maximum inlet recovery was not sought in the design. For the Phase I tests the inlet configuration was optimized to the extent of applying the Oswatich analysis to obtain maximum recovery from the simple, two shock inlet design. The Phase II inlet design was not optimized in any way. It was merely designed to simulate the external lines of an external-internal compression inlet. The model did not have any internal compression.

Based upon its contraction, the Phase I inlet model had a potential pressure recovery of  $P_{t_2}/P_{t_0} = 0.043$  at the test Mach number. The maximum recovery actually obtained was 0.028, which corresponds to  $\eta_p = 0.65$ . The low value of  $\eta_p$  obtained is probably due to the lack of adequate constant area shockdown length within the inlet throat. Shock induced boundary layer separation is a problem in high Mach number inlets just as it is in wind tunnels, and adequate constant area length must be provided if the potential pressure recovery is going to be approached in practice.

The Phase II inlet model had a potential recovery of only  $P_{t_2}/P_{t_0} = 0.029$  because the inlet contraction was not as great as that of the Phase I model. The actual recovery of  $P_{t_2}/P_{t_0} = 0.017$  represented an  $\eta_p$  of .59. Here again the low value of  $\eta_p$  was probably due to inadequate constant area shockdown length.

During parts of a ramjets flight trajectory the inlet may operate subcritically, that is, with its terminal shock system partially or completely expelled. It is desirable that this aspect of engine operation be investigated on the ground in a

ramjet test facility. Consequently tests were made under the current contract to determine the permissible limit of subcritical operation. A throttling plug was driven into the inlet model exhaust tube to expell the terminal shock. For Phase I model configuration D, and Phase II configurations A and B, with which the tests were made, the facility model nozzle flow broke down at the first sign of spillage and no subcritical operation was possible. Model 1D was tested for limit of subcritical operation with  $\frac{A_{ST}}{A_N - A_i}$  equal to 1.25 and  $A_i/A_N = 0.43$ . This was a second

throat area 6% greater than the minimum starting and running throat area.

The limit of subcritical operation tests with IIA (open gap) model configuration were run at  $\frac{A_{ST}}{A_N - A_i} = 1.04$  and 1.14 or 24% and 36% greater than the minimum running throat area. For the IIB (closed gap) model,  $\frac{A_{ST}}{A_N - A_i} = 1.14$  was used, which is 78% greater than the minimum running second throat area for this configuration.

It is rather surprising that no subcritical operation was possible at the second throat settings used. Adequate overall pressure ratio was available. At the existing Mach number level, the initial shock wave in the inlet terminal shock system is probably an oblique shock followed by flow separation; so that, even with the shock expelled, the aerodynamic configuration would be fairly clean. Subcritical operation must be possible at some value of second throat area; however, a penalty in minimum operating pressure ratio will have to be paid since it apparently will be quite a bit larger than the minimum running second throat area. At  $\frac{A_{ST}}{A_N - A_i} = 1.4$  the minimum running pressure ratio was 270, compared to the value  $\lambda_{min} = 152$  at  $\frac{A_{ST}}{A_N - A_i} = 0.64$  for the Phase II

closed gap model.

The presence of the throttling plug in the inlet model during the Phase II tests seemed to have an adverse influence on minimum operating pressure ratio. The reason for this effect has not been determined. The pressure recovery data points obtained with the throttle installed are marked in figures 20 through 34 by a flag.

#### 5.9 NOZZLE MACH NUMBER DURING THE PHASE II TESTS

The Phase II inlet model was equipped with a pitot pressure tap at the tip of the spike. This tap provided an indication of nozzle centerline Mach number for each run. Since diffuser second throat area was changed by translating the inlet model axially, centerline Mach number data was obtained for a variety of axial locations. These data are plotted as a function of axial location in figure 46. The poor accuracy of the transducer used for this measurement is responsible for the scatter in the data. It is apparent, though, that the general level of Mach number found from these data compares well with the centerline Mach number found in the nozzle calibration.

### 6.0 EMPIRICAL EQUATIONS FOR ESTIMATION OF RAMJET FACILITY SECOND THROAT DIFFUSER PERFORMANCE

The test data obtained from the current program, along with existing data on wind tunnels and ramjet facility models, indicate that the efficiency of the pressure recovery process as defined herein is essentially independent of both aerodynamic and geometric parameters if adequate shockdown length is provided in the diffuser throat. The corrected efficiencies obtained from all ramjet facility model data analyzed range from  $\eta_p = 0.38$  to  $\eta_p = 0.70$ . If the Phase I  $A_i/A_N = 0.53$  data (high cowl lip angle and large inlet) are eliminated, the variation is from  $\eta_p = 0.50$  to  $\eta_p = 0.70$ . For those remaining configurations which had an adequate constant area second throat length, the corrected efficiency only varied from 0.60 to 0.70. The analyzed data included data from ramjet facility models designed for side inlets as well as for axisymmetric inlets. Consequently it seems reasonable that an efficiency of  $\eta_p = 0.65$  be assumed when estimating the pressure recovery of bypass flow second throat diffusers. This gives the following empirical equation for estimating running pressure recovery at high Mach numbers (see equation 4.9).

$$\frac{P_{T2}}{P_{T0}} = \frac{1.05}{\left(\frac{A_N}{A_{NT}}\right) \left(\frac{A_{NE}}{A_N}\right) \left(\frac{1 - A_i/A_N}{\frac{A_{NE}}{A_N} - \frac{A_i}{A_N}}\right) \left(\frac{A_{ST}}{A_N - A_i}\right)} \quad 6.1$$

Half of the parametric ratios which are required to solve for pressure recovery are geometric ratios apparent from the test setup ( $A_N/A_{NT}$  &  $A_i/A_N$ ). The ratio of effective to geometric nozzle exit area,  $A_{NE}/A_N$ , must be estimated for design of the facility nozzle, and the exact value will be obtained when the nozzle is calibrated. The diffuser contraction,  $A_{ST}/A_N - A_i$ , is the only

remaining ratio to be evaluated. Its minimum value will depend upon whether or not an adjustable diffuser is used.

For a fixed bypass flow diffuser the contraction is limited by the starting process area requirements. In section 5.4.3 it was concluded that the ideal one-dimensional estimate of minimum starting second throat area was reasonably accurate for high Mach number closed gap configurations ( $K_1 = 1.0$  in equation 4.13)

$$\left(\frac{A_{ST}}{A_N - A_i}\right)_{\text{MIN START}} = \frac{0.62 - \left(\frac{A_i}{A_i}\right)\left(\frac{A_i}{A_N}\right)}{1 - A_i/A_N} \quad 6.2$$

By substituting this in equation 6.1, an expression for running pressure recovery in high Mach number, fixed bypass diffuser, closed gap configurations is obtained.

$$\left(\frac{P_2}{P_0}\right)_{\text{MIN RUN FIXED DIFF}} = \frac{1.05}{\left(\frac{A_N}{A_{NT}}\right)\left(\frac{A_{NE}}{A_N}\right)\left(\frac{0.62 - \left(\frac{A_i}{A_i}\right)\left(\frac{A_i}{A_N}\right)}{1 - A_i/A_N}\right)} \quad 6.3$$

For open gap configurations, the minimum starting throat area obtained above should be multiplied by about 1.13, and the pressure recovery divided by this figure.

If an average  $K_2$  of 17.5 is assumed, an expression for minimum running second throat area can be obtained which is valid for adjustable diffuser, closed gap configurations (equation 4.14)

$$\left(\frac{A_{ST}}{A_N - A_i}\right)_{\text{MIN RUN ADJUSTABLE}} = \frac{17.5 \left\{ \frac{(P_2/P_1)_{0.2} + 1}{(P_2/P_1)_{\text{SEP}}} \right\} \left(1 - \frac{A_{NE}}{A_N}\right)}{\left\{ \left(\frac{A_N}{A_{NT}}\right)\left(\frac{A_{NE}}{A_N}\right) \right\}^{0.6} \left(1 - \frac{A_i}{A_N}\right)} \quad 6.4$$

This, in turn, can be substituted into 6.1 to give a relationship for estimating running pressure recovery for adjustable diffuser, closed gap arrangements.

6.5

$$\left(\frac{P_r}{P_{t0}}\right)_{\text{MIN RUN ADJUSTABLE}} = \frac{0.06}{\left\{ \left(\frac{A_N}{A_{NT}}\right) \left(\frac{A_{NS}}{A_N}\right) \right\}^{0.4} \left( \frac{\left(\frac{P_r}{P_t}\right)_{\text{RUN}} + 1}{\left(\frac{P_r}{P_t}\right)_{\text{START}}} \left(1 - \frac{A_{NS}}{A_N}\right) \right) \frac{A_{NS} - A_i}{A_N}}$$

A factor of roughly 1.25 should be used to correct running throat area and pressure recovery for the open gap configuration with moderate cowl lip angles.

Equations 6.3 and 6.5 above provide a handy means of estimating the bypass flow second throat diffuser pressure recovery for the running condition; and corrections are given so that estimates can be made for both open and closed gap configurations. For the open gap configuration, the apparent pressure recovery during starting can be as low as 67% of the running pressure recovery; while for the closed gap configuration, the starting recovery is about 90% of the running recovery. With these figures estimates of starting pressure recoveries can be made.

The basic equation for pressure recovery, 6.1, above should give an estimate of pressure recovery which is accurate to within 10% for well designed diffuser if the diffuser contraction is known. For moderate cowl lip angles (less than 20° say), equation 6.2 should be good to within 10% also, giving an estimate of pressure recovery for fixed diffusers which is within  $\pm 20\%$ . The limited data on adjustable bypass flow diffusers for ramjet facilities would indicate an accuracy of plus or minus 40% for equation 6.4 giving minimum running throat area, which means that estimates of running pressure recovery made using equation 6.5 could be off by as much as 50%. In reality, the error will probably be smaller than this if all of the values needed in the equation are known accurately (some of this data was lacking when the correlation of outside data was made to obtain  $K_2$ ). With the accuracy

obtainable using equations 6.3 and 6.5, it probably is not necessary to run special model tests to obtain pressure recovery data since the correlation included data from unusual configurations. Nevertheless, model tests may be necessary to develop the optimum diffuser contours for unusual inlet configurations.

The well versed reader will note that, although many of the explicit equations for pressure recovery, etc. are limited to high Mach numbers ( $5.0 < M < \infty$ ), accuracy can be obtained at lower Mach numbers by using the flow tables.

## 7.0 REMARKS CONCERNING THE USE OF BOUNDARY LAYER REMOVAL AND STARTING BLEED OFF

Although neither boundary layer removal nor starting bleed off was successfully attempted during the current test program, the test results shed some light on the practicability of such techniques. Both of these techniques have been proposed as possible ways of improving the running pressure recovery of the bypass flow second throat diffuser to lower the overall pumping requirements.

Boundary layer removal would have three effects at most. First of all it might improve the efficiency of the recovery process in the second throat diffuser. For well designed diffusers having corrected efficiencies approaching 0.65 without removal, the efficiency might be increased to 0.90 by such removal. Secondly, for a given diffuser throat area, removing the boundary layer actually reduces the potential recovery since it increases the area ratio through which the flow is expanded before shutdown. Finally, and perhaps most significant, boundary layer removal should permit considerably more diffuser contraction after starting. To take advantage of this, though, an adjustable diffuser is necessary. If an adjustable diffuser is used, significant improvements in bypass diffuser pressure recovery can undoubtedly be obtained (reference 3). The real question, though, is whether the overall pumping requirements are reduced by boundary layer removal. To check this, an analysis was made of the effect of boundary layer removal on pressure recovery, assuming that the removal of the boundary layer resulted primarily in reduced boundary layer displacement thickness and consequently a lower minimum running diffuser throat area. The results indicated that, although the pumping requirements downstream of the bypass flow second throat diffuser were reduced, this reduction was more than offset by the pumping requirements of the boundary layer removal.

Starting bleed off was discussed briefly in section 2.5 as a means of starting the facility with the diffuser throat set at

minimum running area. In order for this to have any meaning at all, there has to be a difference between minimum running and minimum starting diffuser second throat area. With the Phase I, high cowl angle configuration there was no difference between starting and running throat area, so a starting bleed off system would have proven useless. With the Phase II model it was possible to contract the diffuser after starting so one might expect some advantage of bleed off, however, certain aspects of the problem indicate that the value of a starting bleed off system may be questionable even with moderate cowl angles. To accomplish flow removal it is necessary to have a gap at the nozzle exit. During the tests it was found that the minimum running throat area with the open gap was larger than the minimum starting area with the closed gap. Consequently the minimum running pressure ratio with a fixed diffuser designed for starting would be lower than the minimum running pressure with a diffuser set at minimum running area and having a starting bleed off system, unless some method were available for closing the bleed gap after starting.

## 8.0 CONCLUSIONS

1. For well designed bypass flow second throat diffusers, the efficiency of the pressure recovery process, as defined herein, is relatively insensitive to stagnation temperature, Reynolds number, and changes in inlet and diffuser entrance geometry ("well designed diffusers" refers to those with adequate constant area shockdown length).
2. The test variables affected pressure recovery primarily through their influence on the area ratio through which the bypass flow expanded before shockdown. This effect involved the portion of the total flow entering the bypass diffuser and the geometric contraction which could be applied to the flow in the diffuser ( $A_{byp}^* A_{ST}$ ).
3. The influence of inlet throat size,  $A_i^*$ , and inlet geometric capture area,  $A_i$ , on minimum starting diffuser throat can be predicted reasonably accurately by using one-dimensional theory (equation 4.12) .
4. It appears that an equation which accounts for nozzle boundary layer displacement thickness, nozzle expansion ratio, and the strength of model induced disturbances can be used to correlate minimum running diffuser throat area, (equation 4.14).
5. Reduction of the cowl flare angle from  $30^\circ$  to  $15^\circ$  between the Phase I and II models had the largest affect on pressure recovery of any of the test variables and resulted in an increase in pressure recovery from 37% of normal shock to 65% of normal shock. The increase in permissible diffuser contraction (reduced minimum running throat area) was responsible for the improved pressure recovery.
6. For both the Phase I and Phase II models, leaving an open gap between the nozzle exit and diffuser pickup resulted in an increase in both minimum starting and minimum running throat area with a consequent decrease in maximum pressure recovery.
7. From the Phase II data it appears that the starting pressure ratios for the open gap are considerably (1.5 times) higher

than running pressure ratio while the difference is not as great with the closed gap.

8. With both the Phase I and Phase II models flow broke down at the first sign of inlet spillage for all diffuser second throat settings tested, i.e. subcritical operation was not possible.
9. In the light of the test results, there appears to be little or no value in either boundary layer removal or starting bleed off.
10. Further improvements in diffuser corrected efficiency may be obtained by increasing the constant area shockdown length in the diffuser.

#### 9.0 RECOMMENDATIONS

1. Additional tests should be made with the low cowl lip angle and a larger inlet to nozzle exit area ratio
2. Additional tests should be made to better define the influence of diffuser second throat constant area length

## REFERENCES

1. Anderson, D.E., "The Effect of Engine Size on Free-jet Test Cell Performance," AEDC TN-57-19, November 1957
2. Anderson, D.E., "Performance of a Free-jet Diffuser with Small Inlet and Throat Size," AEDC TN-57-20, November 1957
3. Latvala, E.K., "Performance of a Scale Model Free-jet Engine Test Installation Incorporating Diffusers with Square Outer Fairings," AEDC TN-58-100, February 1959
4. Staniforth, R., "Supersonic Tunnel Design for Testing Engine Intakes," ARC R&M 3212, NGTE R229, or ARC 20, 758, Oct. 1958
5. Feldmann, Gafarian, and Bitondo, "Aerodynamic Research for the Design of Altitude Free-jet Test Sections for Ramjet Test Facilities," North American Aviation Report AL-1265, May 1951
6. Feldmann, "Aerodynamic Research for the Design of Altitude Free-jet Test Facilities for the Investigation of Side Inlet Ramjets," North American Aviation Report AL-1428
7. Hunczak, "An Investigation at Mach Numbers 2.98 and 2.18 of Axially Symmetric Free Jet Diffusion with a Ramjet Engine," NACA RM E51 L24, February 1952
8. Herman, Thompson, and Melnik, "Theoretical and Experimental Investigation of a Supersonic Conical Inlet Model with Shroud Type Diffuser in a Free Jet Tunnel", University of Minnesota, Rosemount Research Laboratory, Research Report 154, November 1958
9. Grunnet, J.L., "Model Studies of the Free-jet Altitude Test Facility for the G-38 (D-53) Engine" Report written under contract to Wright Aeronautical Division, Curtiss-Wright Corporation, April 1957
10. Fasken, S.D., "Design of Ramjet Engine Ground Test Facilities," Institute of the Aeronautical Sciences Preprint No. 841, July 1958
11. Lee, J.D., "Axisymmetric Nozzles for Hypersonic Flows," WADC TN 59-228, June 1959

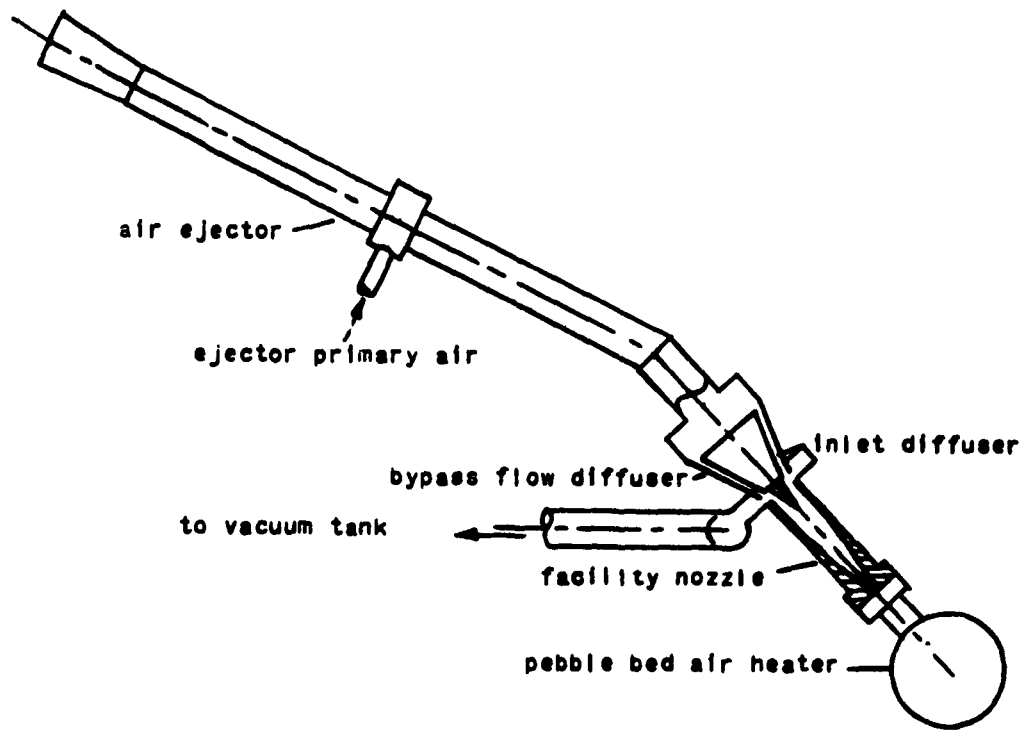
12. Bartz, D.R., "A Simple Equation for Rapid Estimation of Rocket Nozzle Convective Heat Transfer Coefficients," *Jet Propulsion Magazine*, January 1957
13. McLafferty, G.H., "Hypersonic Inlet Studies at UAC Research Laboratories," Combustion and Propulsion, Fourth AGARD Colloquium, April 1960 (Pergamon Press 1961)
14. Hermann "Supersonic Inlet Diffusers and Introduction to Internal Aerodynamics," Honeywell, 1956
15. Eckert and Drake, "Heat and Mass Transfer," 2nd Edition, McGraw Hill, 1959
16. Ames Staff, "Equations, Tables, and Charts for Compressible Flow," NACA Report 1135, 1953
17. Wegener and Lobb, "NOL Hypersonic Tunnel No. 4 Results II: Diffuser Investigation," NAVORD Report 2376, May 1952
18. Schurmeier, "Design and Operation of a Continuous-Flow Hypersonic Wind Tunnel Using a Two-Dimensional Nozzle," AGARDograph 38, May 1959
19. Yu, Ying-Nien, "A Summary of Design Techniques for Axisymmetric Hypersonic Wind Tunnels," AGARDograph 35, November 1958
20. Church, Jones, and Quentmeyer, "Performance Evaluation of Fixed and Variable-Area Rocket Exhaust Diffusers Using Single and Clustered Nozzles with and without Gimbaling," NASA TN-D-1306, July 1962

TABLE I INSTRUMENTATION

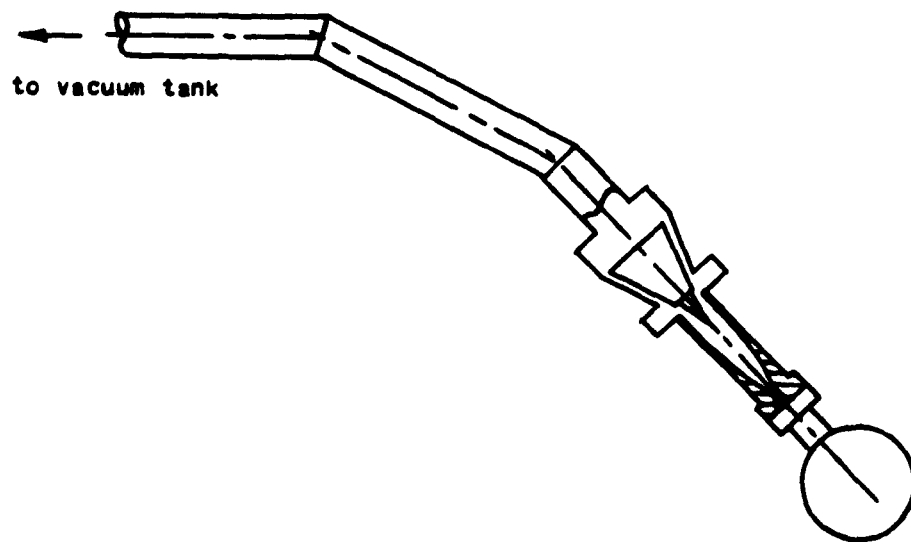
Phase I Instrumentation		<u>Instrument</u>	<u>Manufacturer</u>	<u>Range</u>	<u>Accuracy Within</u>
<u>Measurement</u>		gauge	Helicoid	0-2000 psig	± 5 psi
nozzle stag press		unshielded T-C			
nozzle stag temp		transducer	Hastings-Raydist	0-70 mm hga	± 2% of reading
nozzle exit static		transducer	"	"	"
bypass bleed		transducer	"	"	"
plenum press		transducer	"	"	"
bypass pipe		transducer	"	"	"
stagn pressure		transducer	"	"	"
bypass pipe		transducer	"	"	"
static pressure		transducer	"	"	"
inlet spike		transducer	Consol. Electrodyn	± 25 psig	± 0.25 psi
static pressure		transducer	Statham	0-100 psig	± 0.30 psi
inlet model		transducer	Consol. Electrodyn	± 25 psig	± 0.25 psi
stagn pressure		transducer	Statham	0-50 psia	± 0.50 psi
inlet meter		transducer	Statham	0-50 psia	± 0.50 psi
static pressure		transducer	Rosemount Eng.	3000° R	± 1%
bypass diffuser		manometer		90 hg	± 0.05 hg
static pressure		manometer		90 hg	± 0.05 hg
bypass diffuser		transducer	Consol. Electrodyn	0-50 psia	± 0.50 psi
stagn press 1		transducer	Statham	0-50 psia	± 0.50 psi
bypass diffuser		transducer	Statham	0-50 psia	± 0.50 psi
stagn press 2		transducer	Statham	0-50 psia	± 0.50 psi
bypass diffuser		shielded T-C	Rosemount Eng.	3000° R	± 1%
stagn temp		shielded T-C	Rosemount Eng.	3000° R	± 1%

TABLE I (CONTINUED)

Phase II Instrumentation		<u>Instrument</u>	<u>Manufacturer</u>	<u>Range</u>	<u>Accuracy Within</u>
<u>Measurement</u>		gauge	Helicoid	0-2000 psig	± 5 psi
nozzle stagn press		unshielded T-C			
nozzle stagn temp		transducer	Hastings Raydist	0-70 mm hg	± 2% of reading
nozzle exit static press		transducer	Statham	0-100 psig	± 0.50 psig
inlet spike stagn press		transducer	Statham	0-5 psia	± 0.05 psia
inlet spike static press		transducer	Statham	0-50 psia	± 0.50 psi
inlet model stagn press		transducer	Statham	0-50 psia	± 0.50 psi
inlet meter static press		transducer	Statham	0-50 psia	± 0.50 psi
bypass diff static press		manometer		90 hg	± 0.05 hg
bypass diff stagn press 1		transducer	Statham	± 25 psig	± 0.25 psi
bypass diff stagn press 2		transducer	Consol Electrodyn	± 25 psig	± 0.25 psi
bypass diff stagn temp		shielded T-C	Rosemount Eng.	3000° R	± 1%

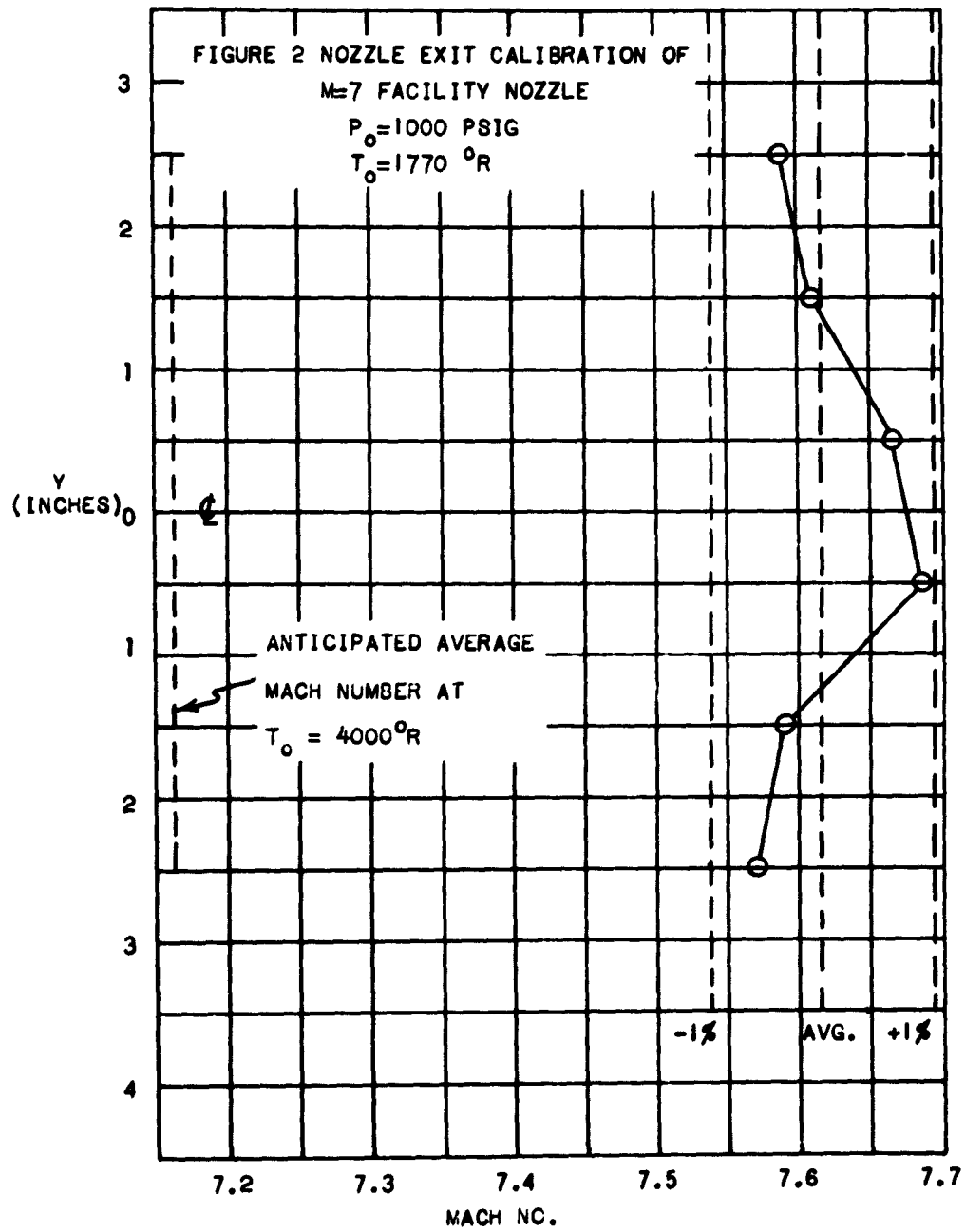


A. Configuration Used for Initial Tests



B. Configuration Used for Majority of Tests

FIGURE 1 GENERAL LAYOUT OF FACILITY MODEL TEST SETUP



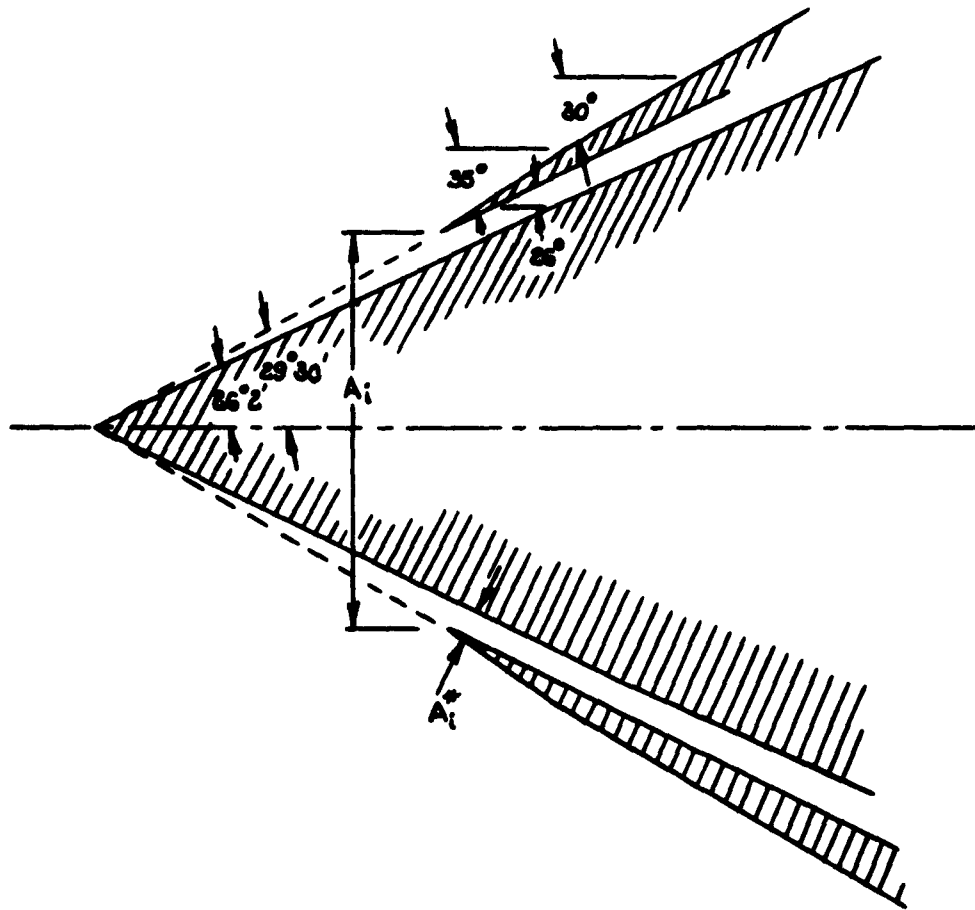


FIGURE 3 PHASE I INLET CONFIGURATION

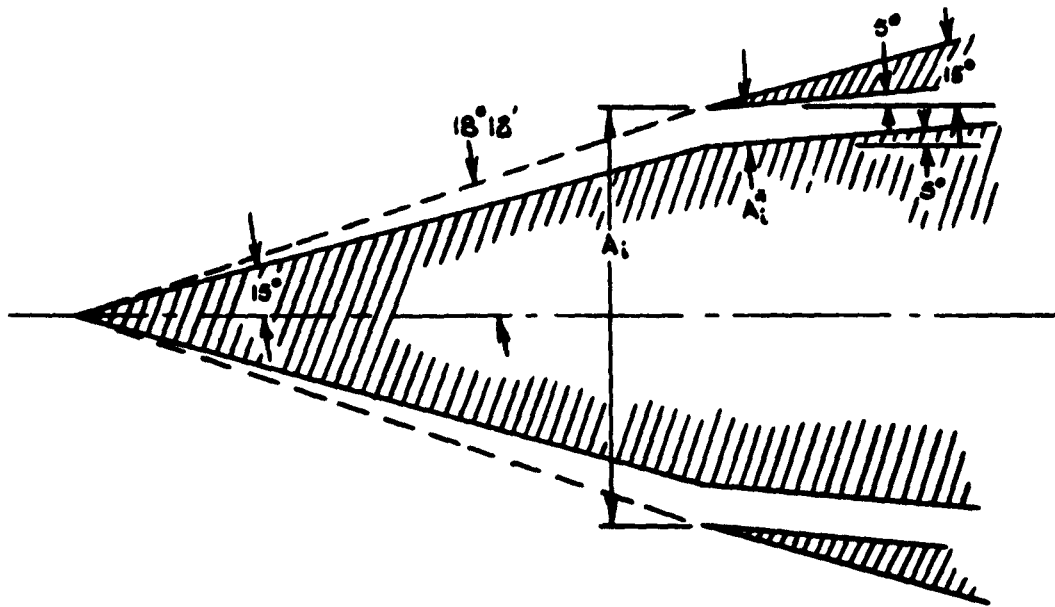
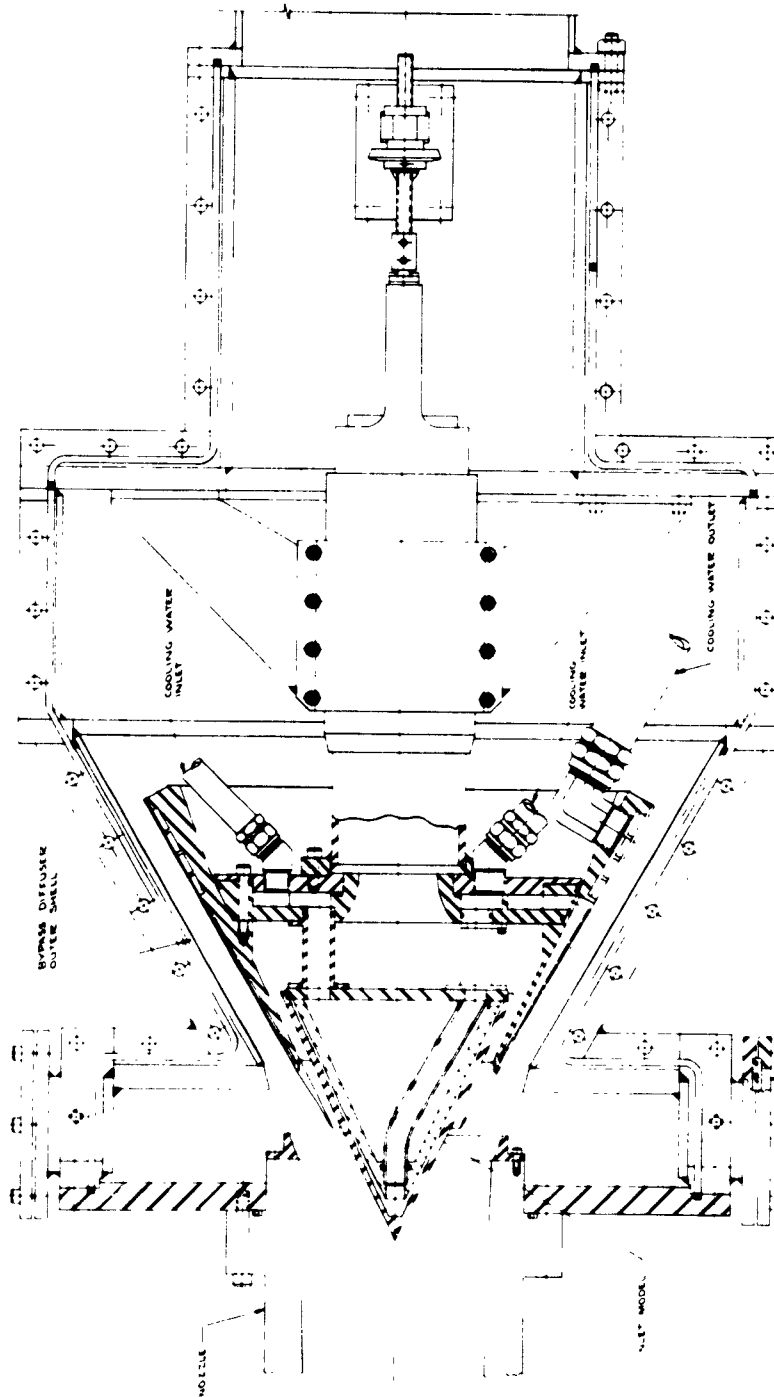


FIGURE 4 PHASE II INLET CONFIGURATION



1/4" = 1' - WINDOW

FIGURE 5 PHASE I FACILITY MODEL CONSTRUCTION

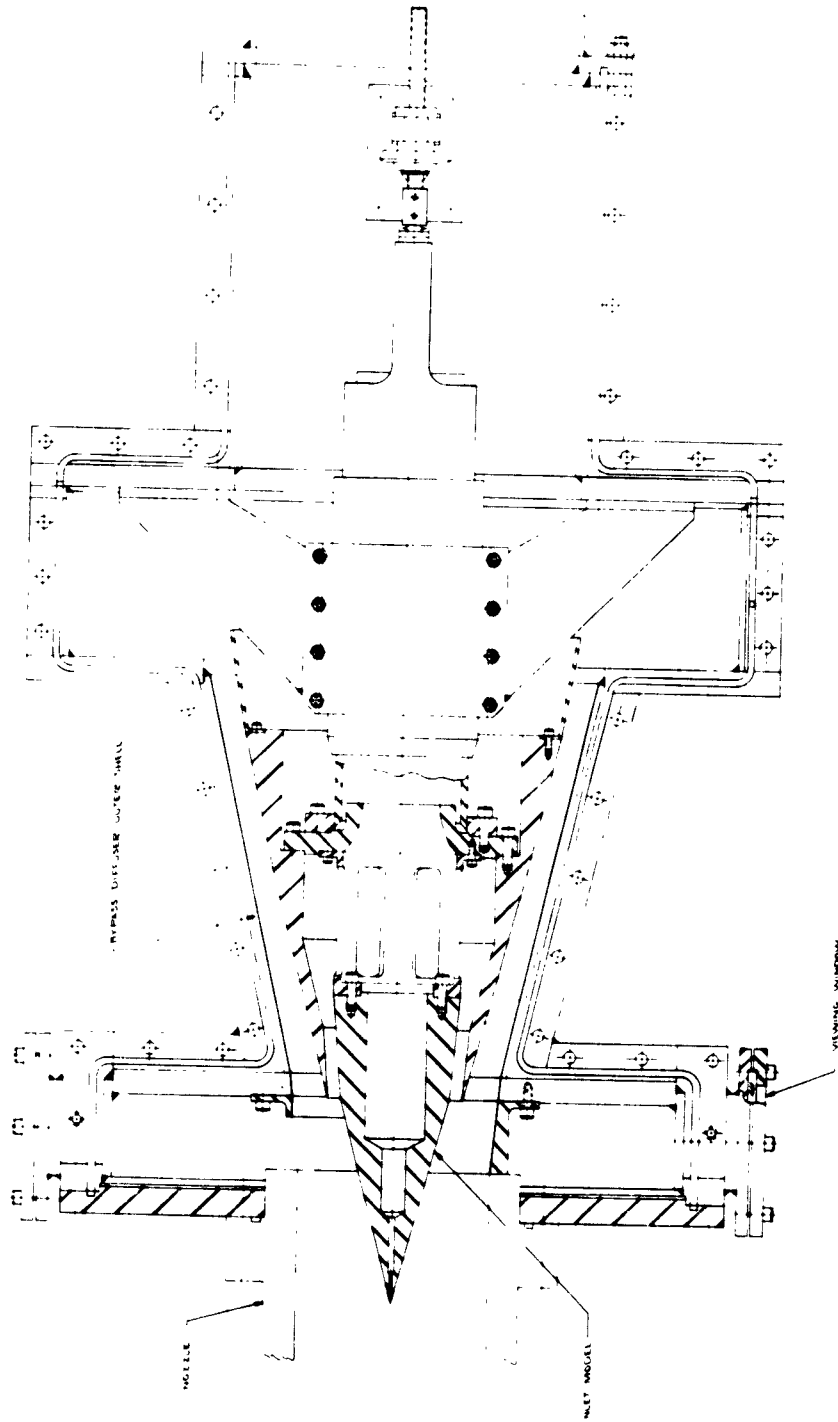
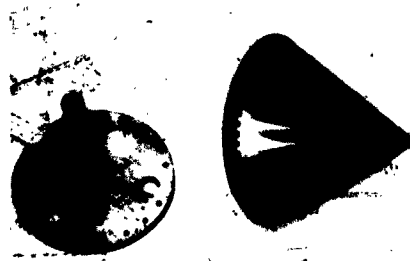


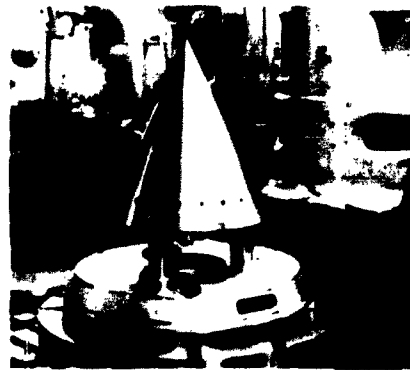
FIGURE 6 PHASE II FACILITY MODEL CONSTRUCTION



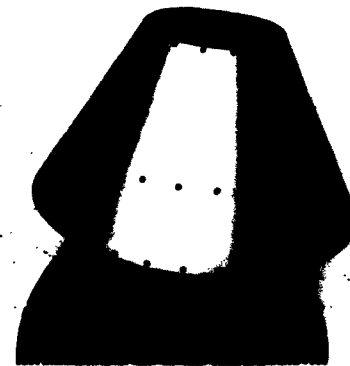
SPIKE



BULKHEAD



SPIKE-BULKHEAD ASSY.



COWL

PHASE I INLET MODEL CONSTRUCTION

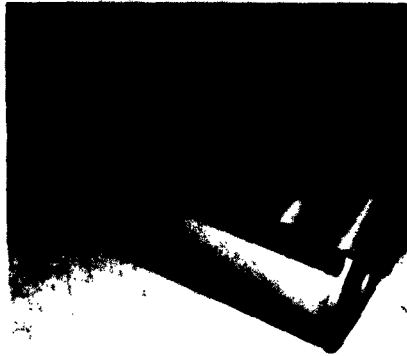


PHASE I INLET IN FACILITY



PHASE II INLET IN FACILITY

FIGURE 7 PHOTOS OF PHASE I AND PHASE II INLET MODELS



QUICK OPENING VALVE



INITIAL PHASE I SETUP



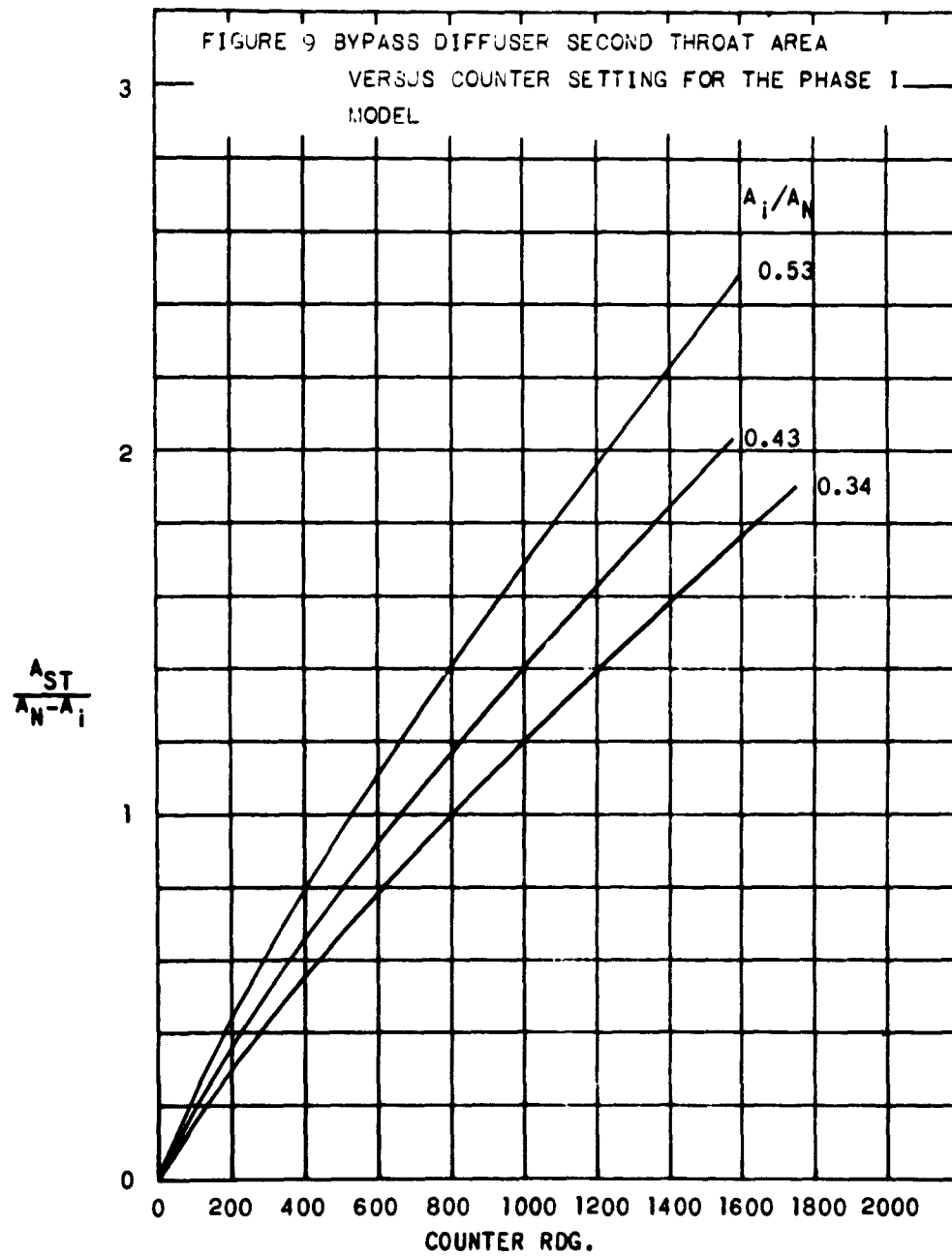
STANDARD PHASE I FACILITY MODEL CONFIGURATION

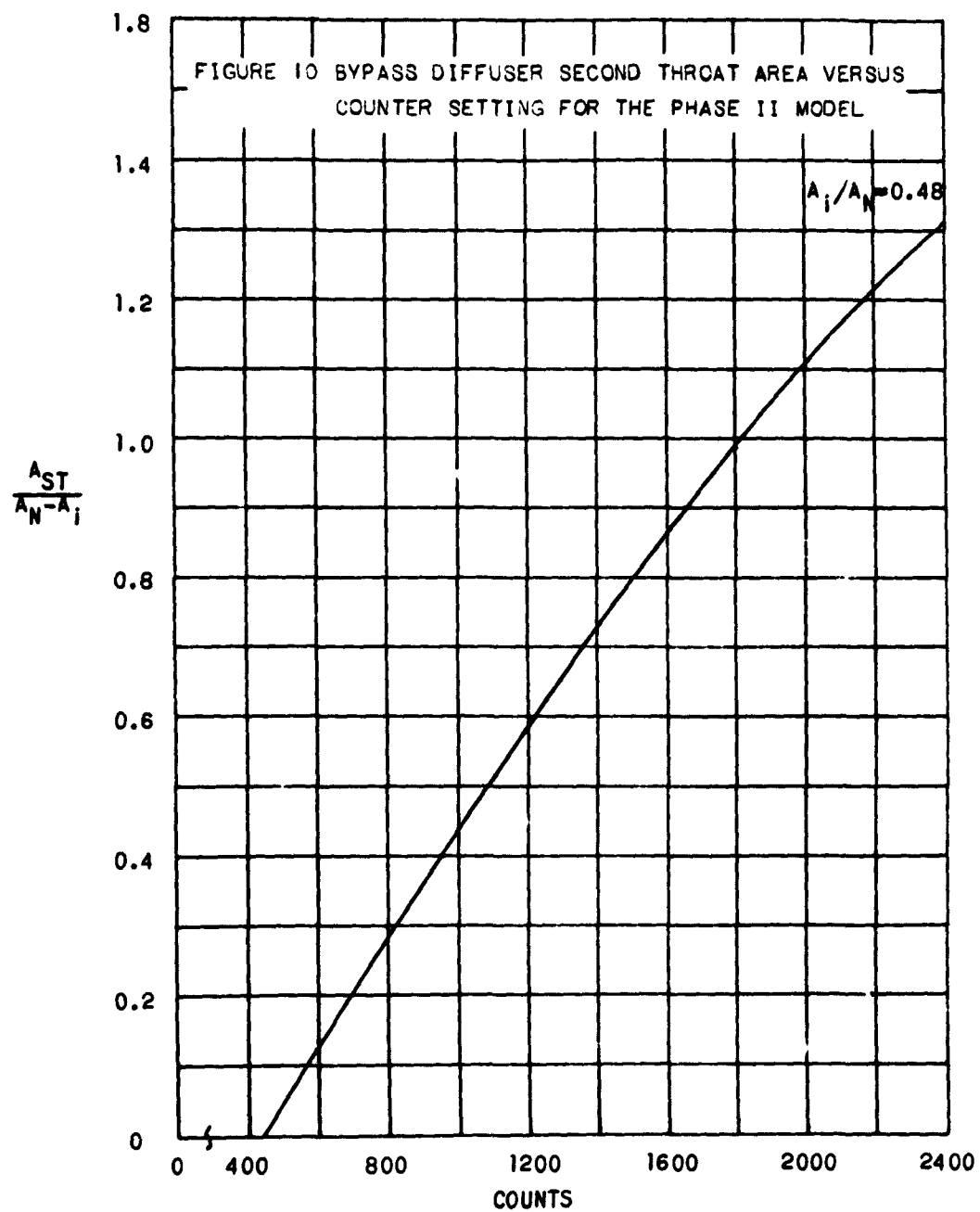


PHASE II FACILITY CONFIGURATION



FIGURE 8 PHOTOS OF PHASE I AND PHASE II FACILITY MODELS





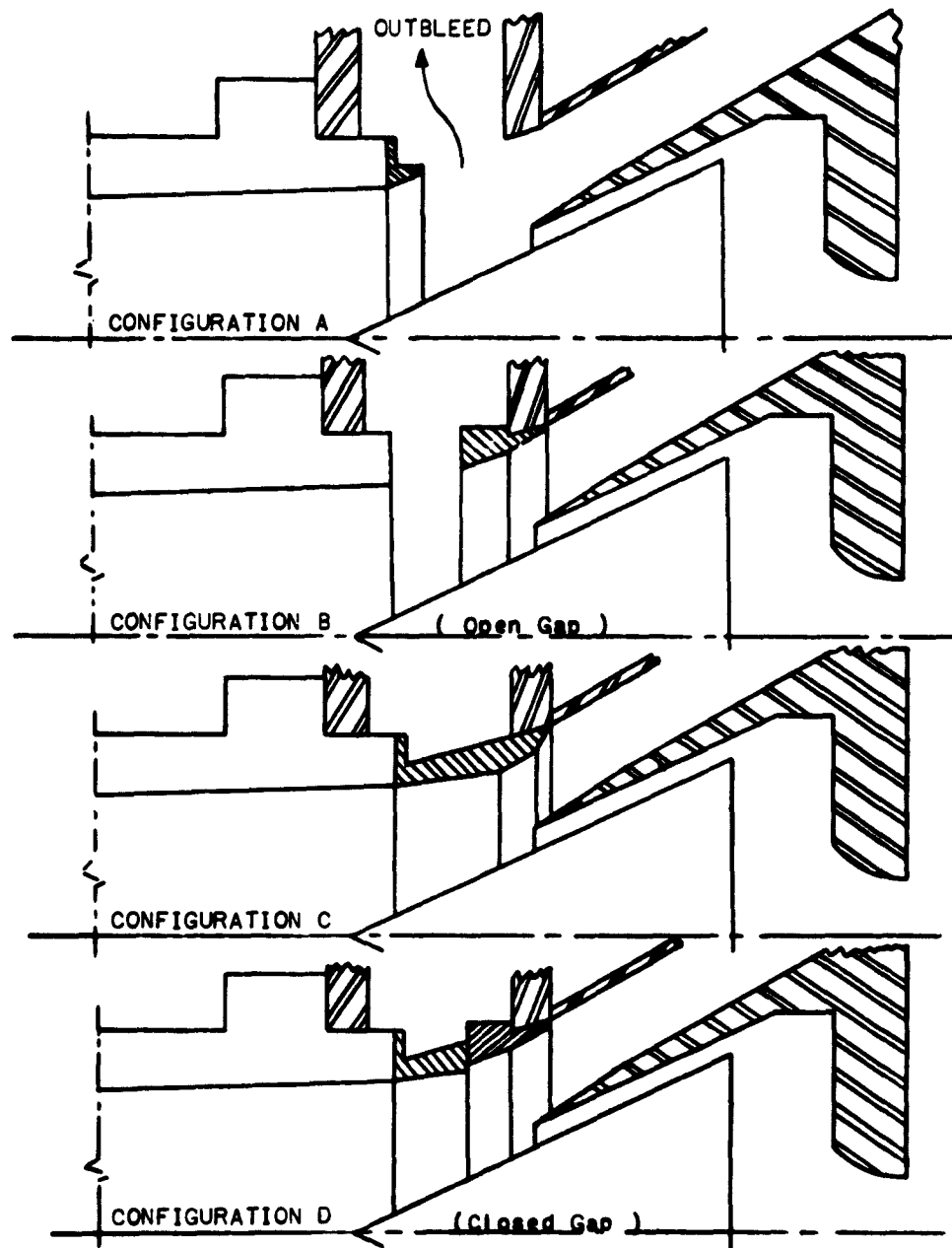
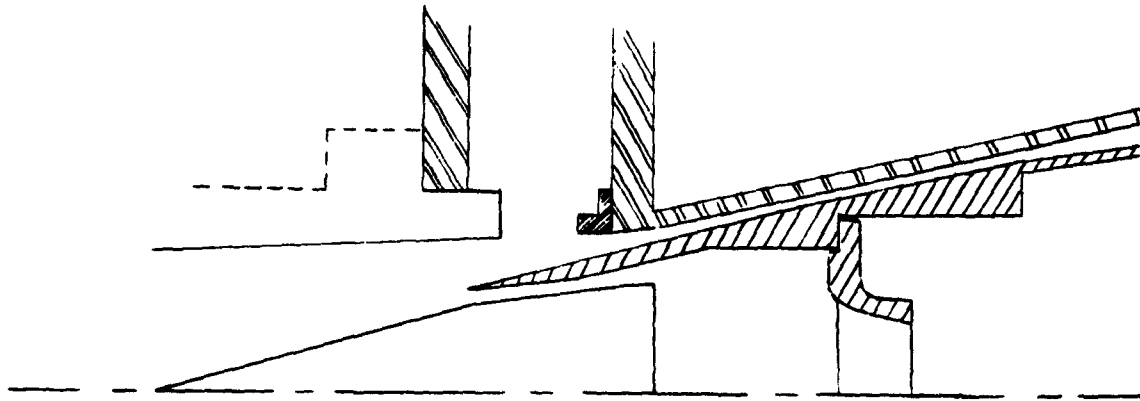
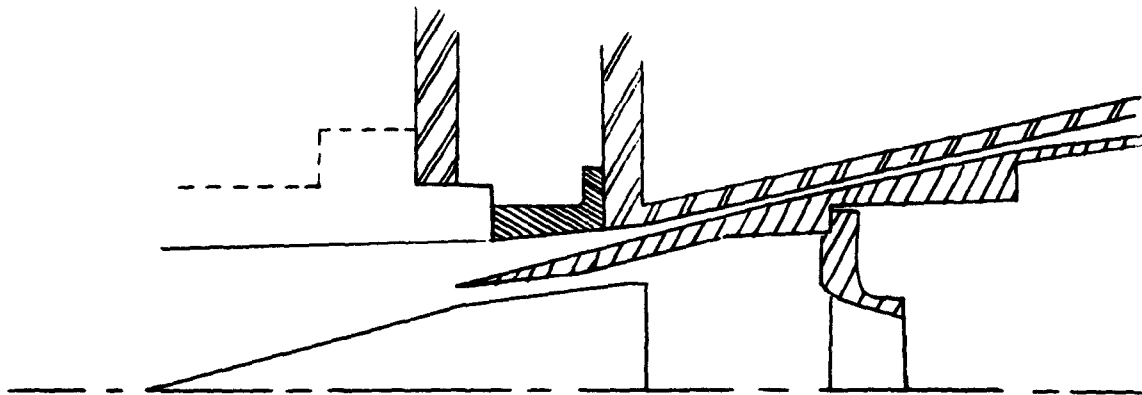


FIGURE 11 DIFFUSER ENTRANCE CONFIGURATIONS TESTED WITH THE PHASE I MODEL



Configuration A. Open Gap



Configuration B. Closed Gap

FIGURE 12 DIFFUSER ENTRANCE CONFIGURATIONS TESTED WITH THE PHASE II MODEL

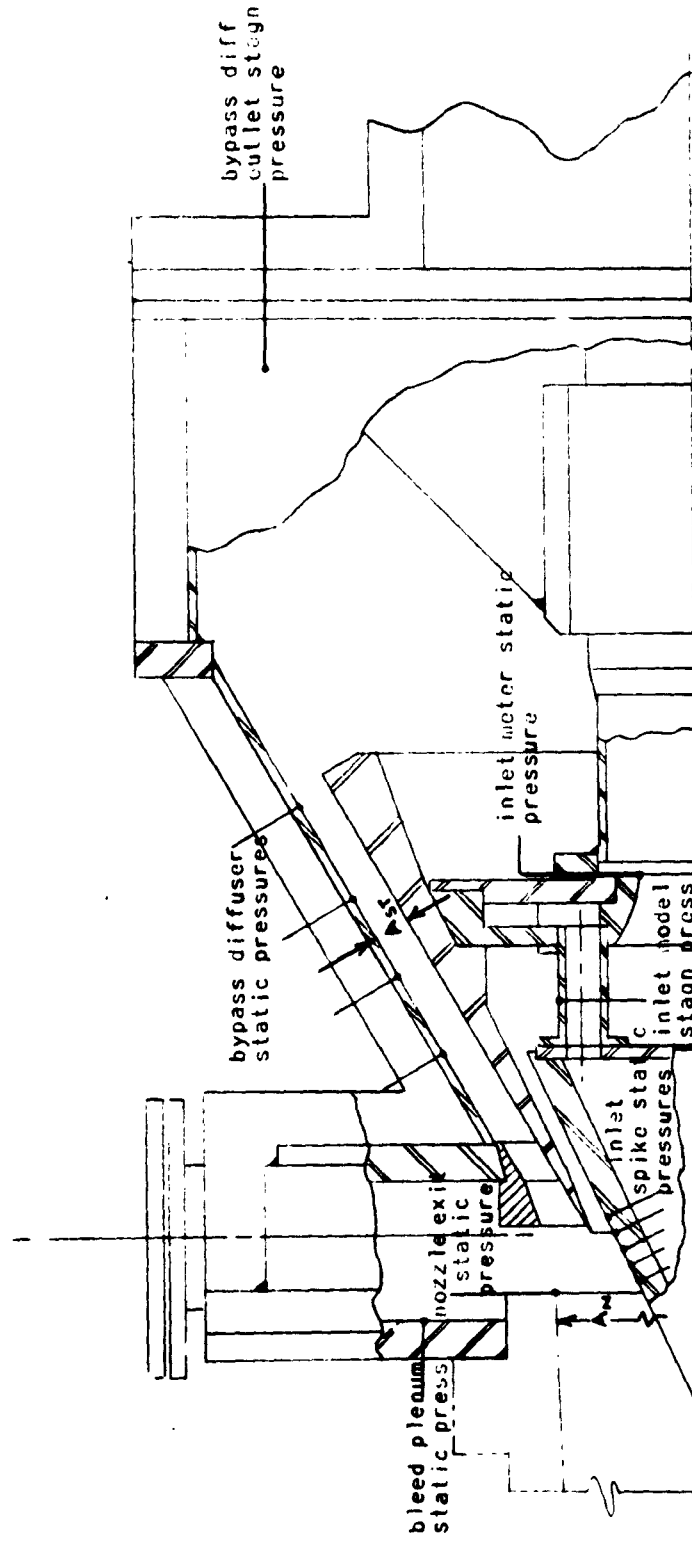


FIGURE 13 THE LOCATION OF PRESSURE TAPS ON THE PHASE I MODEL

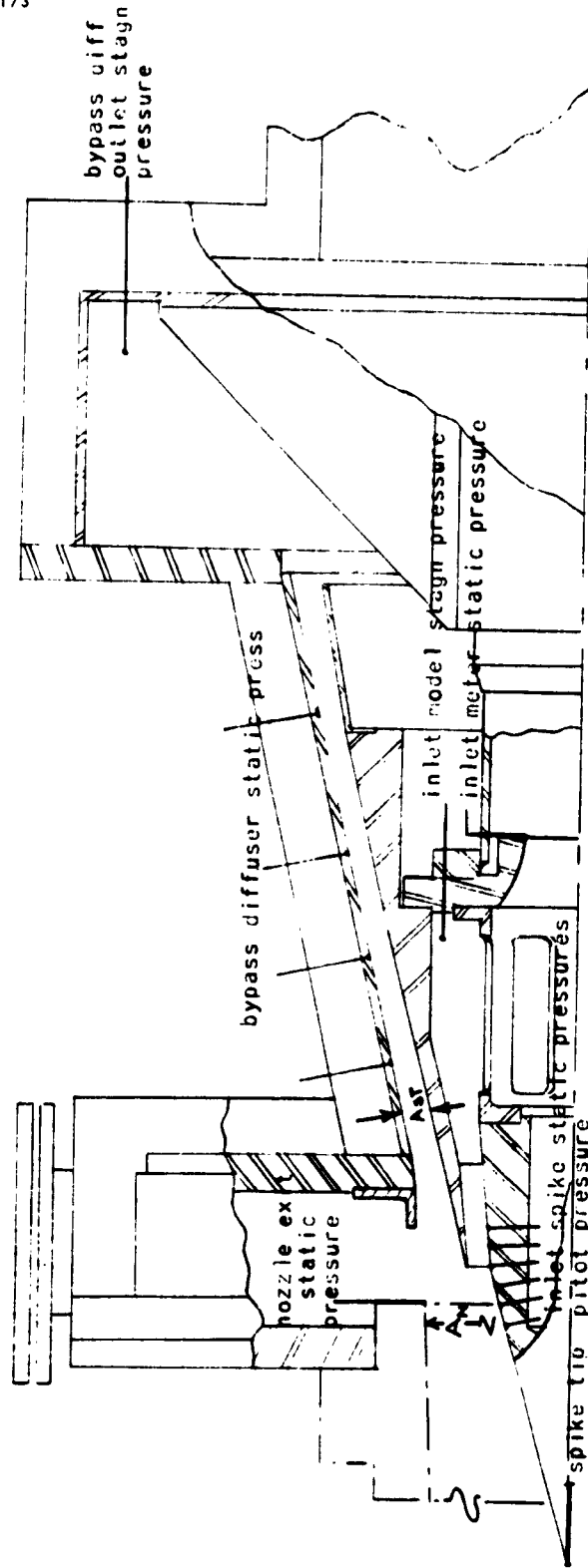
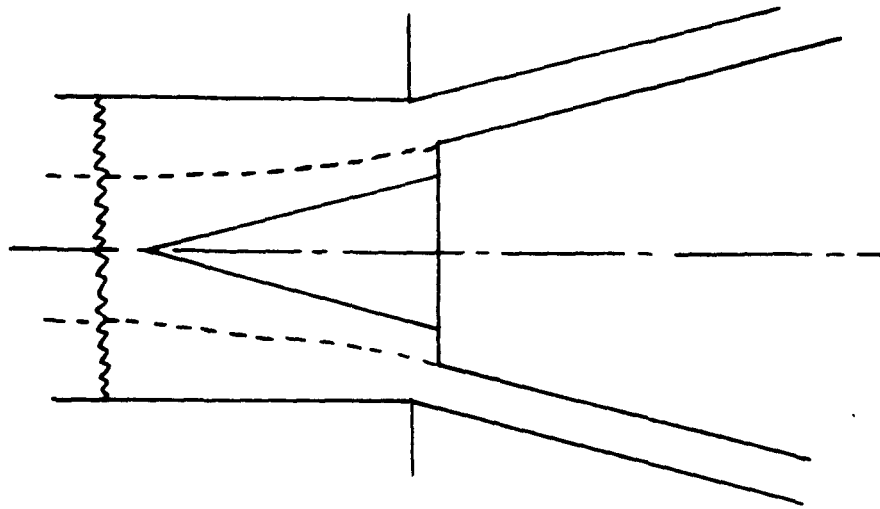
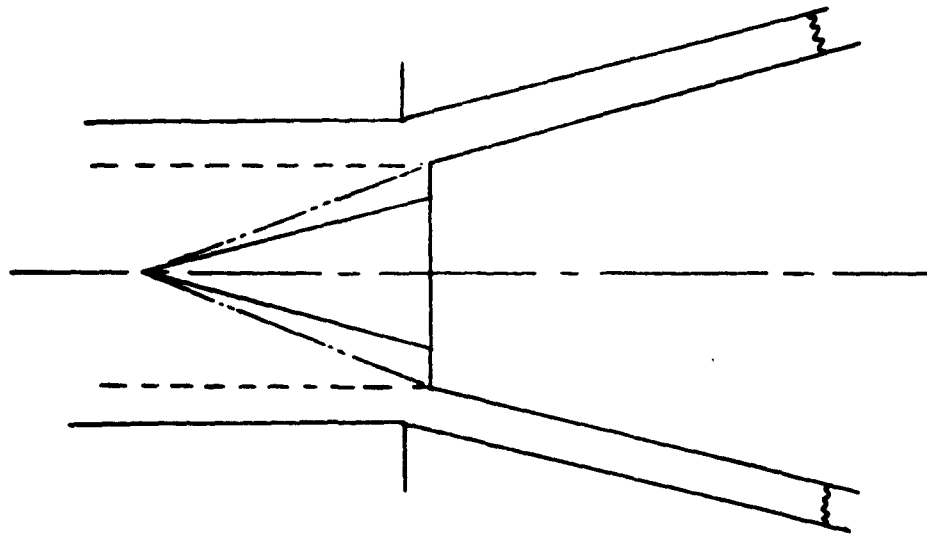


FIGURE 14 THE LOCATION OF PRESSURE TAPS ON THE PHASE II MODEL

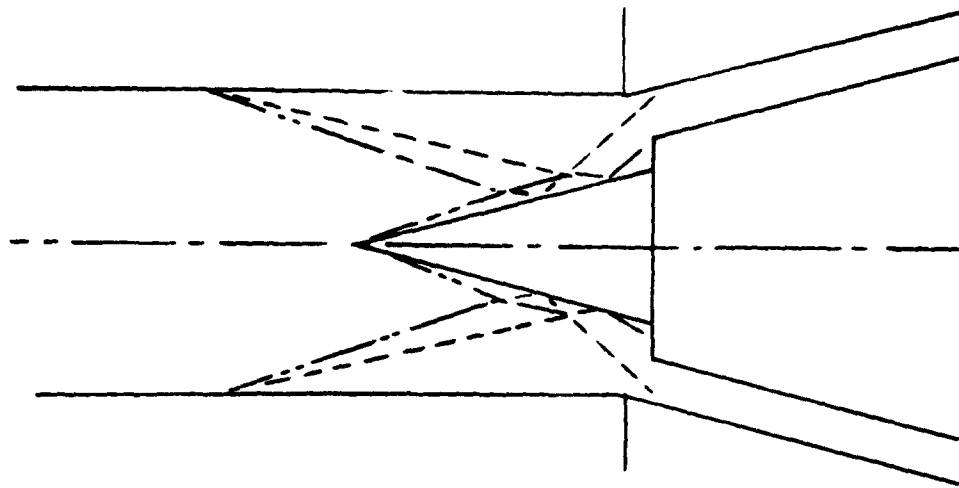


Before Starting

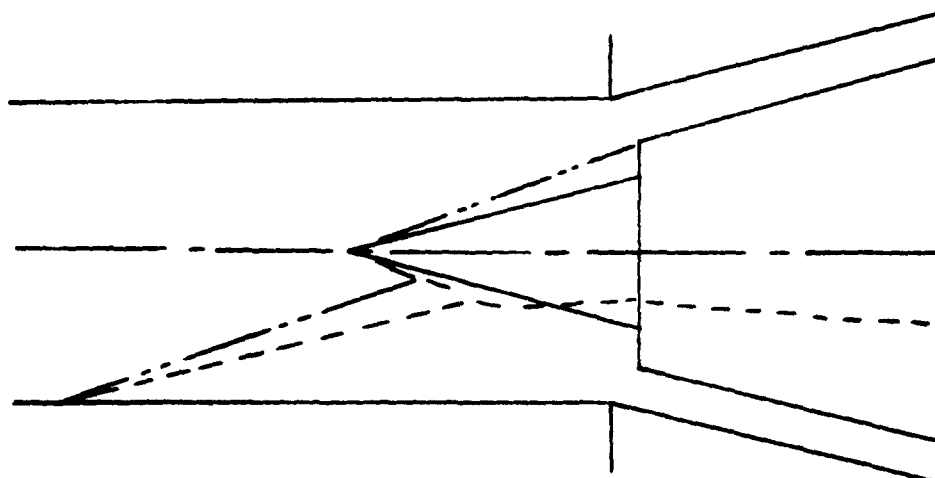


After Starting

FIGURE 15 DESCRIPTION OF THE STARTING PROCESS WITH A NORMAL SHOCK

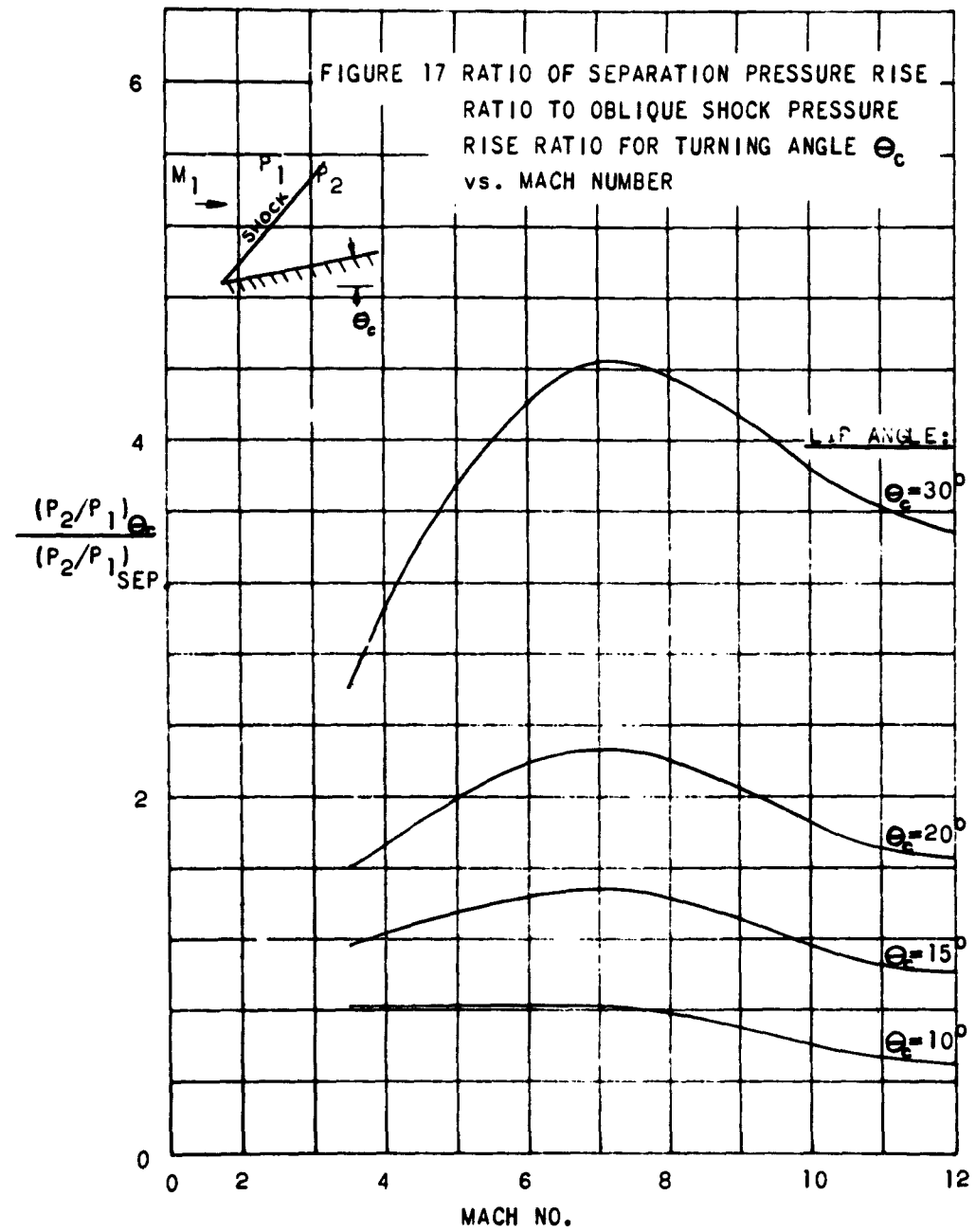


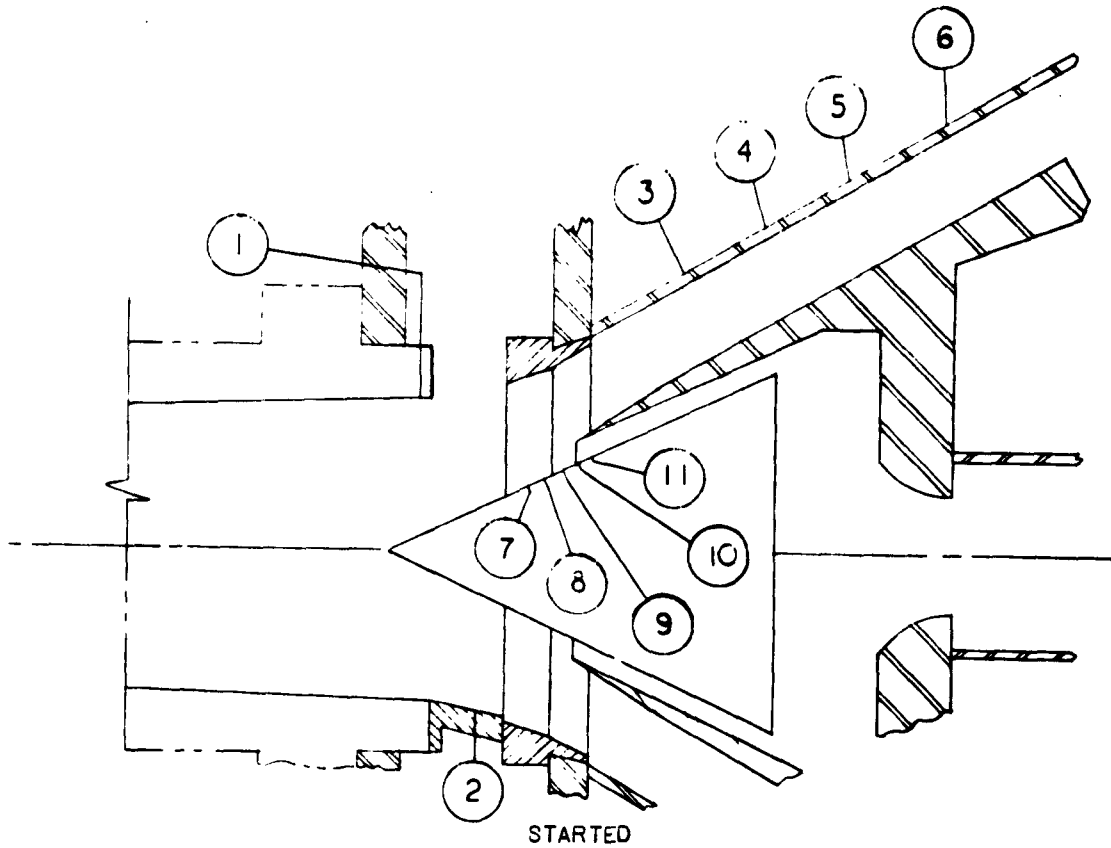
A. Jet Centered



B. Jet Flopped to One Side

FIGURE 16 DESCRIPTION OF THE STARTING PROCESS WITH FLOW SEPARATION IN THE NOZZLE



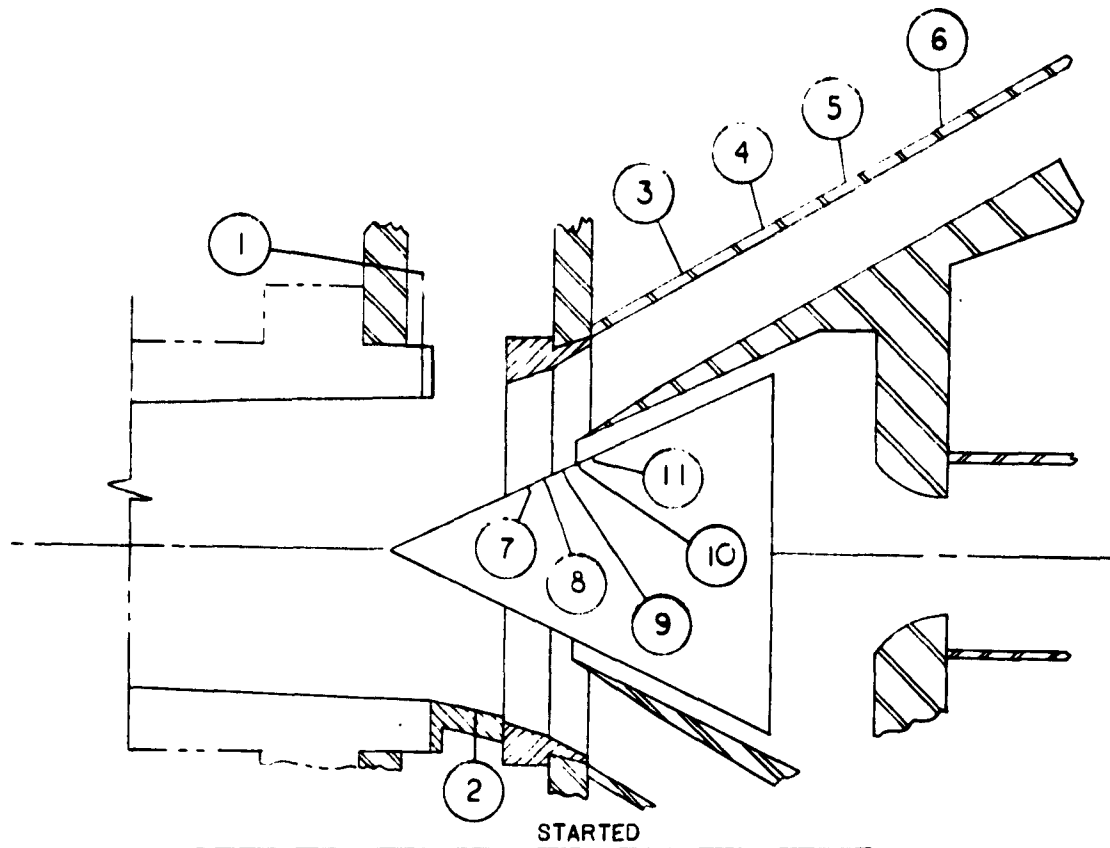


TAP	OPEN GAP		CLOSED GAP	
	UNSTARTED	STARTED	$T_o = 2500^{\circ}R$	$T_o = 3500^{\circ}R$
1	0.00212	0.000552	0.00090	0.00064
2			0.00199	0.00084
3	0.000676	0.00610	0.00099	0.00036
4	0.000574	0.000957	0.00146	0.00070
5	0.000977	0.000937	0.00155	0.00094
6	0.00158	0.00122	0.00168	0.00128
7	0.00414	0.00224	0.00360	0.00301
8	0.00434	0.00224	0.00360	0.00296
9	0.00530	0.00304	0.00409	0.00340
10	0.00404	0.00457	0.00516	0.00513
11	0.00311	0.00224	0.00360	0.00274

LEADER THROAT CLOSED

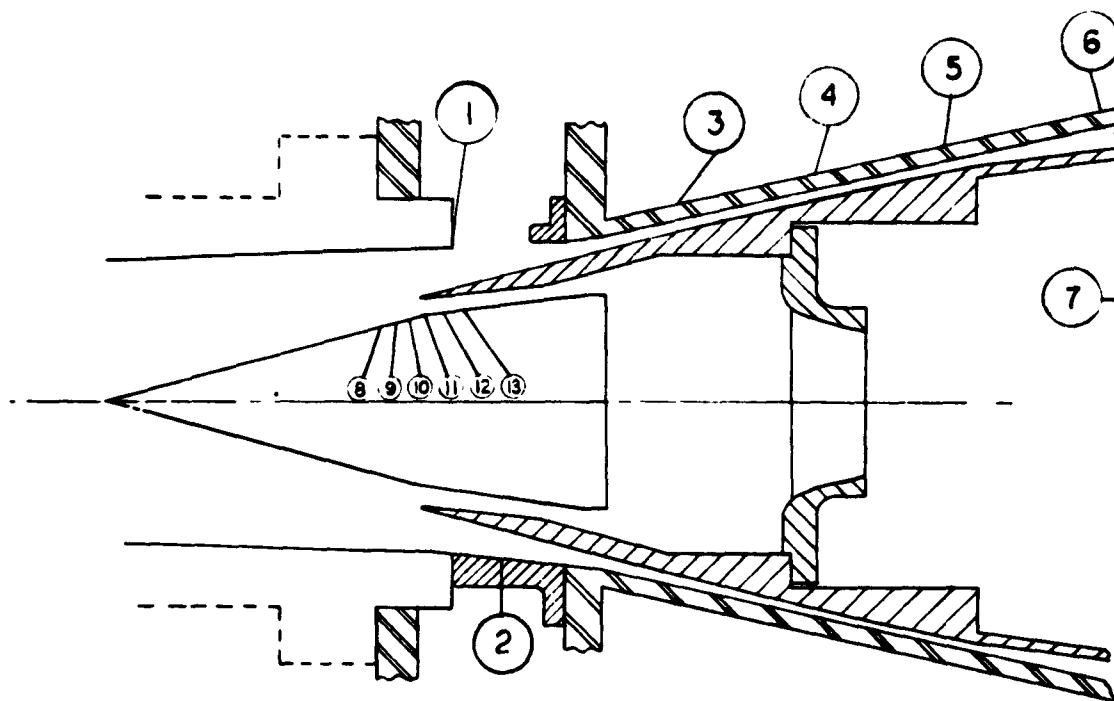
} INSIDE COWL

FIGURE 18 PHASE I MODEL PRESSURE DISTRIBUTION,  $A_1/A_N = 0.34$



TAP	$A_i/A_N = 0.44$		$A_i/A_N = 0.53$	
	$T_o = 2500^\circ R$	$T_o = 3500^\circ R$	$T_o = 2500^\circ R$	$T_o = 3500^\circ R$
1	0.00068	0.00059	0.00054	0.000335
2	0.00096	0.00196	0.00073	0.00073
3	0.00055	0.00034	0.00054	0.00036
4	0.00096	0.00073	0.00093	0.00073
5	0.00140	0.00116	0.00122	0.00097
6	0.00176	0.00158	0.00137	0.00121
7	0.00384	0.00325	0.00374	0.00321
8	0.00376	0.00316	0.00360	0.00326
9	0.00450	0.00320	0.00360	0.00326
10	0.00471	0.00409	0.00374	0.00331
11	0.00640	0.00611	0.00458	0.00331

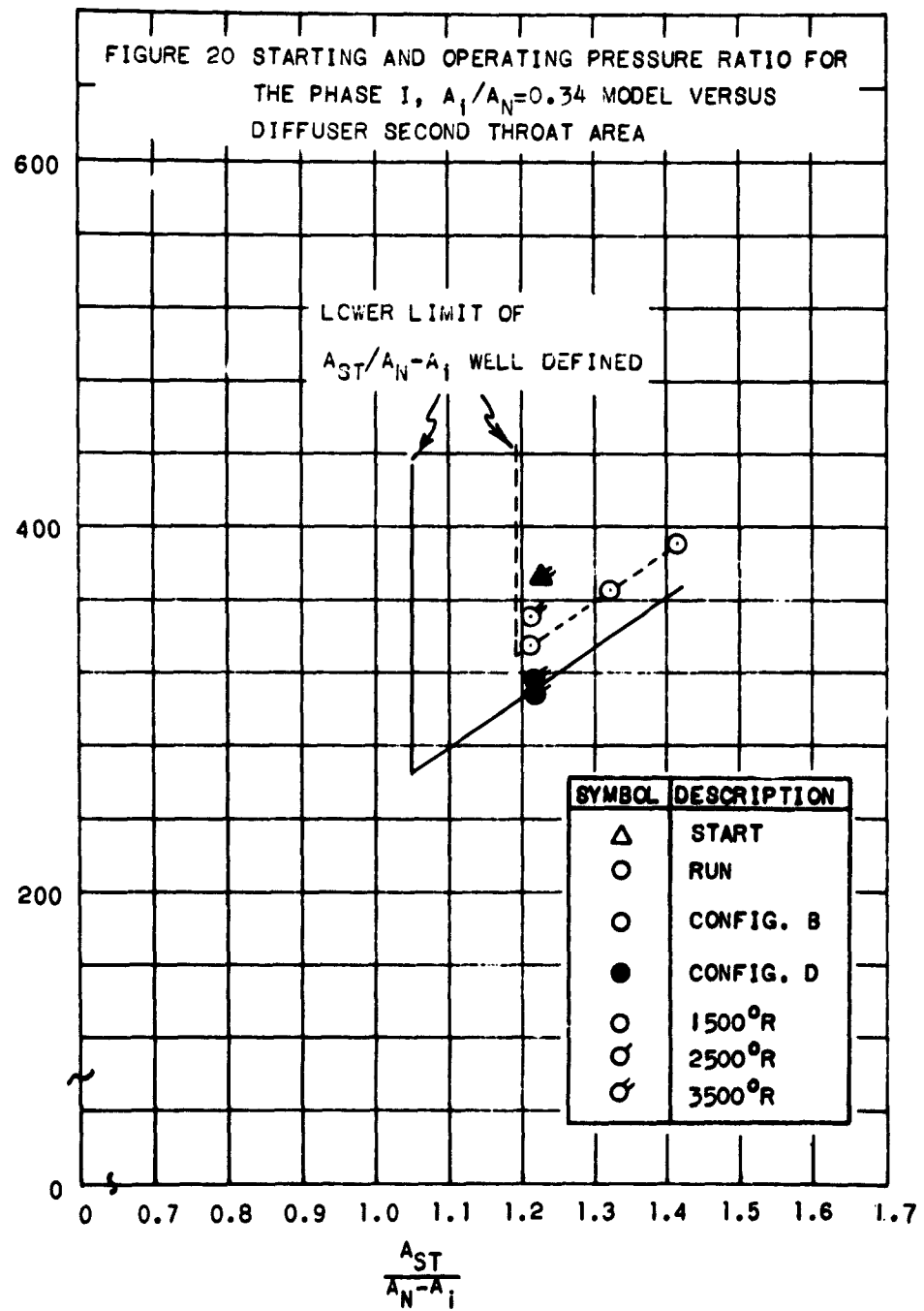
FIGURE 18 (CONTINUED)  $A_i/A_N = 0.44$  &  $0.53$

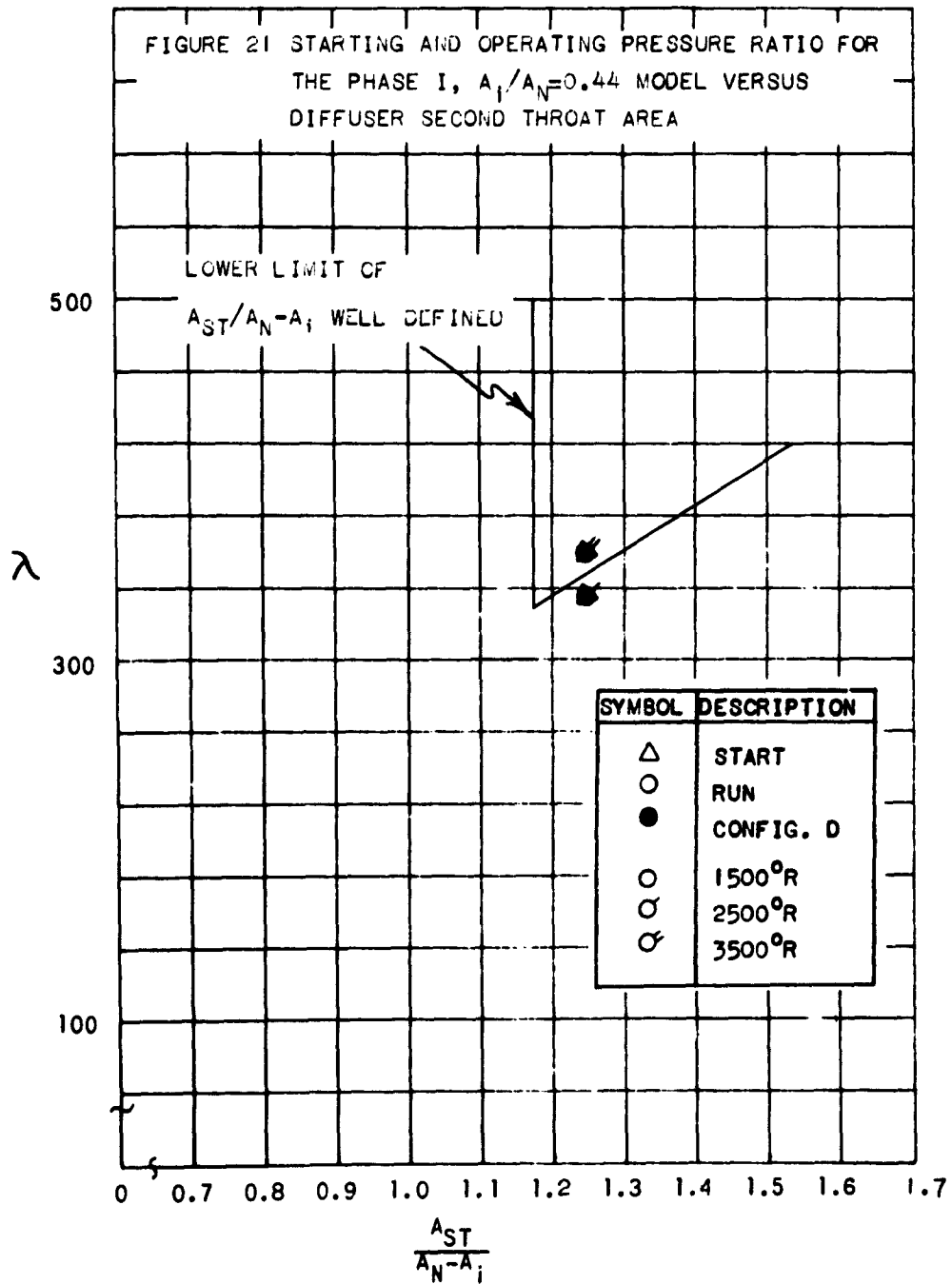


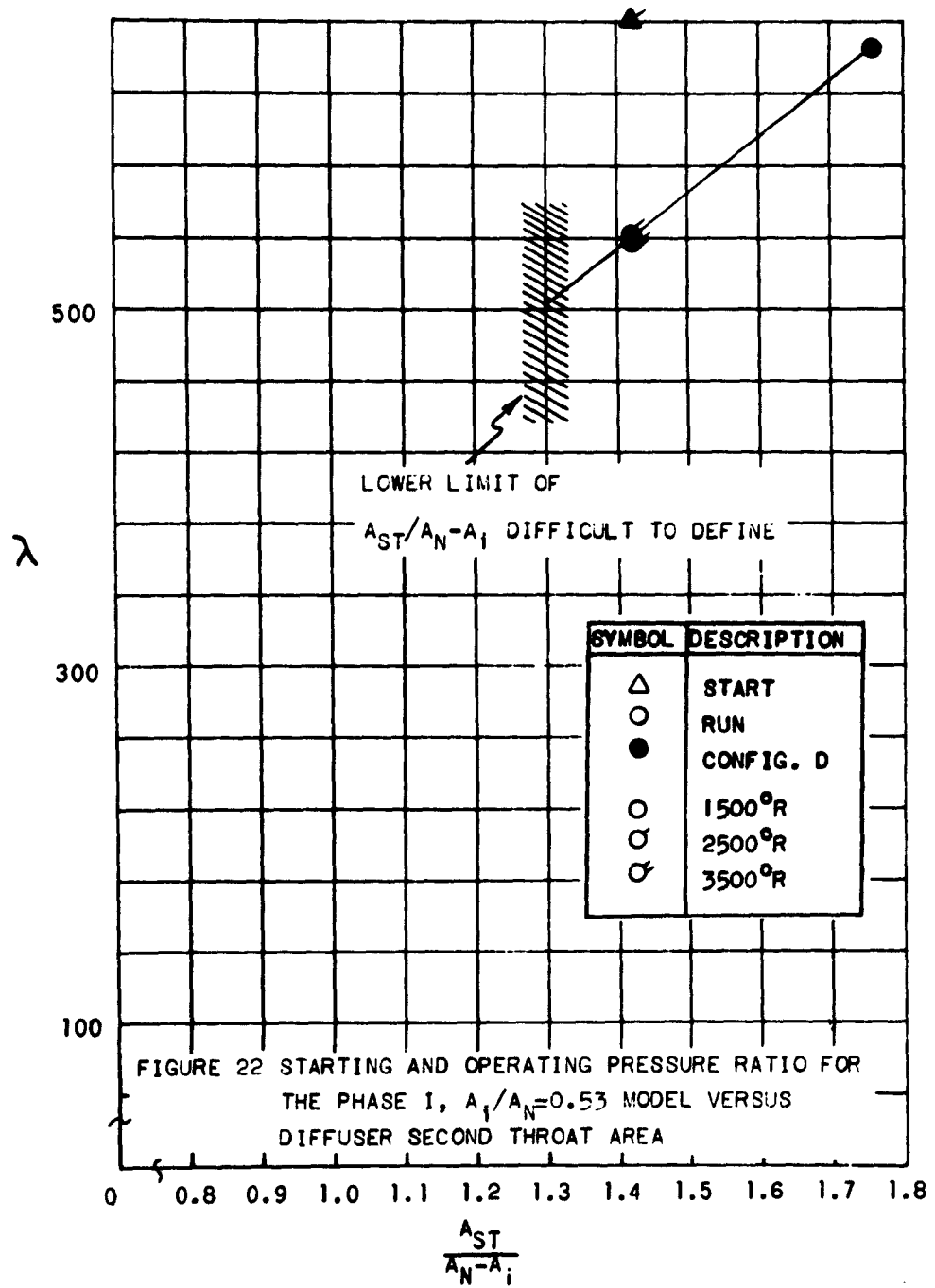
TAP	OPEN GAP		CLOSED GAP	
	UNSTARTED	STARTED	UNSTARTED	STARTED
1	0.00055	0.00015	0.00056	0.00018
2			0.00175	0.00040
3	0.00102	0.00067	0.00102	0.00077
4	0.00073	0.00029	0.00078	0.00105
5	0.00083	0.00053	0.00097	0.00148
6	0.00102	0.00245	0.00116	0.00484
7	0.00210	0.00548	0.00210	0.00624
8	0.00375	0.00103	0.00324	0.00116
9	0.00355	0.00098	0.00300	0.00118
10	0.00332	0.00098	0.00304	0.00118
11	0.00321	0.00132	0.305	0.00139
12	0.00349	0.00195	0.00317	0.00201
13	0.00509	0.00189	0.00357	0.00201

INSIDE COWL

FIGURE 19 PHASE II MODEL PRESSURE DISTRIBUTION







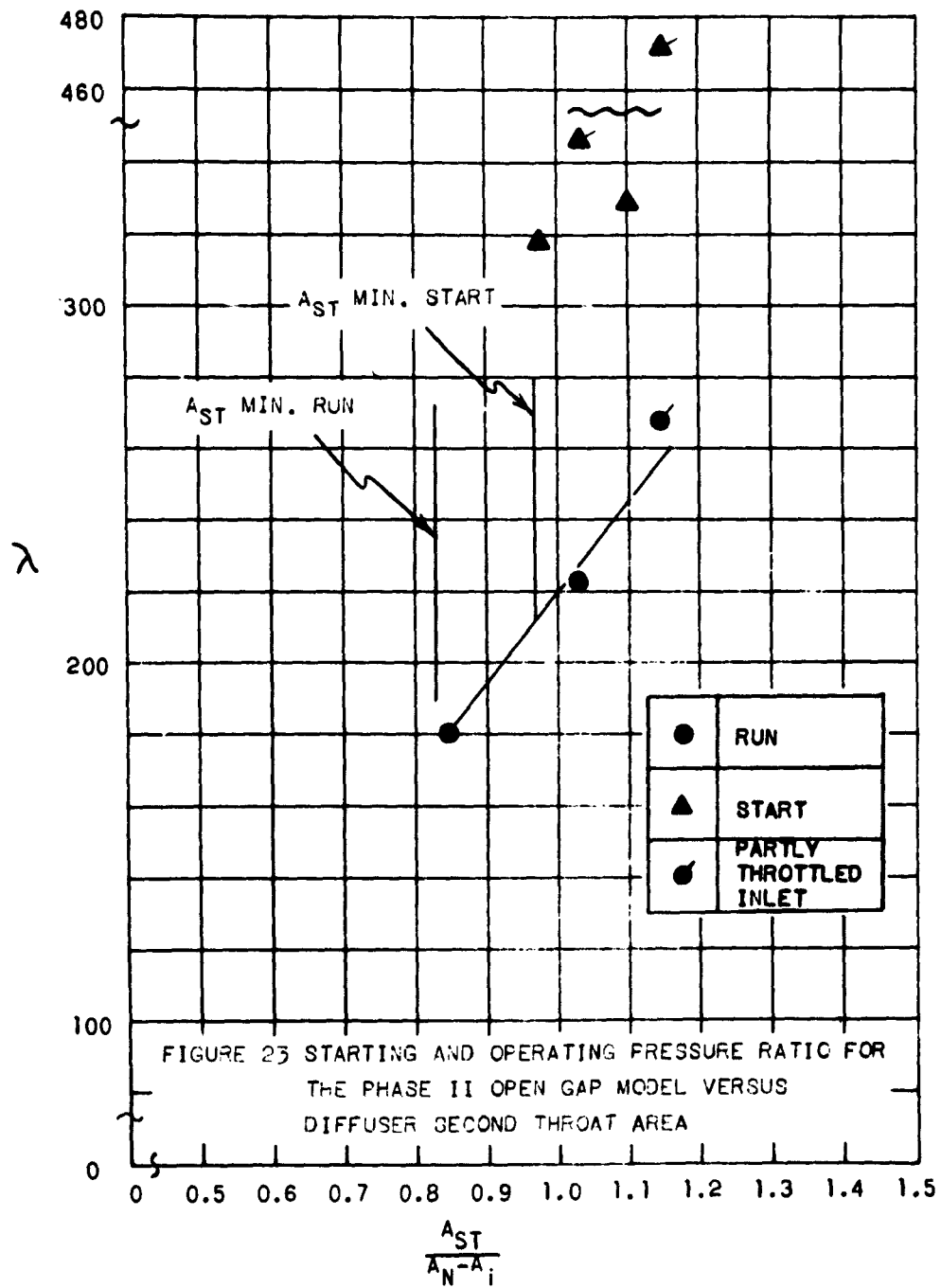
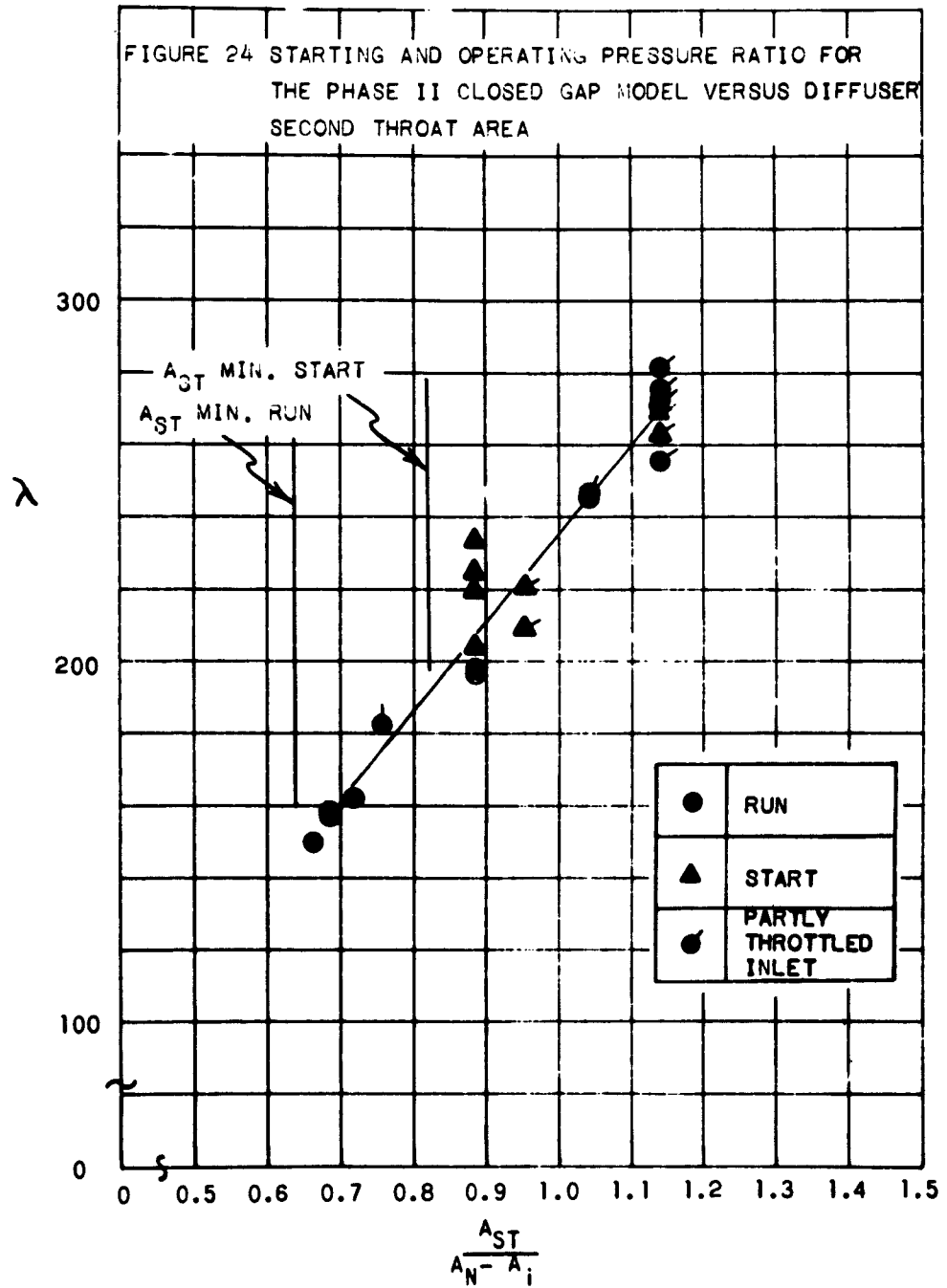
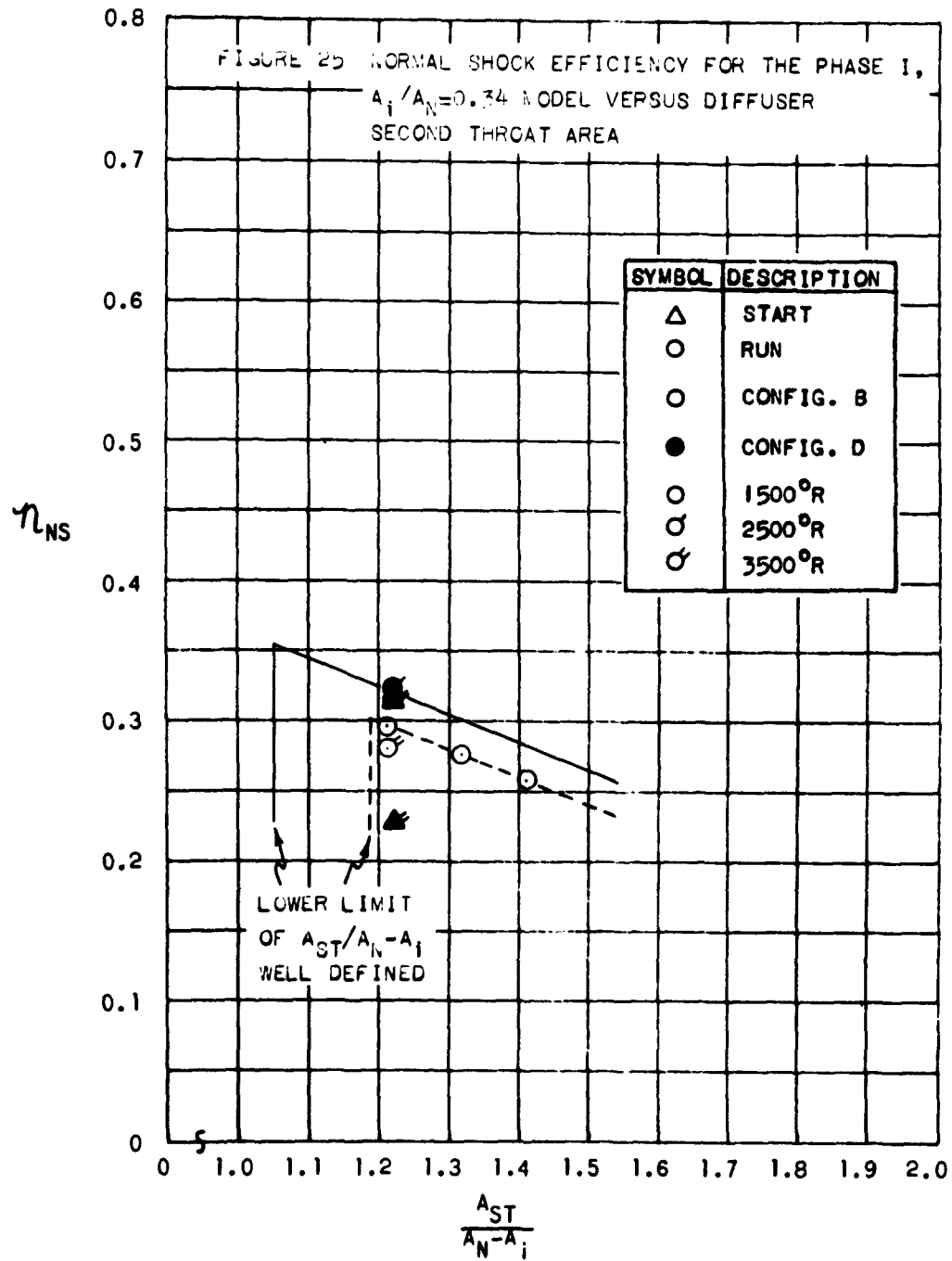
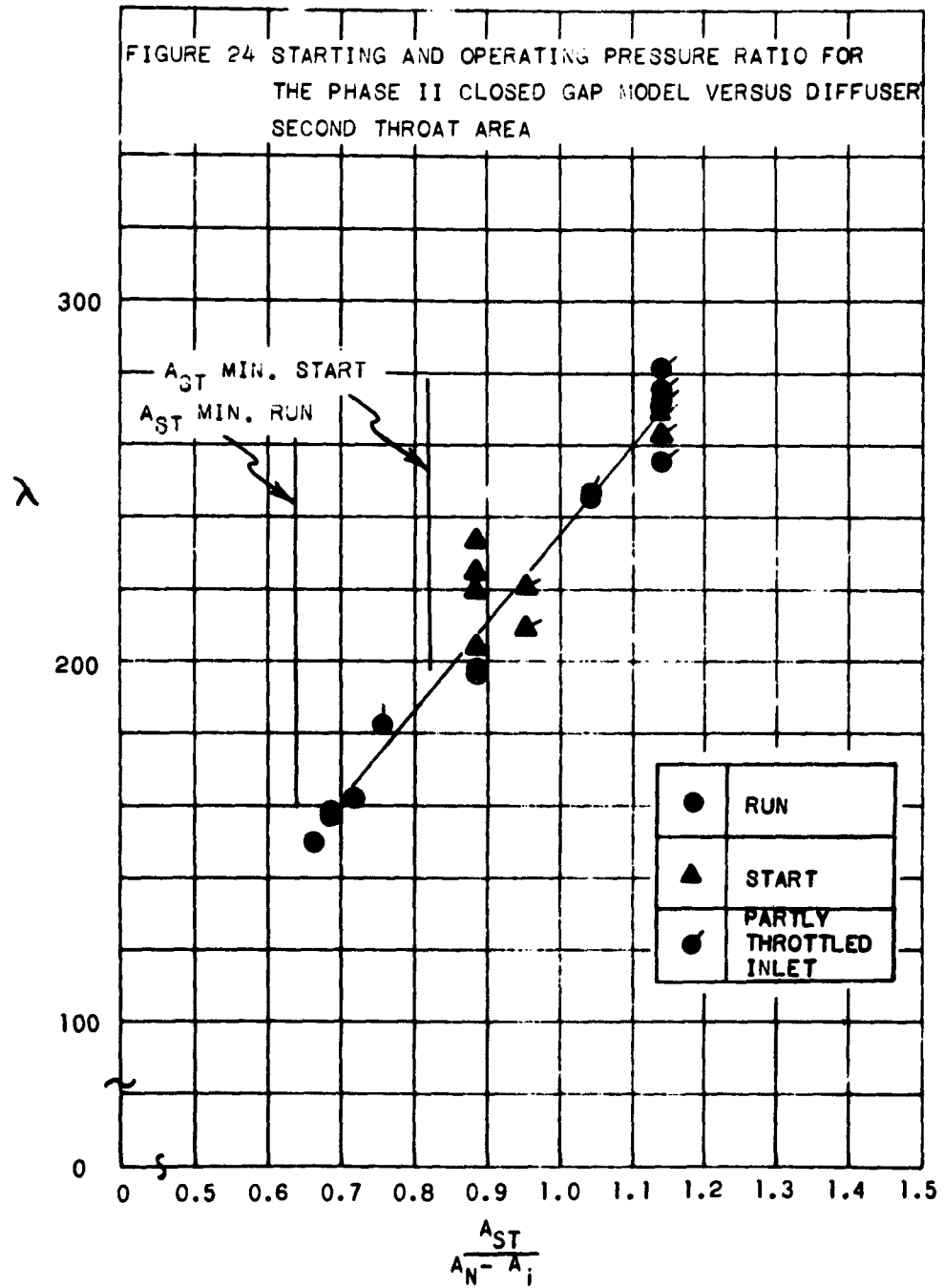
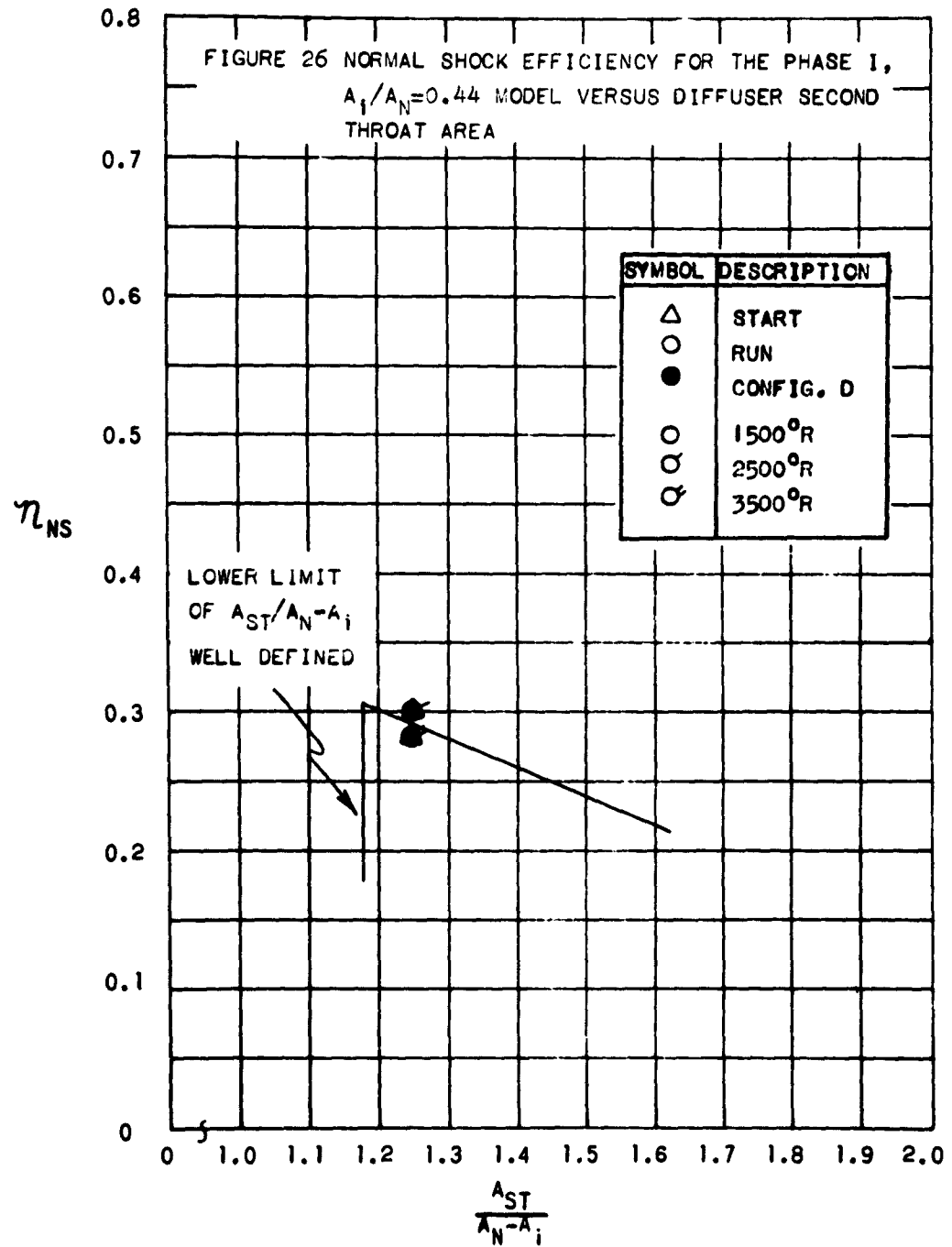


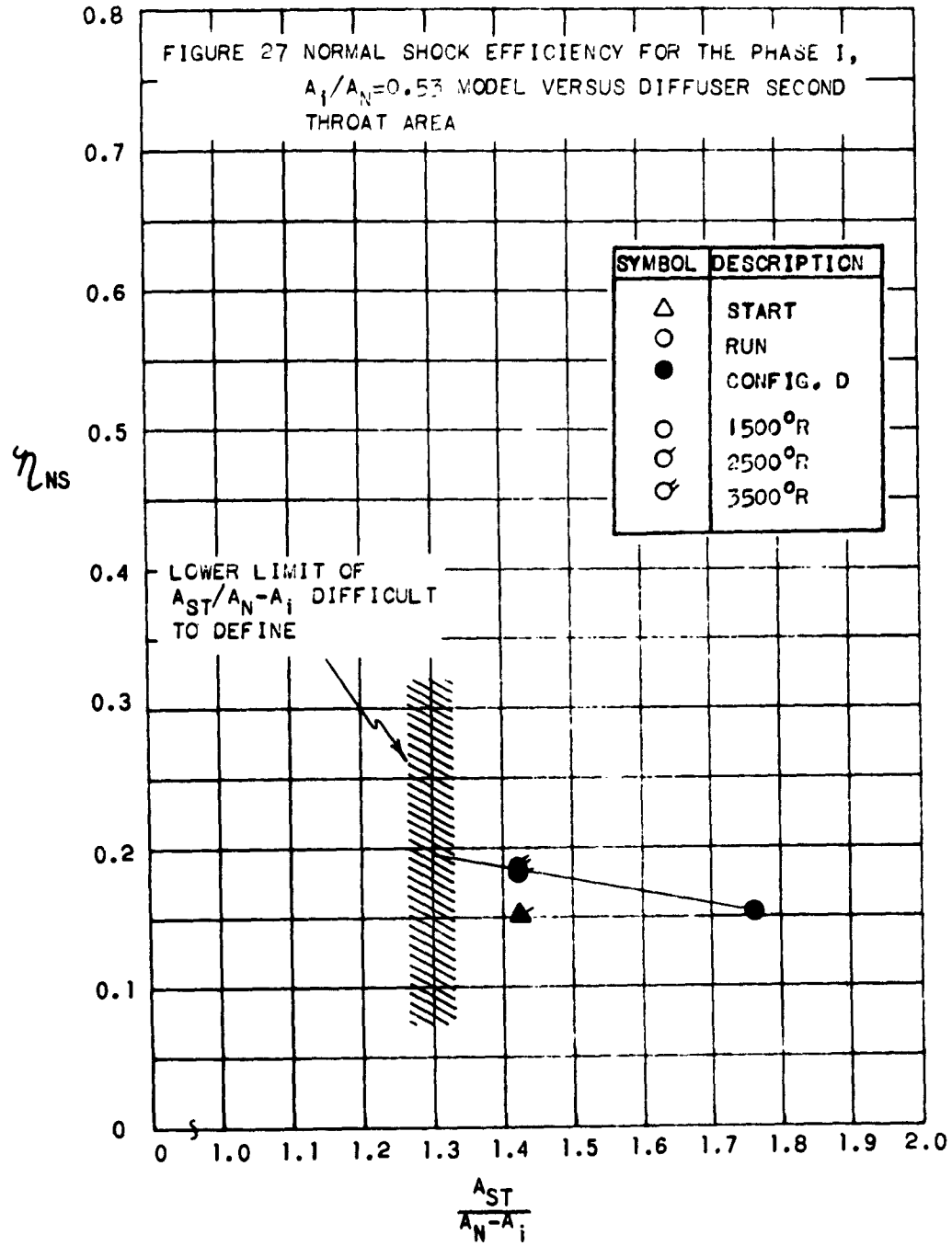
FIGURE 24 STARTING AND OPERATING PRESSURE RATIO FOR THE PHASE II CLOSED GAP MODEL VERSUS DIFFUSER SECOND THROAT AREA

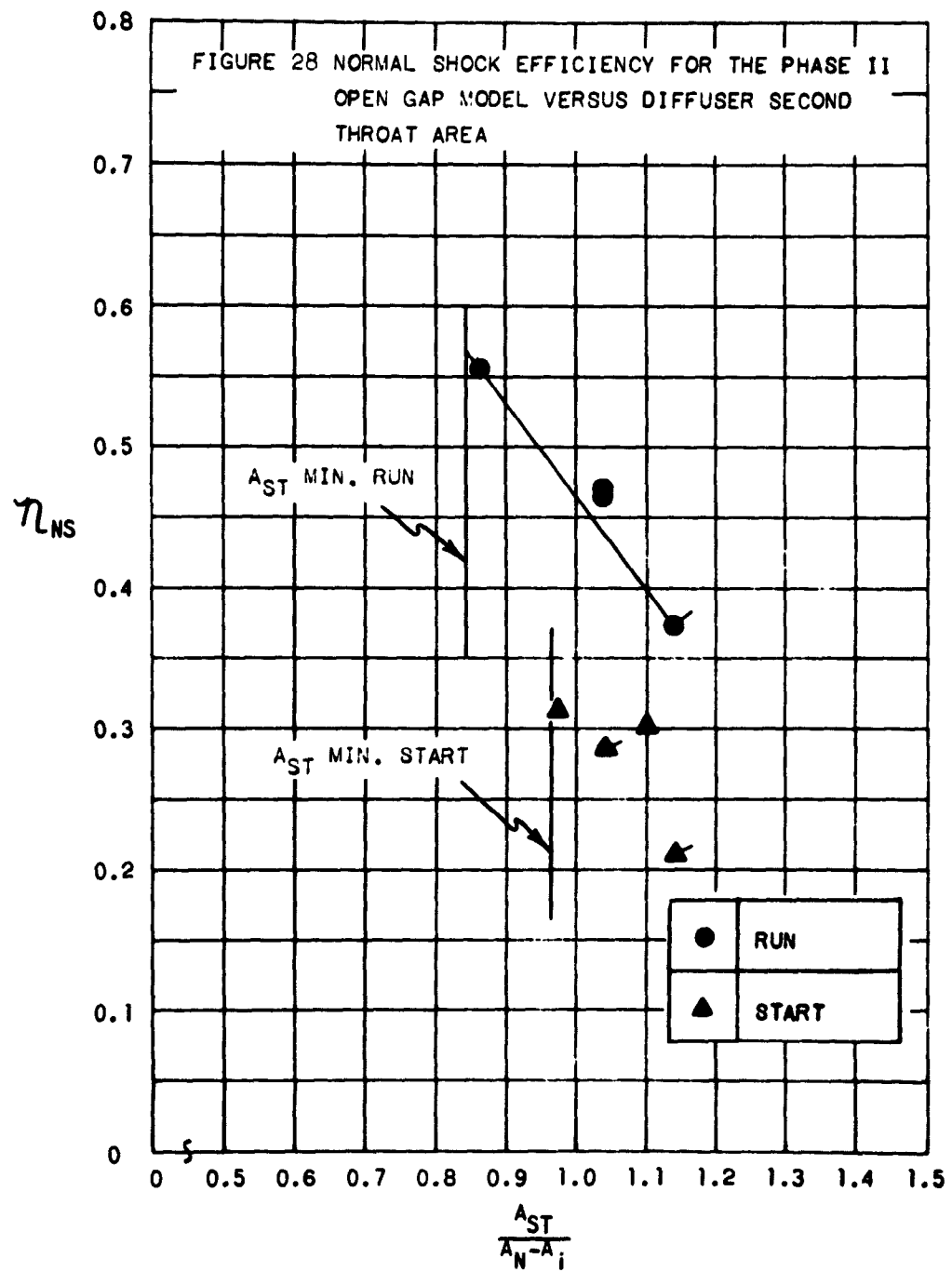


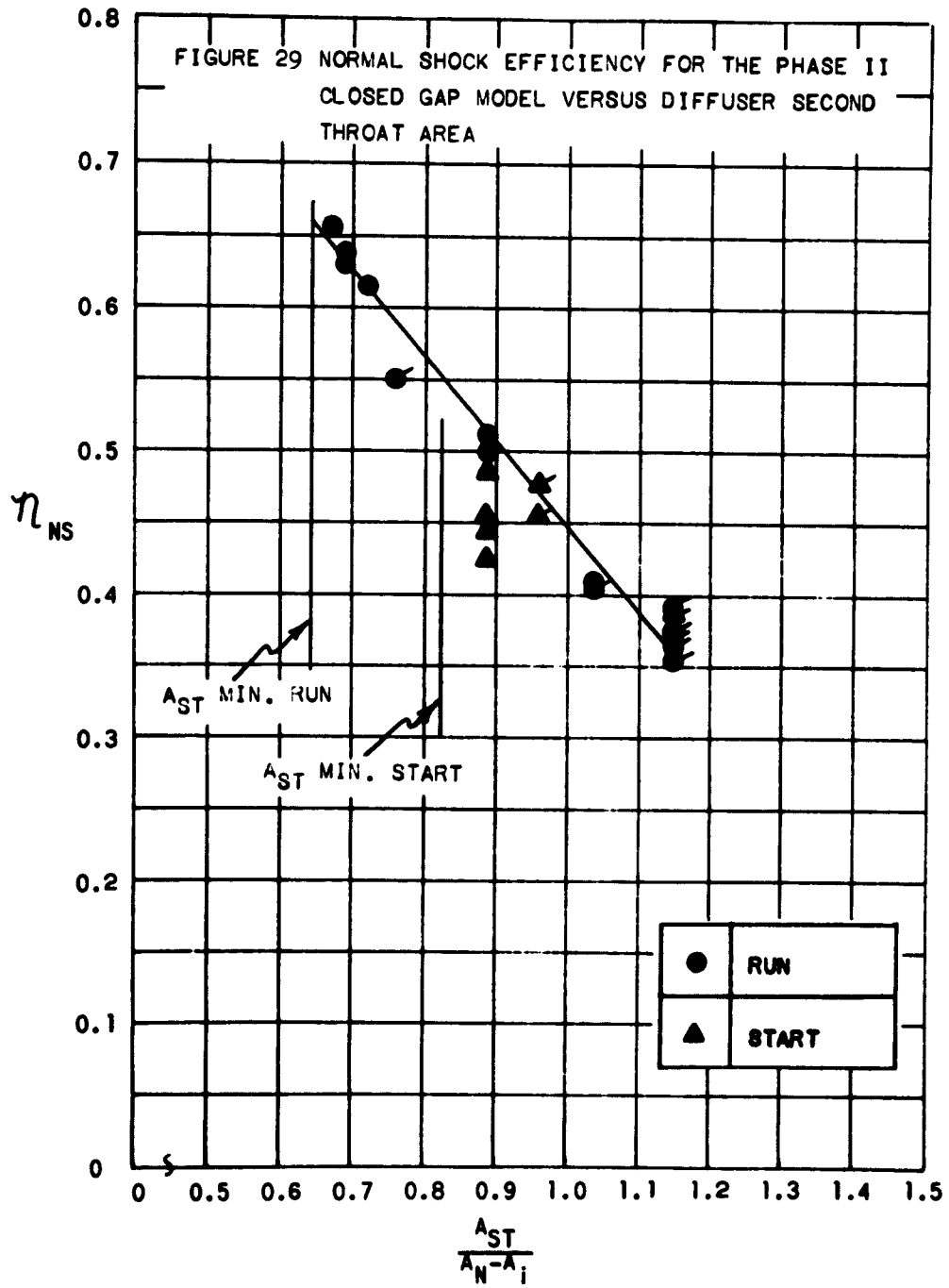


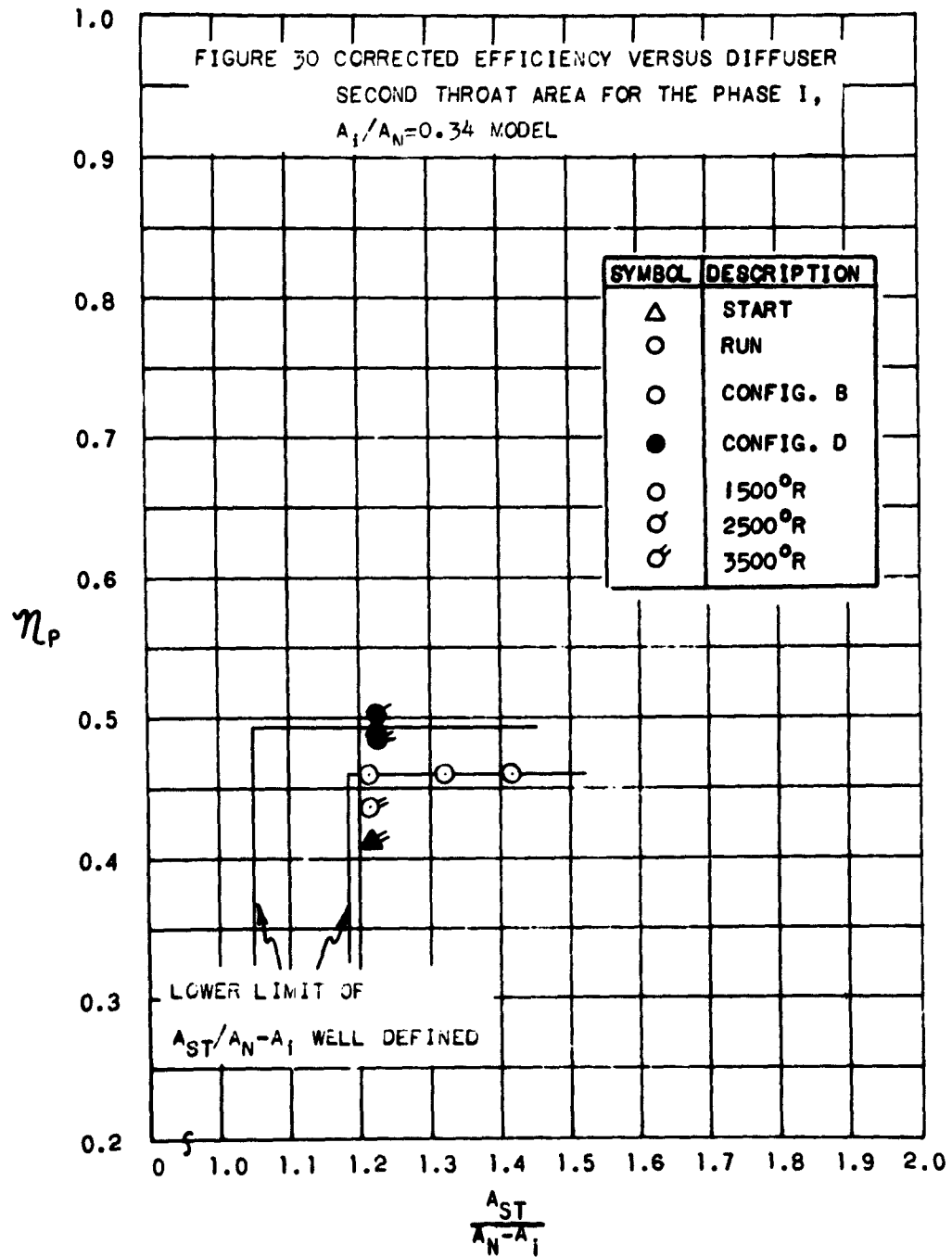


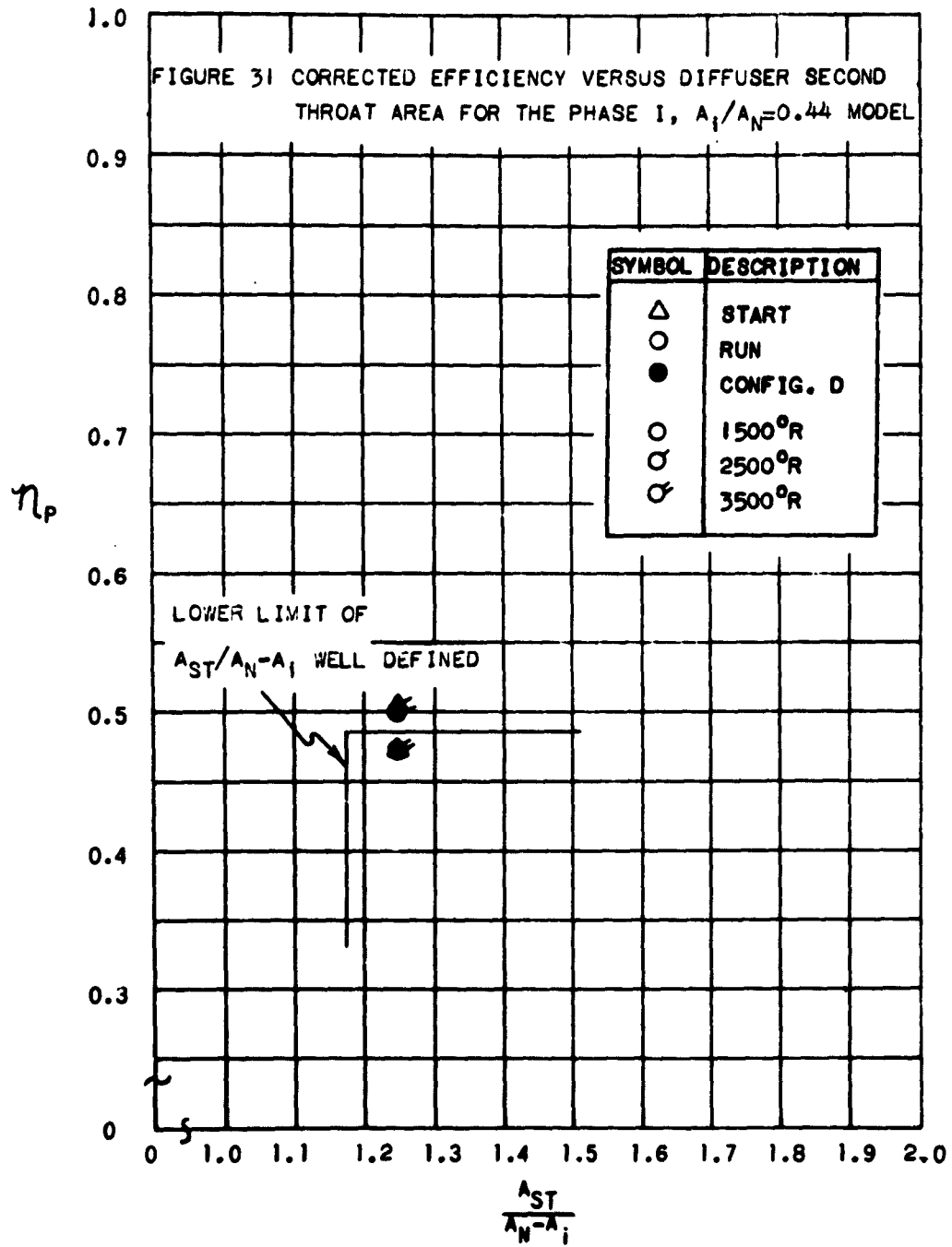


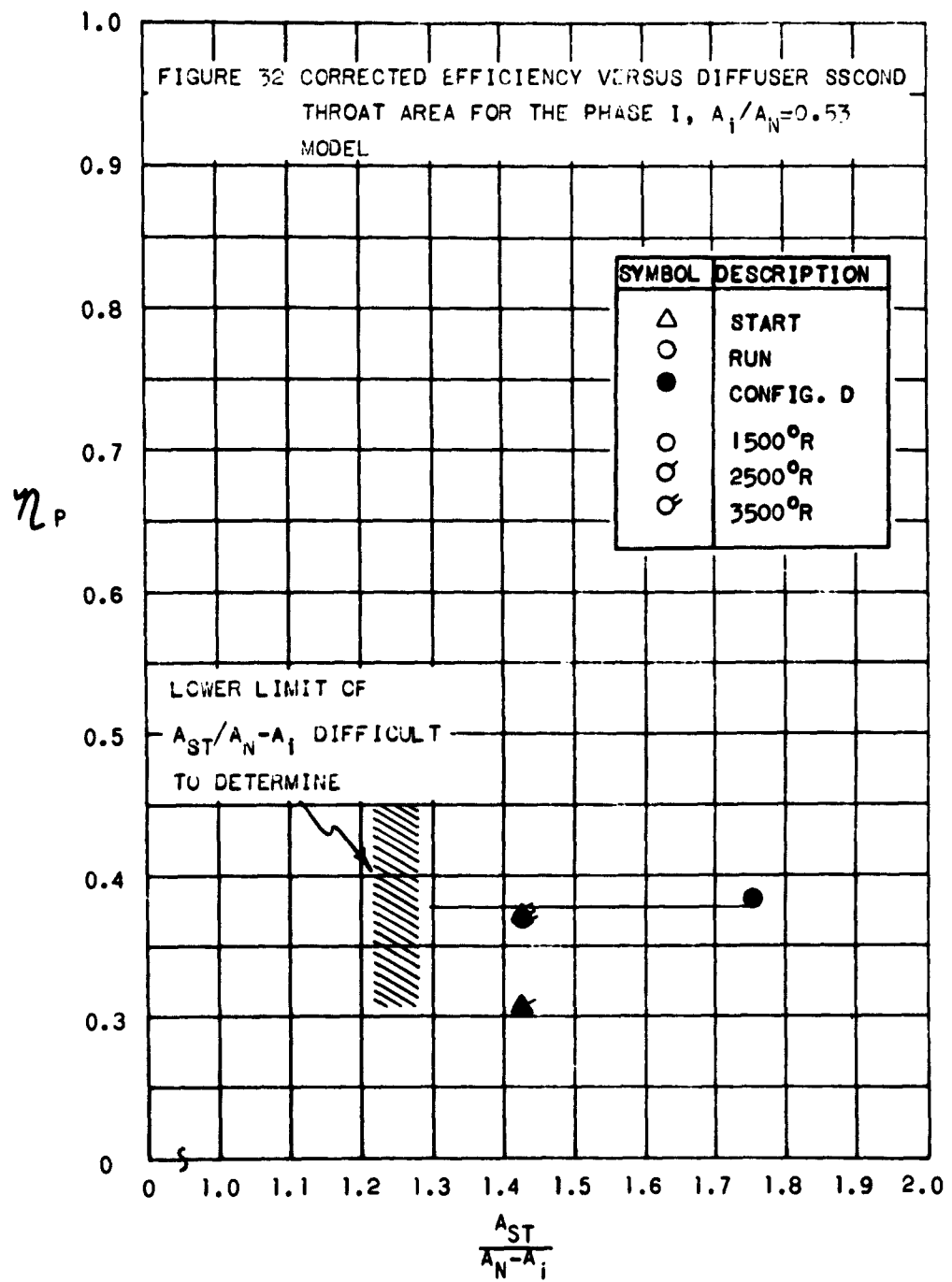


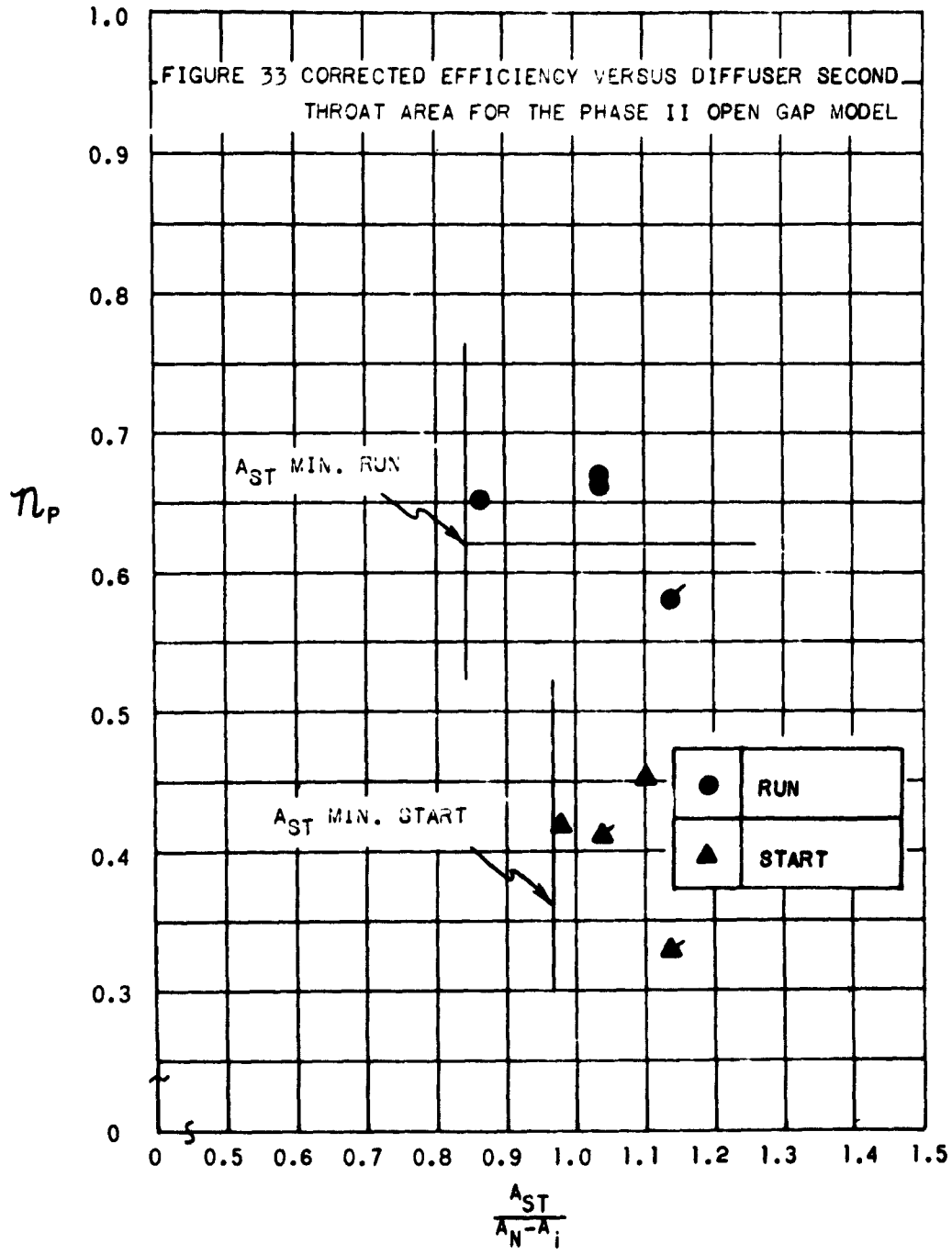


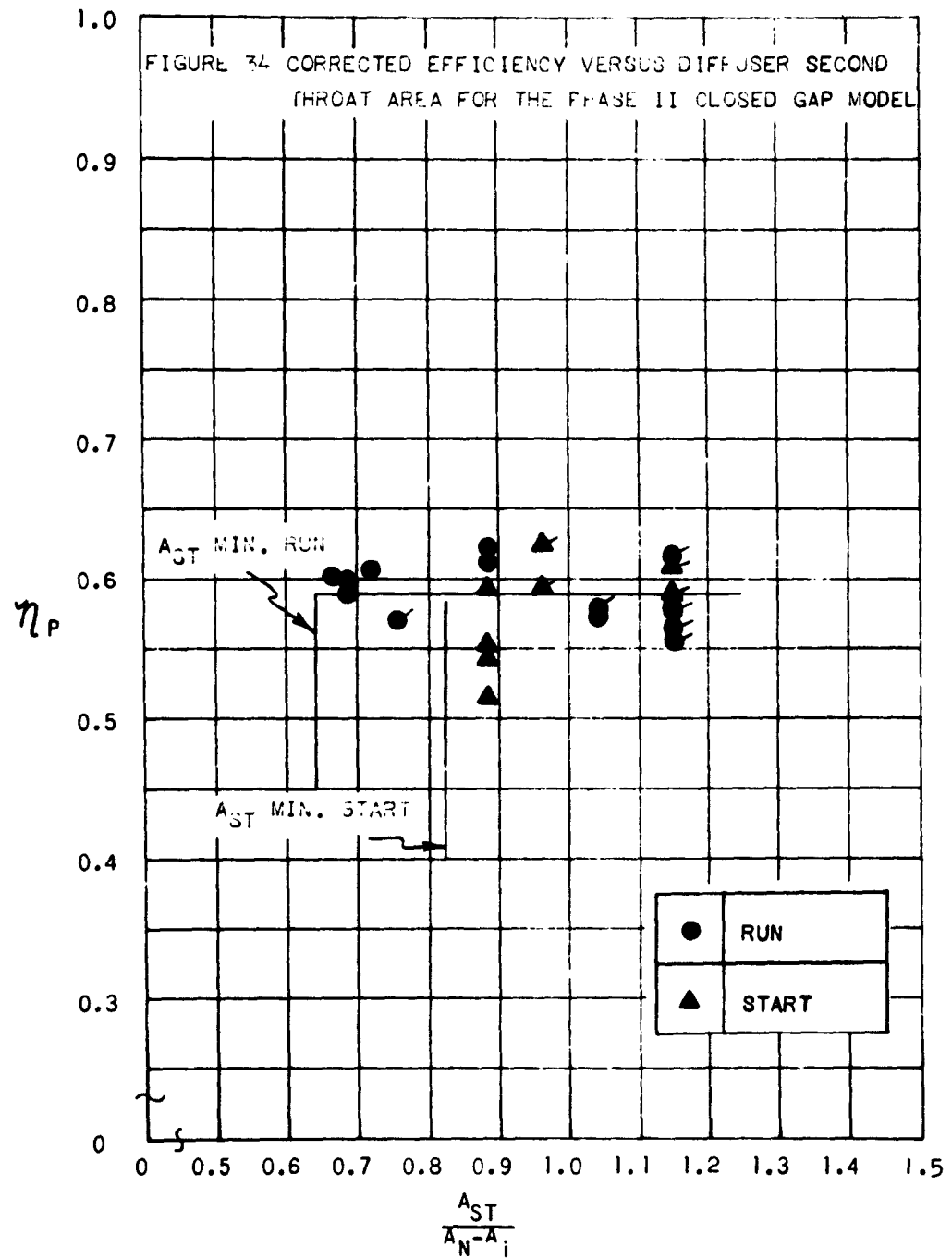












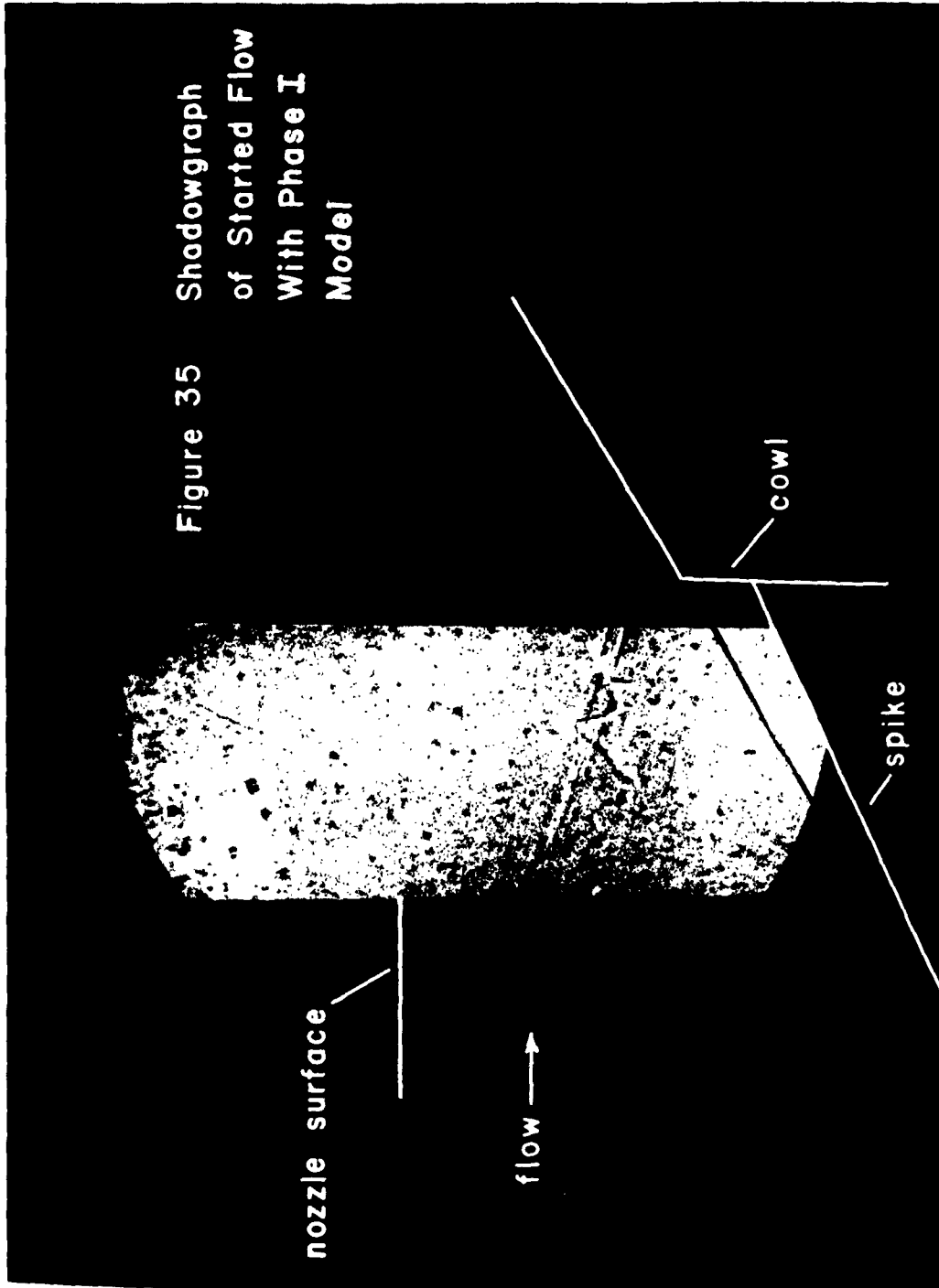


Figure 36 Shadowgraph  
of Started  
Flow With  
Phase II  
Model

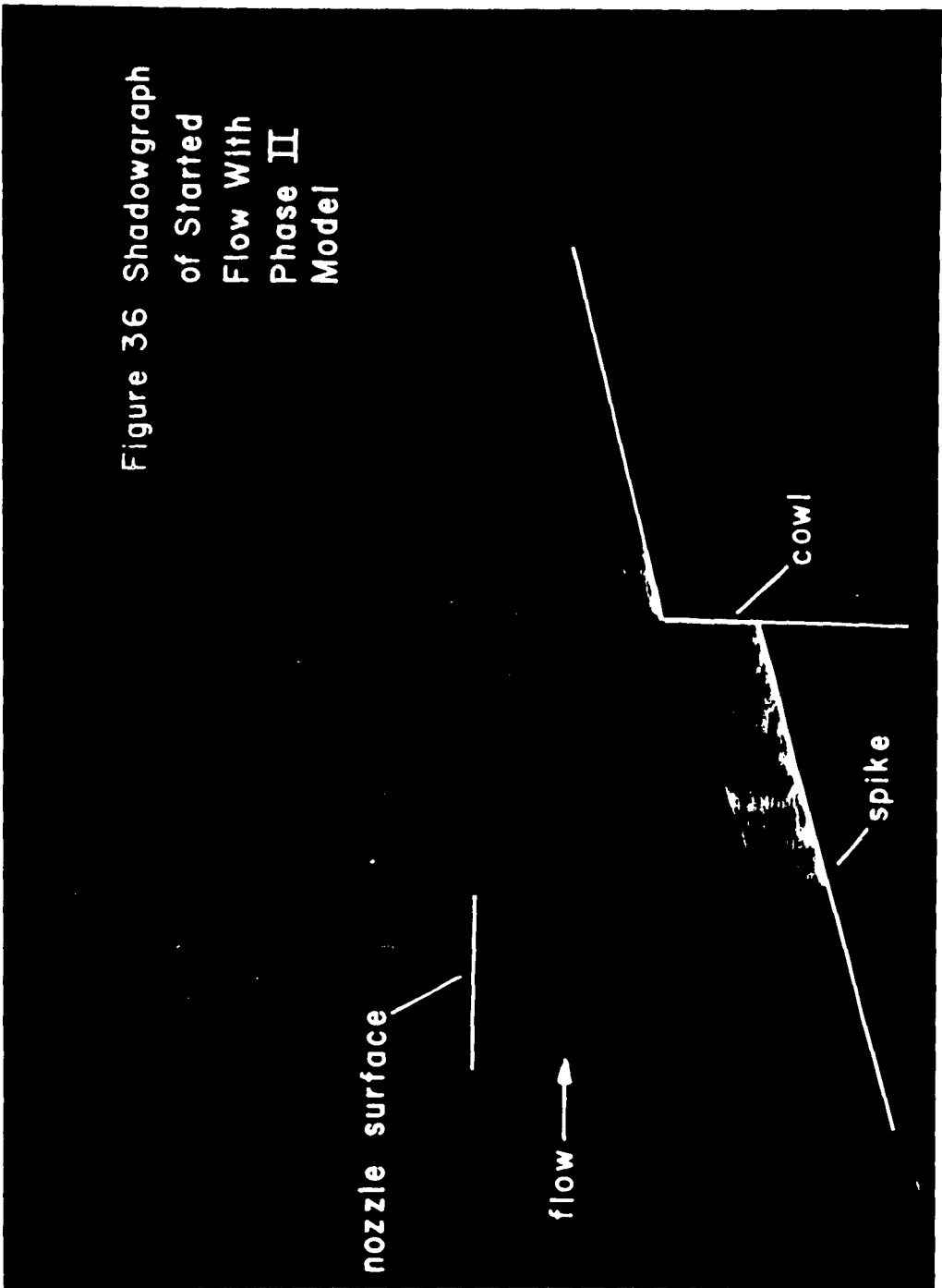
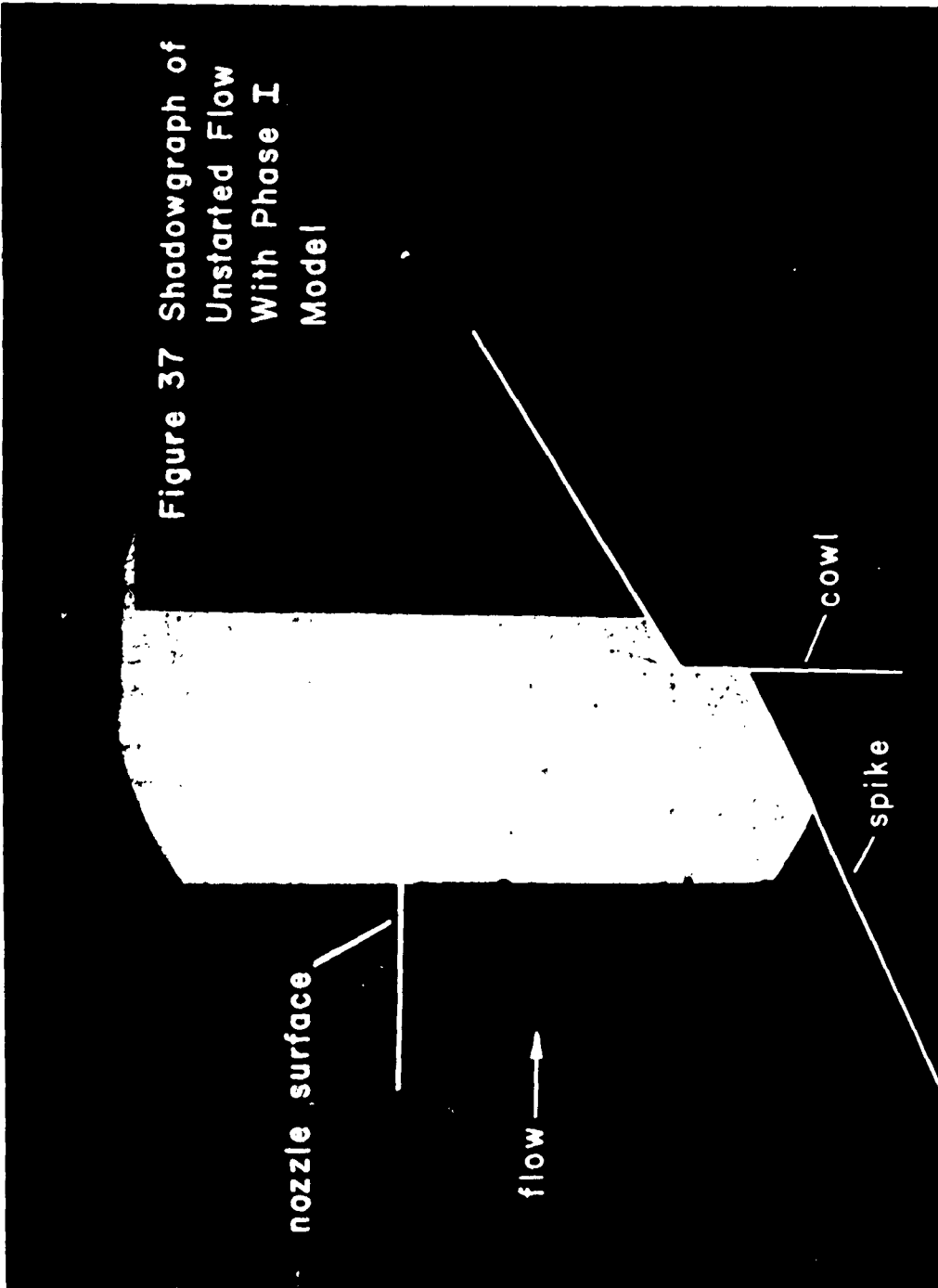


Figure 37 Shadowgraph of  
Unstarted Flow  
With Phase I  
Model



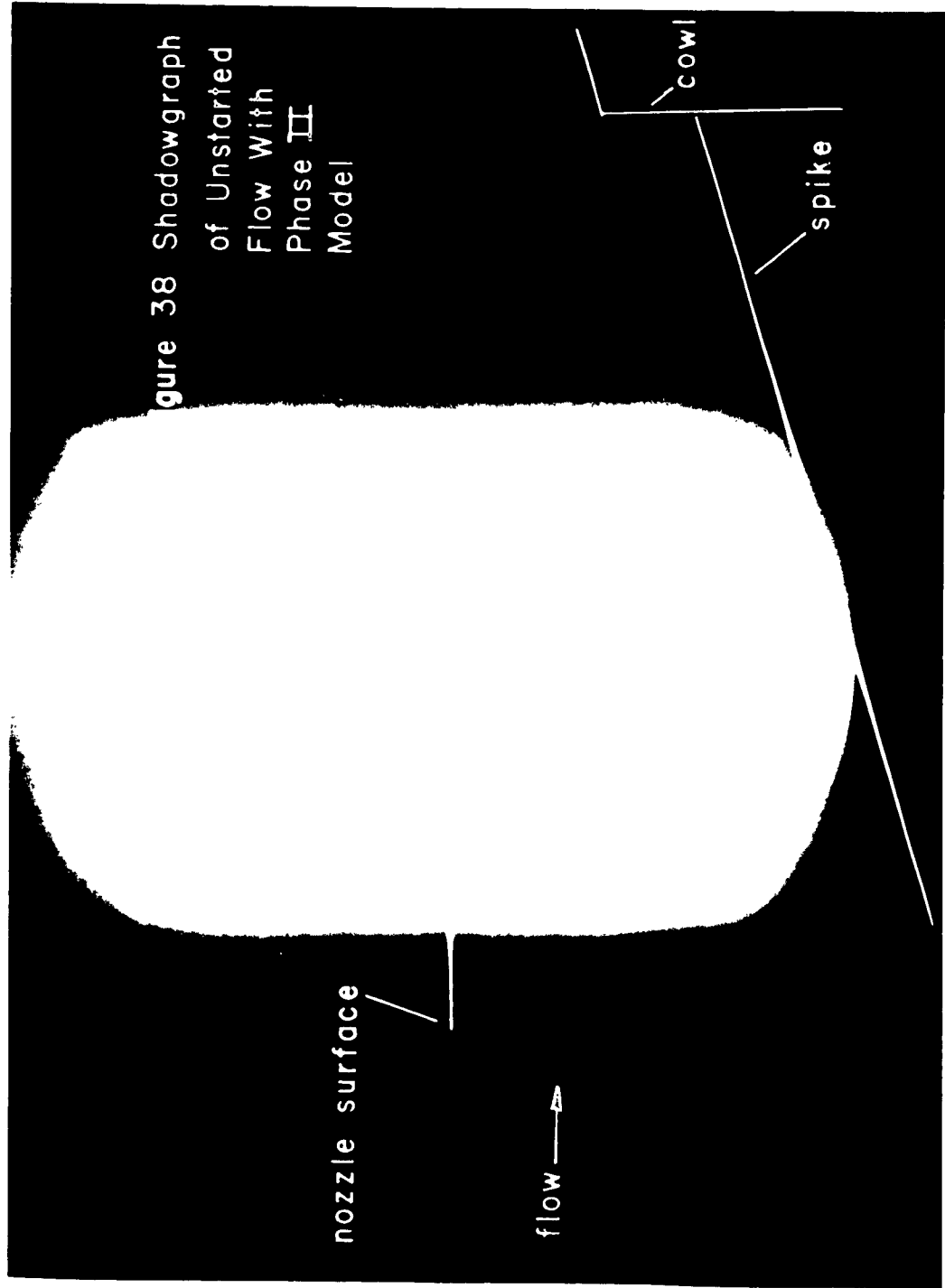


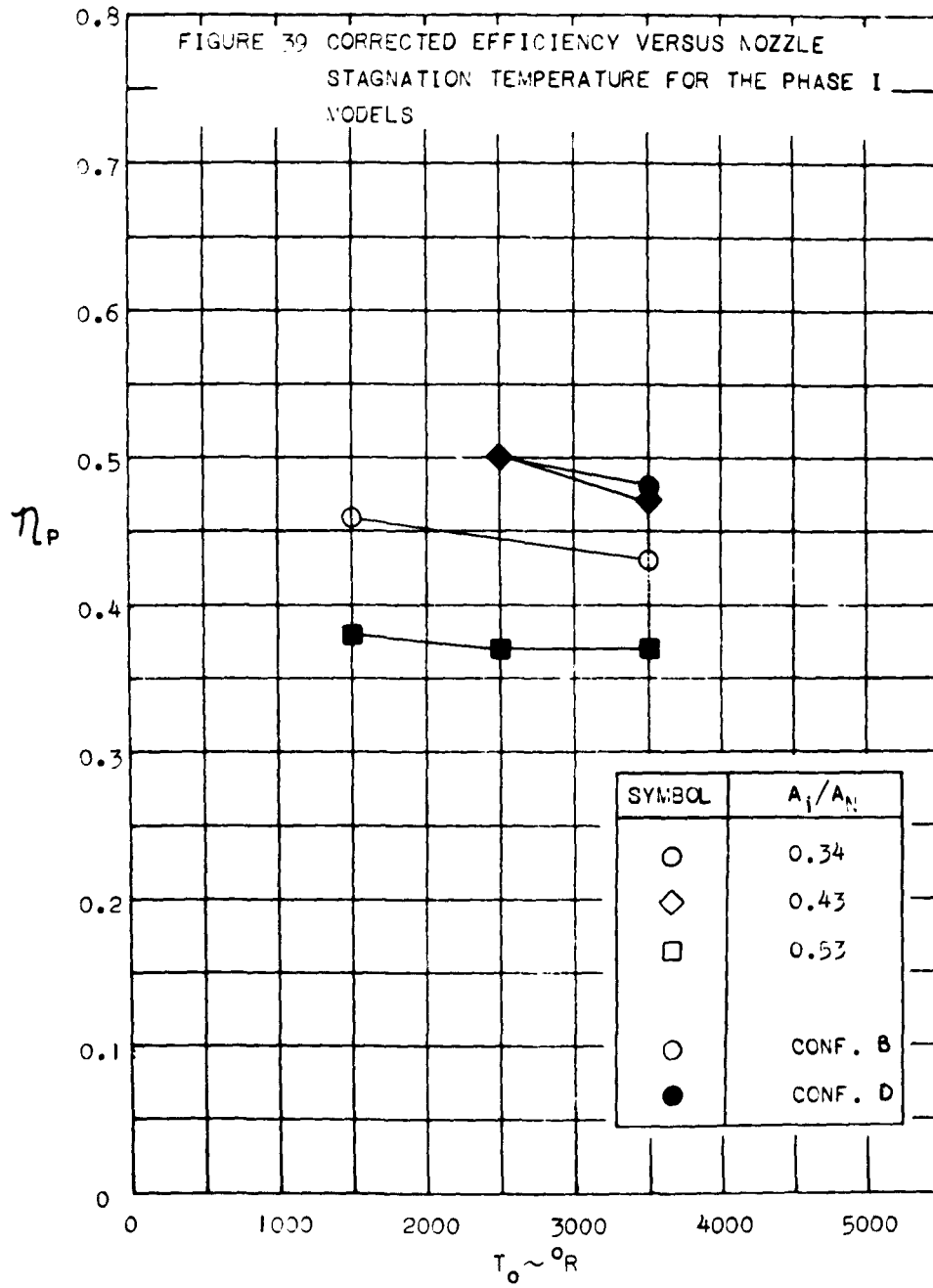
Figure 38 Shadowgraph  
of Unstarted  
Flow With  
Phase II  
Model

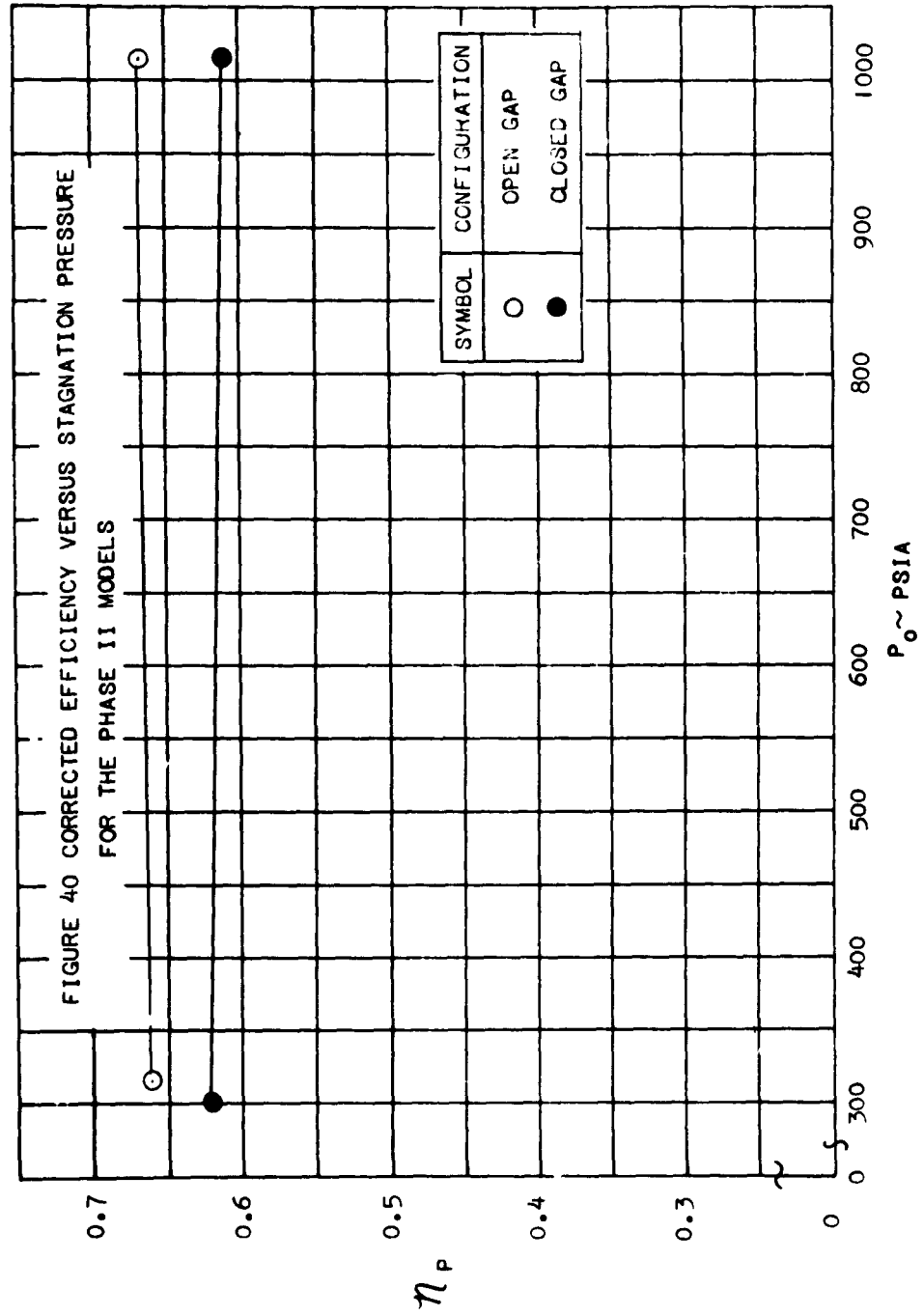
nozzle surface

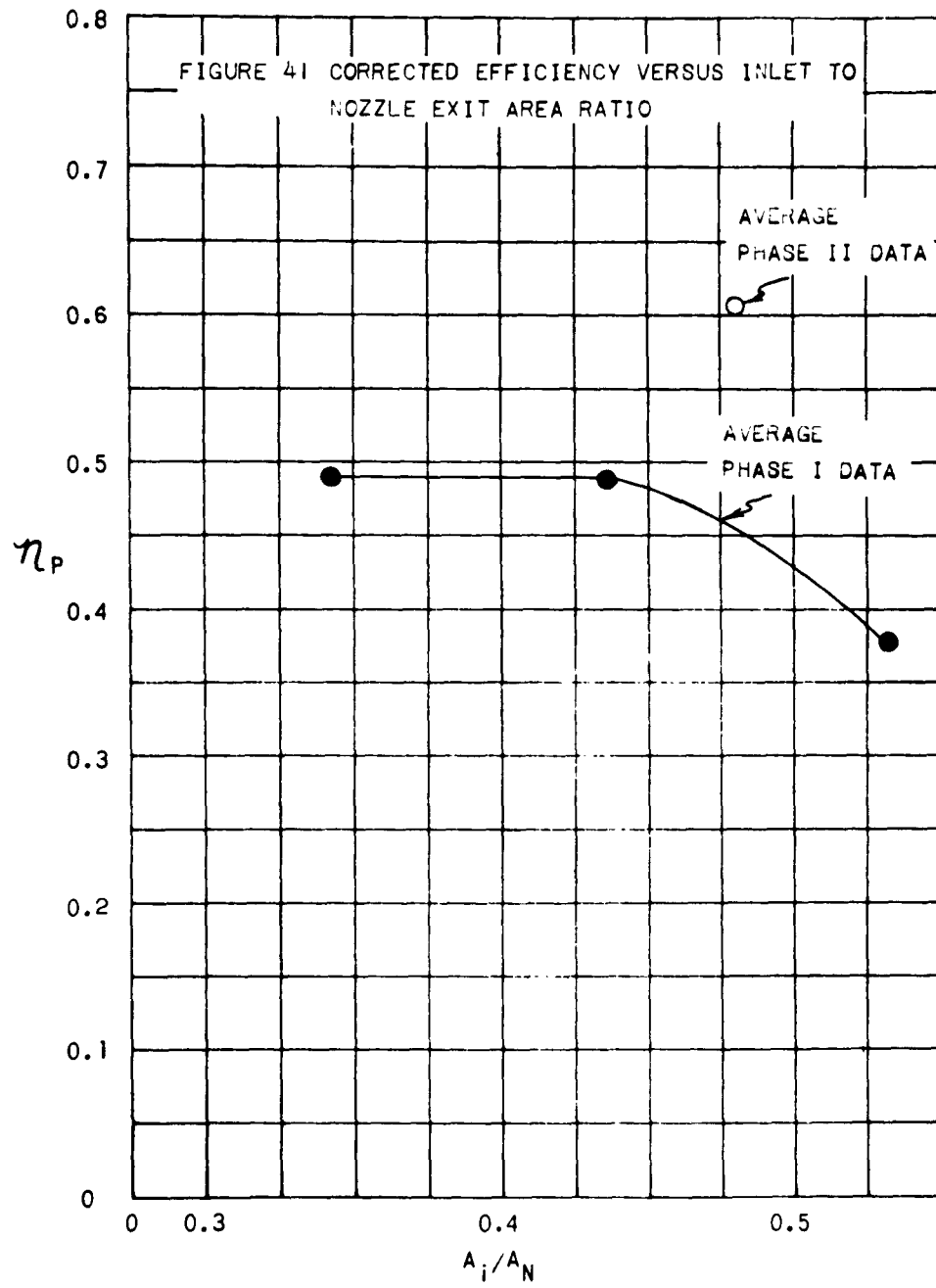
flow →

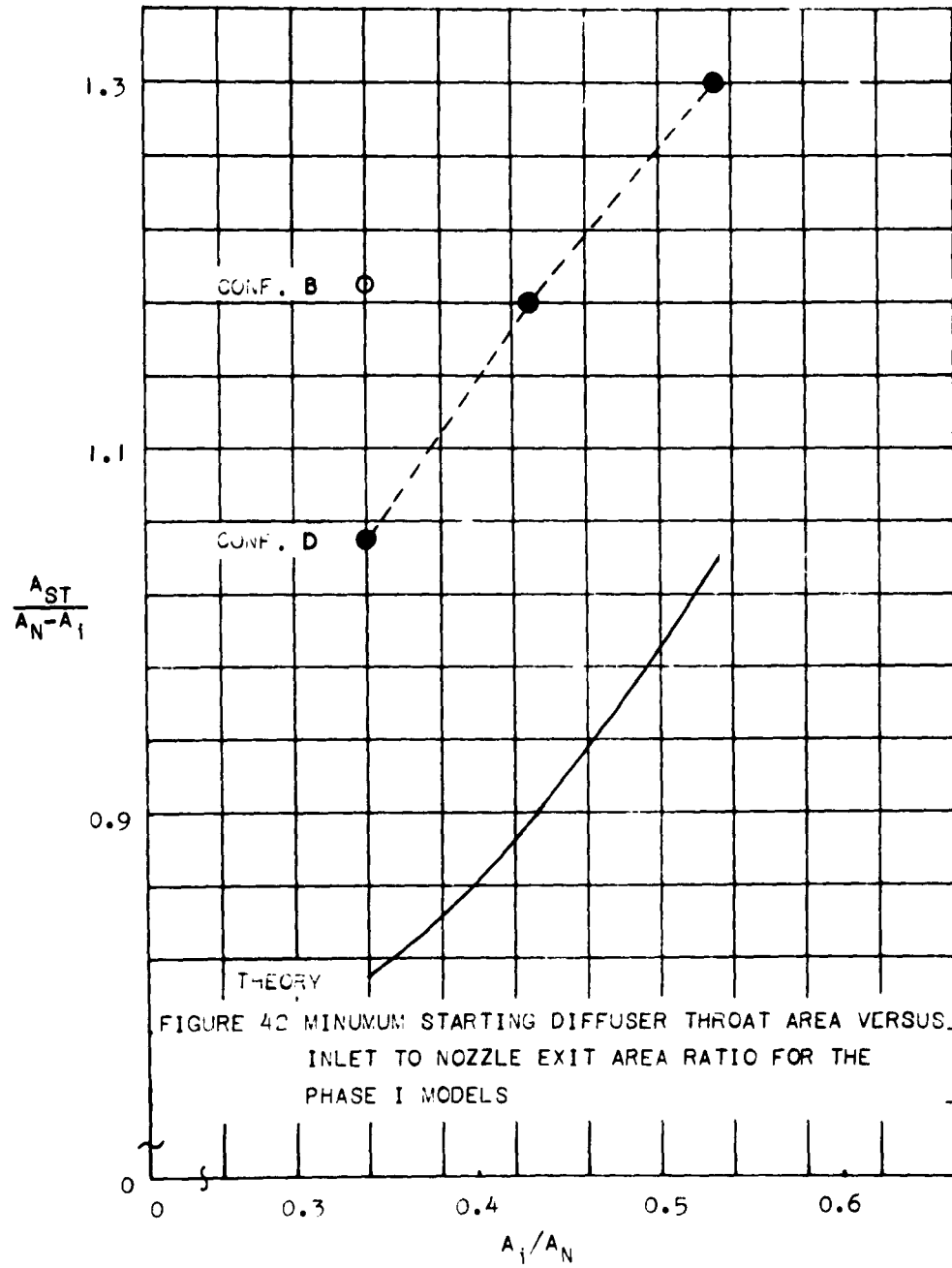
cowl

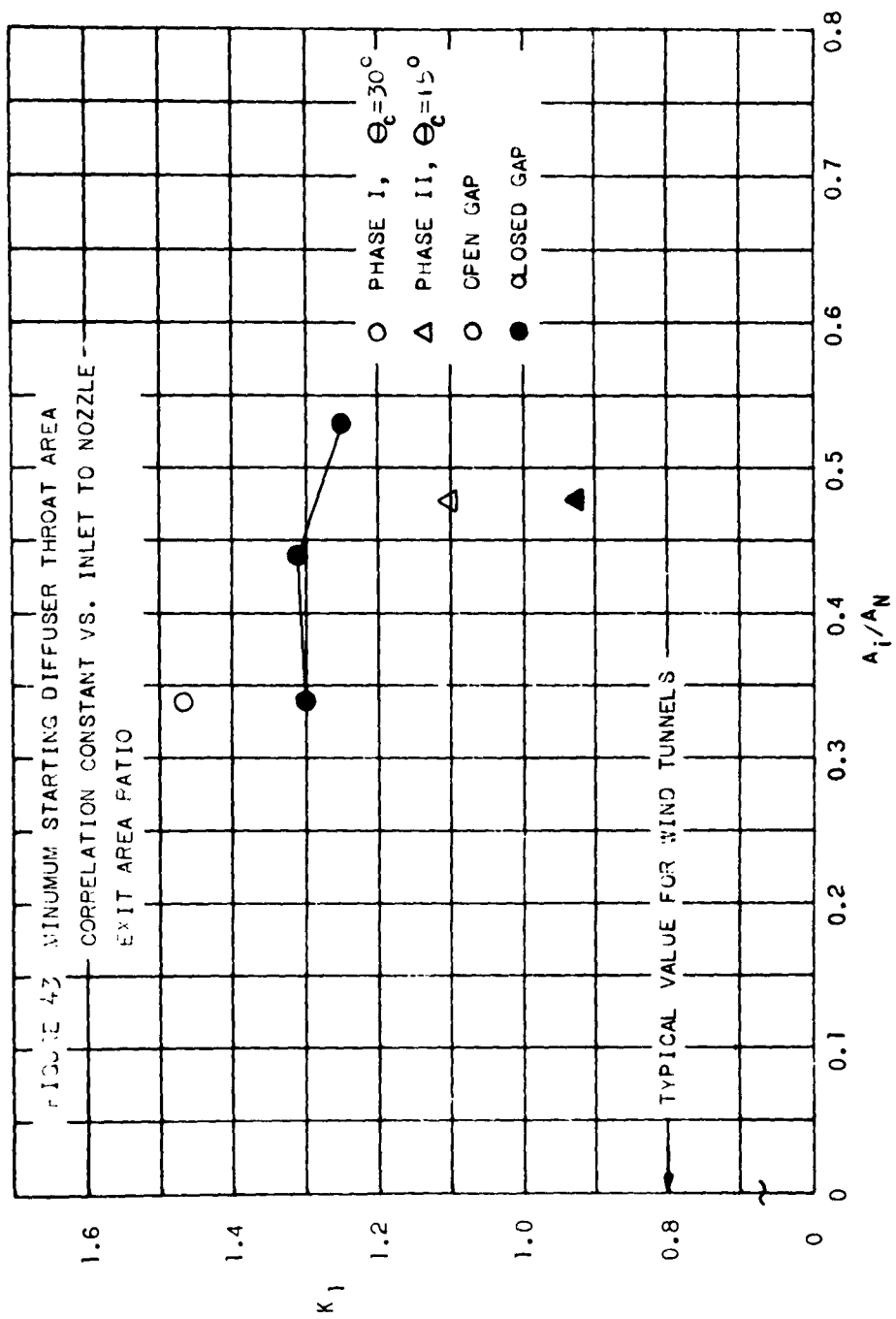
spike

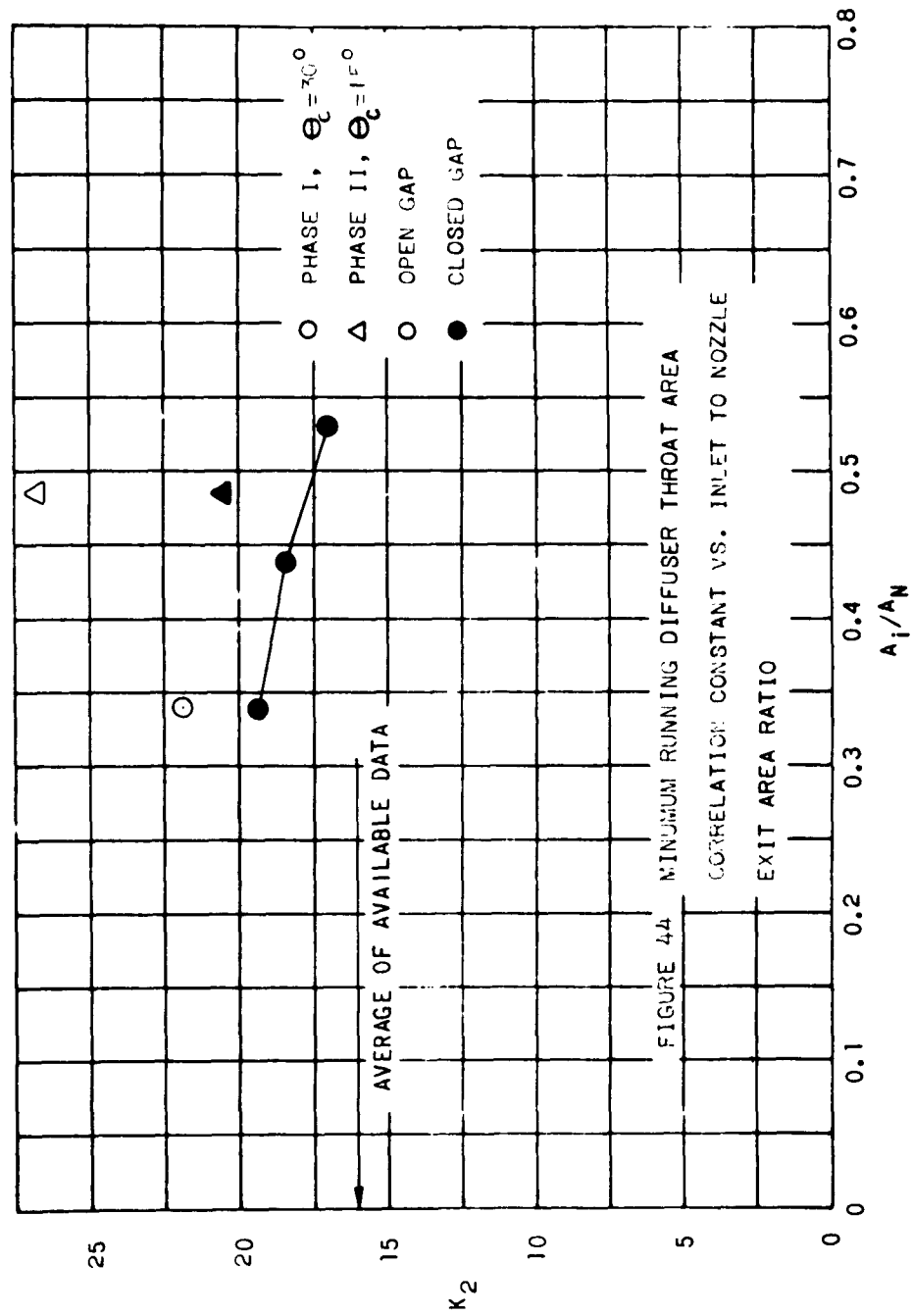












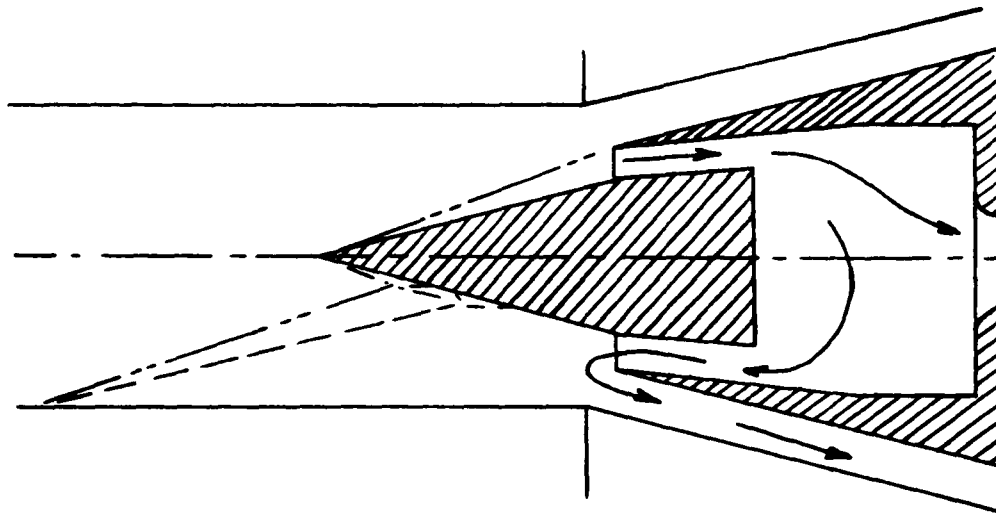


FIGURE 45 THE STARTING FLOW PICTURE WITH THROTTLED INLET

